博 士 論 文

A Physical-layer Approach for Realizing Real-time and Reliable Industrial Wireless Communications

（物理層に着目した産業用高信頼リアルタイム無線通信に関する研究）

Sakdejayont, Theerat

サクデーシャヨン ティラット

指導教員　　**森川 博之 教授**

Abstract

This thesis focuses on physical-layer approaches for realizing real-time and reliable industrial wireless communications. To achieve industrial wireless communications, wireless systems are required to operate in real-time and reliable performance. Conventionally, industrial control systems (ICS) has been implemented by wired systems. This incurs several disadvantages including high wiring and maintenance costs, restricted machine deployment, and low reachability. Realizing industrial wireless communications is still a challenging task in terms of real-time capability, reliability, security, and low power consumption. In particular, current wireless standards are limited to satisfy the real-time and reliability requirements due to their constraints in physical-layer designs, which are originally intended for traditional wireless applications. Therefore, this thesis aims to improve the real-time capability and the reliability via physical-layer approaches.

This thesis aims to reduce physical-layer transmission overhead for improving the real-time capability while maintaining good reliability. For realizing real-time and reliable wireless communications, the system should simultaneously adopt several techniques including forward error correction, interference avoidance, single-hop topology, contention-free channel access, channel equalization, and diversity. Essentially, the transmission overhead, which affects real-time capability, usually occurs for achieving channel equalization and diversity. Specifically, preamble transmission is required to learn about wireless channels, which in turn is used in a channel equalization algorithm to eliminate negative effects of the channels. In addition, transmit diversity requires some levels of cooperation among multiple transmitters in order to realize constructive signal combination at a receiver. Both preamble transmission and transmit cooperation are considered as a large overhead for short data payloads of ICS. Therefore, this thesis studies methods to (1) shorten the preamble transmission and (2) reduce the transmit cooperation.

(1) By exploiting the fast and frequent transmissions in ICS, we propose a subcarrier-selectable short preamble for channel estimation in an OFDM (orthogonal frequency division multiplexing) system. To shorten the preamble transmission in traditionally wireless systems, the well-studied blind estimation and scattered-pilot schemes might be applied to estimate the channel by exploiting long payload transmission time. However, for the small payloads of ICS, a short preamble is necessary for acquiring channel information in a short amount of time. In this thesis, we introduce the subcarrier selectivity to the preamble design. By doing so, the channel correlation in both time and frequency domain can be utilized to obtain accurate channel estimation. Our simulation results verify that the proposed short preamble can improve the real-time capability of ICS in time and frequency correlated channels.

(2) To reduce the transmit cooperation while achieving good reliability, we propose symbol-level packet combining using RSSI (received signal strength indicator) to make naturally real-time concurrent transmission (CT) become reliable. CT is real-time cooperating scheme and thus promising for ICS. CT makes all transmitters transmit an identical signal at the same time without any other cooperation. However, compared to beamforming-based and orthogonal precoding schemes which require additional channel sounding or frequency and phase synchronization, CT cannot guarantee the non-destructive combination of signals at a receiver and may cause reliability degradation in the reception. To cope with this, we adopt receive diversity to perform symbol-level packet combining using RSSI. The proposed method is studied and evaluated by simulation and experiments in CT environments based on IEEE 802.15.4 and IEEE 802.11 DSSS standards.

In summary, this thesis addresses the real-time capability and reliability aspects of industrial wireless communications via physical-layer approaches. The main contributions of this thesis includes a novel design of short OFDM preambles utilizing not only frequency but also time correlated channels, and symbol-level packet combining using RSSI for reliable CT. Our studies verify that the proposed methods can potentially contribute to the improvement of the real-time capability and reliability in industrial wireless communications.

Contents

List of Figures

List of Tables

Chapter 1

Introduction

1.1 Background and Motivations

Wireless communications are moving toward new directions of the technology developments. The next generation of the wireless communications will involve more in communications of *things* in addition to communications of *humans*. Fig. 1.2 illustrates several usage scenarios of the next generation of wireless communications and their corresponding directions of developments. The communications of physical objects in the cyber-physical systems, the Internet of Things (IoT) and machine-to-machine networks requires new dimensions of performance criteria and therefore needs a new set of design, which differs from the communications of humans as being developed since 1990. At the beginning of 1990, the wireless communications are developed for delivering short messages and, later on, voice calls. Until now, the development is mostly focused on the throughput or massive broadband (upper half of the triangle in Fig. 1.2. For instance, nowadays we are able to surf the Internet, send photos, stream music and videos, and even organize a meeting via a video teleconference. Additional important aspects of the next-generation wireless communication developments are real-time capability and reliability. These characteristics are essential for realizing industrial wireless communications in manufacturing factories.

Meanwhile, in a view of industrial revolution, the next fourth industrial revolution is being said to built on the digital revolution and is expected to become the next generation of industrial control systems (ICS). One of most well-known project is called Industry 4.0. It is promoted by a German government towards the computerization of manufacturing, or so called a "smart factory". The previous three industrial revolutions are depicted in Fig. 1.1. The next generation of ICS is cyber-physical systems where physical, digital and biological worlds are fused together. Multiple cyber-physical systems communicate and cooperate with each other and with human over a communication network or the Internet. They facilitate the current automation system to the next level of factory automation where human are less involved to the process. This revolution is needed to be carried out multiple technological fields such as robotics, artificial intelligence, information networks including wireless communications.

This is where two demanded technologies meet and create a relationship in the research and development field as industrial wireless communications. This thesis considers industrial wireless communications as a research background, in which where we focus on improving real-time capability and reliability of industrial wireless communications via physical-layer approaches. This section discusses our research motivations, which include

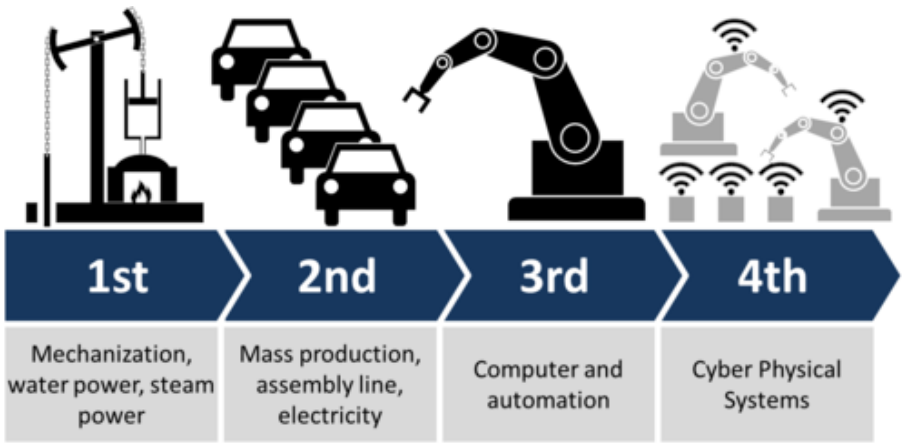

Fig. 1.1 Industry revolutions [1].

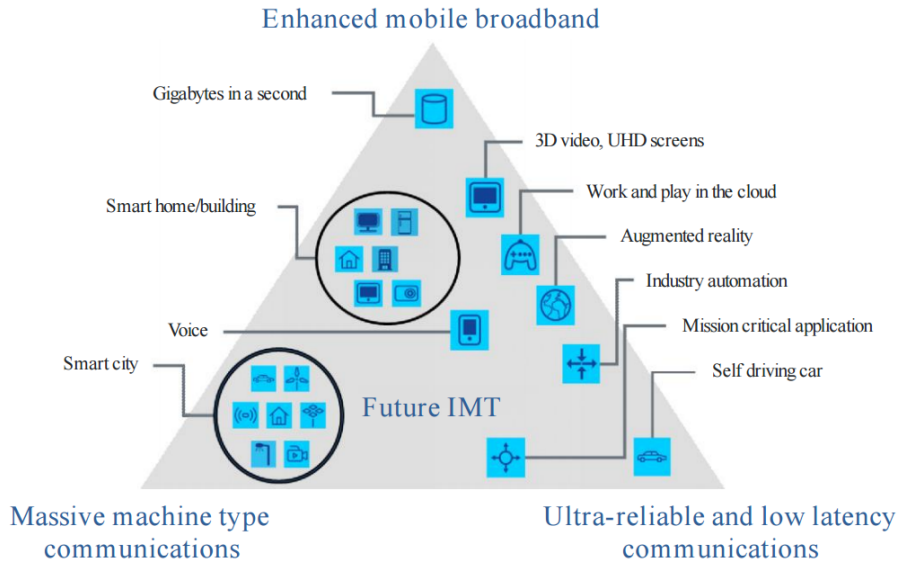

Fig. 1.2 Next generation of wireless communications [2].

alleviating disadvantages of wired systems, challenging stringent requirements of ICS, and overcoming limitations of existing industrial wireless standards.

1.1.1 Disadvantages of Wired Communications

Many of ICS are currently served by wired fieldbus technologies [8,9], e.g., PROFIBUS, PROFINET, EtherCAT, and SERCOS III. Although they provide good performance satisfying requirements of ICS, they have several disadvantages because of their physical attributes. The wired systems have three main drawbacks:

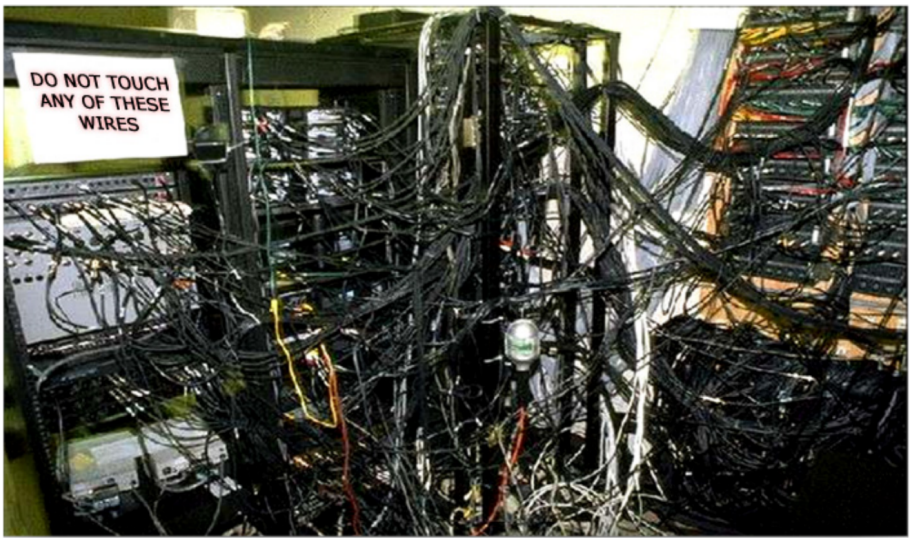

Fig. 1.3 Physical complexity of wiring [3].

- High cost for the installation, wiring, and maintenance of a large number of cables is normally required in factory environments. As illustrated by Fig. 1.3, the wiring can be a mess and complex without a proper management, which requires a high cost. The cost may grow up especially in harsh environments where chemicals, vibrations, or moving parts exist. High levels of protection are required in order to prevent the cables from the potential damages.
- Restricted machine deployment is caused by physical dimensions occupied by the cables. The obstructed physical dimensions make a mobile station not be able to flexibly connect to the communication network. The mobile station needs move within a confined path or area. Moveover, in terms of plant flexibility, a floor plan of the factory cannot be changed frequently to suit with fluctuating manufacturing demands, since the design of an efficient floor plan or production line is also limited by the restricted deployment of the wired communication system.
- Reachability in harsh environments is low. Wired networks cannot be used for connecting machines in dangerous or hazardous environments, e.g., high-temperature and explosive areas.

In turn, a wireless communication system is a promising candidate to reduce the cost and eliminate the physical deployment constraints of wired communication networks in control systems.

Table 1.1 Real-time requirements of applications in ICS [7].

Real-time requirement	Cycle time	Example of use cases
None	>500 ms	Monitoring, Diagnosis
Soft	∼100 ms	Process automation
Hard	∼10 ms	Factory automation
Isochronous	∼1 ms	Motion control

1.1.2 Performance Requirements of Industrial Wireless Communications

Although the wired system has several disadvantages that could limit their usage scenarios and increase the factory costs, they can provide reliable and real-time connection performances, which are important requirements of industrial wireless communications. In general, the performance requirements of communication systems in ICS can be categorized into four factors.

- Real-time capability: Processes and equipment in ICS require data to be transmitted, processed, and responded as instant as possible. The level of the requirement may differ according to usage scenarios of the data [7, 10]. Fig. 1.4 shows the hierarchy pyramid of layers in factory automation. Generally, a lower layer in the hierarchy requires a higher level of real-time capability. Table 1.1 shows real-time requirements in terms of a cycle time with the corresponding applications in ICS. The cycle time represents how frequent of data input/output an application needs to operate properly. Essentially, the lowest layer, where the communications among sensors/actuators ("slaves" below) and controllers take place, needs the cycle time to be as short as few millisecond (ms).

  Furthermore, it is also crucial that a large number of slaves are able to finish the information exchange within a cycle time for a real-time system. For example, closed-loop control systems may consist of several tens to a hundred of slaves operating together [11].

- Reliability: Since communication networks in ICS deals with physical equipment, unreliable communications may lead to a failure of ICS. The effects of the failure can be extremely severe and include production loss, system shutdown, damage to equipment, and even loss of life. Therefore, ICS requires the communication

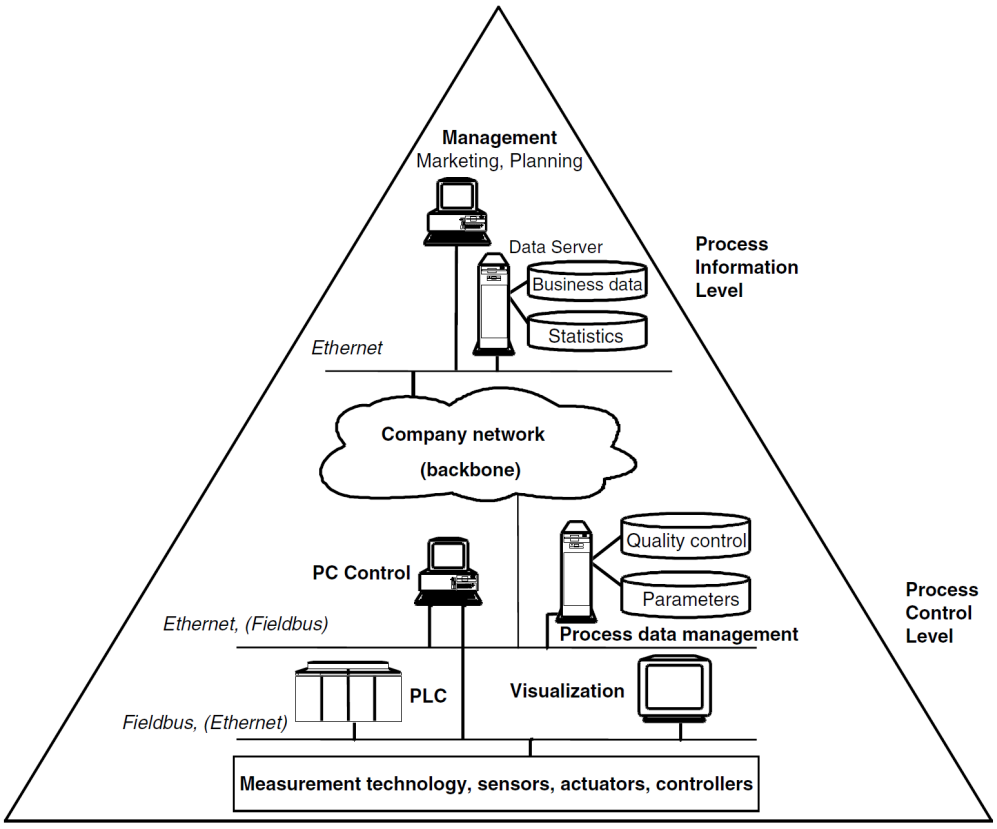

Fig. 1.4 Factory automation hierarchy pyramid [4].

networks to give certain guarantees on success delivery of data. As a numerical example, controls of machine tools, printing machines and packaging machines requires a packet loss rate to be less than 10^{-9} on application level [11].

- Security: Without an exception to a communication network in ICS, security is also an important issue like it is in a traditional network. The security in ICS has strong similarity to that of traditional networks. An attacker may eavesdrop, insert malicious packets, or simply jam the medium to disrupt the network. A number of researches have addressed the security issue by securing a gateway connecting the Internet and the factory network [12] or by employing common techniques, such as encryption and authentication [13].
- Low power consumption: Although the main concern in the design of communication systems for ICS are real-time and reliable communications but not low power consumption, the energy efficiency may become an important issue if the cables for both power and communication are to be completely eliminated. In that case, alternative sources of energy and energy-efficient communication protocols are needed

to be considered. Such energy sources can be via wireless power transmission, energy-harvesting systems, or batteries. On the other hand, several energy-efficient protocols have been researched in the context of wireless sensor networks [14, 15].

The most challenging requirements in shifting from wired to wireless communications in ICS are the real-time capability and reliability. Essentially, this thesis focuses on the improvement of the real-time capability and reliability in industrial wireless communications.

1.1.3 Challenges toward Industrial Wireless Communications

While wireless communication systems have to comply with the stringent requirements, the development of industrial wireless communications remains a big challenge. The limitations are mainly caused by unstable and lossy characteristics of the wireless medium. In this section, we describe characteristics of wireless channels in ICS and current status of wireless technologies designed for ICS.

(a) Industrial Wireless Channels

Industrial environments are often comprised of reflective metallic surfaces, plenty of interference sources, and time-varying factors such as movement of equipment, as illustrated in Fig. 1.5. In principle, the industrial wireless channels can be characterized with similar channel phenomena as modelled in other mobile wireless channels [5,16,17], but they could be in different degrees. The channel characterization of industrial environments such as factories can be referred to [18–20]. The channel phenomena are summarized as follows:

- Large-scale fading: The large-scale fading depicts signal attenuation in large time scale. The change of the large-scale fading is caused by widespread movement and usually can be modelled to be a constant at a specific location over a short period of time. The large-scale fading is expressed by the summation of path loss in a function of a distance and log-normal random variable representing variation among locations in a space. Due to the highly reflective environments in ICS, the degree of signal attenuation with a distance (path loss exponent) is low, compared to normal indoor environments. On the other hand, the variation with the space is large due to the location-specific shadowing effect [18].

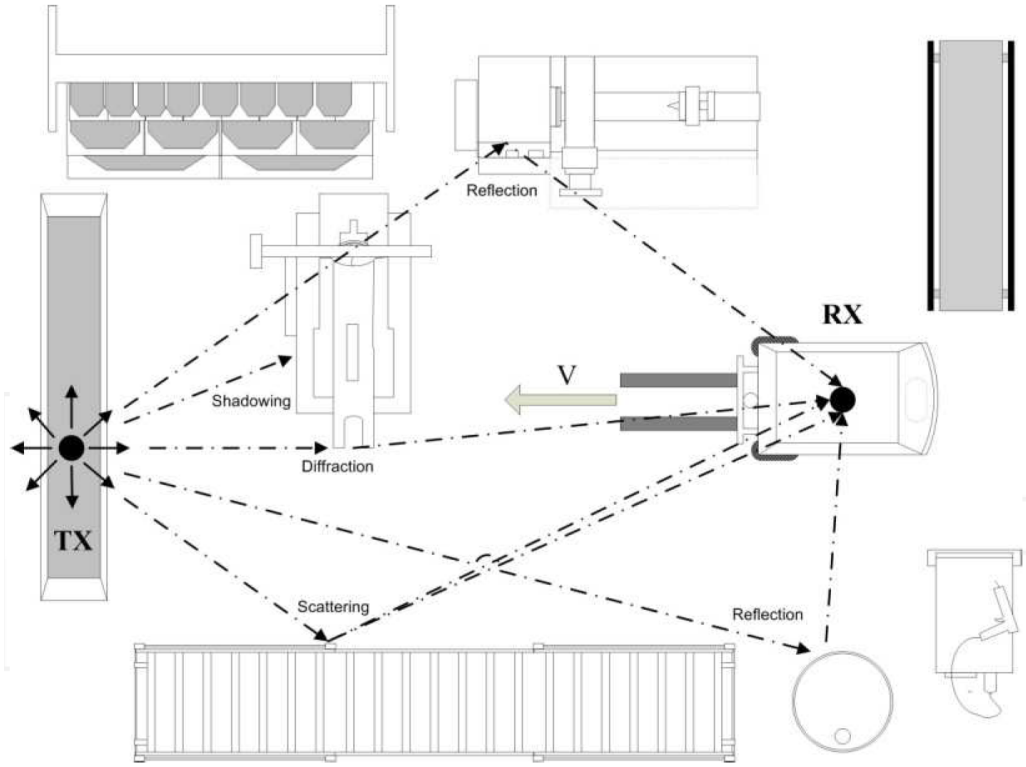

Fig. 1.5 Propagation of electromagnetic waves in an industrial environment [5].

- Small-scale fading: The small-scale fading represents the fast fluctuations of wireless channels. These fast fluctuations are primarily caused by mobility in multipath environments. The small-scale fading can be characterized by two main parameters: multipath delay spread and Doppler frequency. The delay spread and Doppler frequency results in the small-scale fading in frequency and time dimension, respectively.

  The delay spread describes the mean spread of multiple copies of transmitted signals which arrive at a receiver at different times. In time domain aspect, it may result in inter-symbol interference and thus demodulation errors. On the other hand, in the frequency domain, it causes the fluctuation within a frequency band or so called "frequency-selective fading", and hence distorts wideband modulated signals. The opposite phenomenon is called "flat fading". [16] has stated that the delay spread can be as large as 200 ns in industrial environments.

  The Doppler frequency describes the frequency spread which is caused by the mobility of not only a transmitter and a receiver but also surrounding environments. This results in the fast fluctuation of signal amplitudes in the time domain or so called

"fast fading". The opposite phenomenon is called "slow fading", where the channel is rather stable in the time domain. [5] has stated that the Doppler frequency in an environment with fast moving and rotating equipment can be up to 400 Hz.

(b) Current Wireless Technologies

As discussed in Section 1.1.2, the performance requirements of industrial wireless communications are mainly the real-time capability and reliability. However, the current wireless technologies in industrial applications can mostly satisfy only soft real-time requirement (several tens ms of cycle time) and merely satisfy hard real-time requirement (several ms of cycle time). In turn, they can be typically used only in monitoring, diagnosis, and process automation. On the other hand, the applications of factory automation and closed-loop controls like motion control still remains challenging. This causes a delay in the realization of the smart factory and efficient cyber-physical systems. Here, we give examples of current wireless technologies for ICS [21].

- WSAN-FA: WSAN-FA stands for Wireless Sensor Actuator Network for Factory Automation and is based on technologies of WISA (Wireless Interface for Sensors and Actuators) developed by ABB [22]. WSAN-FA is currently an open standardized technology with the lowest achievable cycle time at 2.5 ms, which comes close to the performance requirements for closed-loop applications [11].

  WSAN-FA utilizes the physical layer of Bluetooth (IEEE 802.15.1), which is a standard for building wireless personal area networks. WSAN-FA extends the Bluetooth protocol with an improvement of a frequency hopping algorithm and several additional techniques such as TDMA (time division multiple access), channel blacklisting, and frequency diversity. With 1-byte data frame, WSAN-FA can simultaneously support 32 slaves at 2.5-ms cycle time.

- IWLAN: IWLAN or Industrial Wireless Local Network [23] is a proprietary technology developed by Siemens.

  IWLAN is based on the physical layer of IEEE 802.11n, which is a standard for broadband local area networks. Instead of CSMA/CA (Carrier sense multiple access with collision avoidance), a proprietary polling scheme - a form of point coordination function (PCF) - is utilized for accommodating transmissions of real-time traffics. Although a number of achievable cycle times is not provided in literatures, the cycle time is expected to be similar with IEEE 802.11 with PCF and is approximately several tens of ms.

- WirelessHART: WirelessHART is an open wireless sensor network protocol based on the HART protocol [24] in order to be compatible with existing HART field devices.

  The physical layer of WirelessHART is based on IEEE 802.15.4, which is originally a standard for building low-power personal area networks. WirelessHART adopts multi-hop, time-synchronized, self-organized, and self-healing architecture for realizing industrial wireless sensor networks. However, the real-time performance in terms of the cycle time is still limited at several hundred ms for a network with less than 20 devices.

- ISA100.11a: Similar to WirelessHART, ISA100.11a is also a wireless sensor network protocol based the physical layer of IEEE 802.15.4 [25, 26]. ISA100.11a is developed by the International Society of Automation (ISA). The real-time capability of ISA100.11a is also akin to that of WirelessHart, i.e., the cycle time in the order of hundred ms.

This section has shown that there are still challenges toward industrial wireless communications. In particular, current wireless standards are limited to satisfy the real-time and reliability requirements due to their constraints in physical-layer designs, which are originally intended for traditional wireless applications such as environmental monitoring, file transfer in mobile phones, and high-bit-rate Internet.

Contributions

In a nutshell, this thesis aims to improve the real-time capability and the reliability via physical-layer approaches and has the following contributions.

- This thesis studies the reduction of two physical-layer overheads including preamble transmission and transmit cooperation by considering characteristics and requirements of ICS.
- This thesis proposes a novel design of short OFDM preambles, which can utilize not only frequency but also time correlated channels. The improvement of the real-time capability in correlated channels is verified.
- This thesis proposes symbol-level packet combining using RSSI to make naturally real-time concurrent transmission (CT) become reliable. The reliability performance in CT environments is evaluated.

1.2 Thesis Organization

This thesis contains five chapters. It is organized as follows:

Chapter 1: Introduction

This chapter describes the background and motivations of this thesis to study real-time and reliable industrial wireless communication via physical-layer approaches.

Chapter 2: Real-time and Reliable Industrial Wireless Communications

In this chapter, the design overview of industrial wireless communications is discussed through the survey of related works. In addition to the existing techniques, the extended studies on physical-layer approaches are required to further improve the real-time and reliable wireless communications and are elaborated in this chapter. In particular, we conceptually explain two physical-layer approaches: 1) shortening preamble transmission and 2) reducing transmit cooperation using concurrent transmission.

Chapter 3: Subcarrier-selectable Short Preambles in OFDM systems

This chapter proposes subcarrier-selectable short preambles in order to improve real-time capability. The method for preamble shortening and preamble recovery as well as the corresponding channel estimation are discussed. The improvement in real-time capability is verified by computer simulations.

Chapter 4: Symbol-level Packet Combining using RSSI

This chapter presents symbol-level packet combining using RSSI in order to improve reliability of naturally real-time CT techniques. Important parameters of the method are studies in CT environments. The evaluation by both simulations and experiments verifies the reliability improvement.

Chapter 5: Conclusions

This chapter summarizes the contributions of this thesis as well as suggestions for future improvements.

Chapter 2

Real-time and Reliable Industrial Wireless Communications

In this chapter, we discuss wireless communition techniques from the real-time and reliable aspects. We first provide a design overview based on the survey on wireless communication researches in ICS. After that, we discuss our physical-layer approaches toward real-time and reliable wireless communications. In particular, instead of MAC or network-layer approaches, we focus on an improvement at the physical layer by shortening preamble transmission and reducing transmit cooperation in order to achieve real-time and reliable wireless systems.

2.1 Design Overview

In order to comply to the challenging real-time requirements of ICS in the harsh wireless channels, a number of researches targeting sub-10ms cycle time have come up with strategies to enhance the performance. In this section, we will discuss several technical components required in the design of industrial wireless communications from two points of view: real-time capability and reliability. Fig. 2.1 gives an overview on the important technical components in the design of industrial wireless communications.

- **Real-time capability**:

  (1) Single-hop topology

  A simple single-hop is commonly adopted in order to eliminate routing and forwarding delay [22, 27–31]. Fig. 2.2 illustrates a simple single-hop star topology, in which a master (e.g., a controller) acts as a base station and performs an information exchange with each slave (e.g., a sensor and an actuator) individually. Due to the pre-determined transmission path and the single-hop property, the time required for a routing algorithm and data forwarding can be eliminated.

  (2) Deterministic channel access

  Most researches for improving the real-time capability are based on techniques in MAC layer. The MAC-layer techniques are needed to provide low latency and deterministic channel access timing in order to guarantee good real-time capability. The contention-based techniques such as carrier sense multiple access (CSMA) are typically not adopted in a network designed for ICS. Techniques proposed for applying in ICS can categorized into three main groups: token passing, polling, and time division multiple access (TDMA).

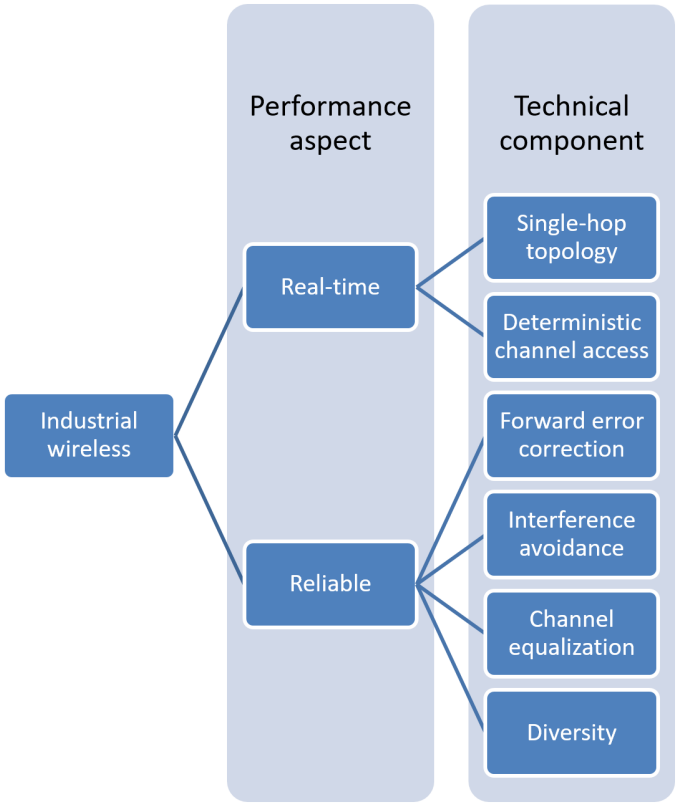

Fig. 2.1 Important mechanisms for real-time and reliable industrial wireless.

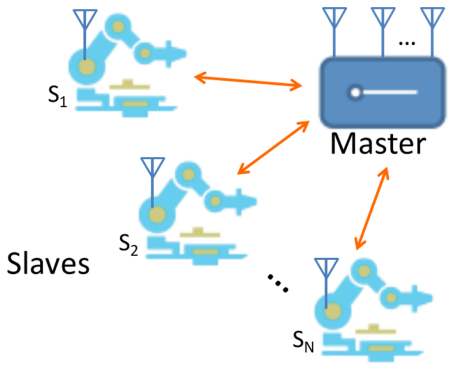

Fig. 2.2 Simple single-hop star topology.

[32] has obtained determinism of channel utilization to some extent by using token-passing protocol to an industrial network. However, the token lost can be problematic even with a token recovery self-healing mechanism.

Polling-based MAC protocols is more centralized protocol, where a network master controls the channel access by inquiring slaves to transmit or receive data. This

concept has been researched based on IEEE 802.11 and Bluetooth in [33, 34].

TDMA-based protocols divide the channel resource into timeslots and assigns them to slaves to access the channel with different timeslots. TDMA has been studied intensively in well-known physical-layer IEEE standards such as IEEE 802.15.1 [35], IEEE 802.15.4 [36–38], and IEEE 802.11 [27, 28]. In particular, Wei et al. [27] has managed to achieve 1-ms cycle time in a network with few devices. Moreover, the communication system has been practically implemented in a gait rehabilitation system [39].

Several variations of TDMA-based protocols have been also proposed. [40] have introduced the combination of TDMA with frequency hopping for low-power wireless sensor networks. The combination of TDMA and CSMA has been studied based on IEEE 802.15.4 [41]. Lastly, considering the shared wireless medium, Lam et al. [30] have proposed another variation of TDMA and named it as packet division multiple access. The similar idea is also adopted by Weiner et al. [29]. The key idea is to transmit a long downlink packet, which can be heard by every slave and only a part of the packet belongs to each slave. That is, the downlink packet header is shared by all slaves and the long packet payload is TDMA-like divided to each slave.

Essentially, the real-time requirement of the factory automation and closed-loop control (few ms) in ICS however cannot be satisfied by those works. Unlike the aforementioned previous works, this thesis therefore takes a physical-layer approach to improve the real-time capability. In particular, we will be looking at shortening preamble transmission (in Section 2.2.1) and reducing transmit cooperation (in Section 2.2.2).

- **Reliability**:

  (1) Forward error correction

  A traditional method to deal with noisy wireless channels is to perform error detection or error correction by adding redundancy to transmitted data. Considering the real-time constraint, [42] have proposed deadline dependent coding, which adaptively adjusts the code rate to achieve optimal performance within the given deadline. However, the error correcting codes may not be able to deal with burst errors, which may occur due to external interference and channel fading.

  (2) Interference avoidance

The external interference can be avoided by adopting frequency hopping and channel blacklisting [22]. Frequency hopping is a spread spectrum technique which make a narrow-band transmission rapidly switch a carrier frequency in order to avoid burst errors caused by an interference at one specific frequency. Channel blacklisting is a mechanism to avoid using some channels according to their performance. These mechanisms are essential when multiple networks share common frequency bands and geolocation.

(3) Channel equalization

Another cause of erroneous communications is channel distortion, which can be alleviated by performing channel equalization. The channel equalization method is to cancel out an adverse effect of the wireless channels. Several works have adopted the method in industrial wireless communications [27–31]; however, its adverse effect on the real-time capability has not been discussed yet and we will discuss this in Section 2.2.

(4) Diversity

Another concept for coping with channel errors is diversity. The diversity generally describes the communication over different independent channels in order to increase the probability of successful communication. The diversity can be obtained in many forms including time, spatial, and frequency diversity.

The time diversity is the simplest type and can be simply implemented by performing retransmissions as well as acknowledgements. However, the retransmission incurs longer transmission time, increased latency, and degraded real-time performance. Blind et al. have studied the trade-off between the real-time capability and the reliability due to the retransmission [43].

The frequency diversity trades spectrum bandwidth with the reliability. It can be implemented in forms of simultaneous transmissions in multiple channels or single transmission with frequency hopping. WISA [22, 35] has adopted both forms of frequency diversity to improve packet reception rate and also avoid interferences from other systems and industrial electromagnetic sources.

The spatial diversity can be obtained by utilizing multiple antennas in a standalone device or by allowing multiple devices to participate in the communication. [29, 31, 44, 45] has studied the use of spatial diversity in wireless industrial networks. Although they have proved that spatial diversity is essential technique to

obtain satisfactory reliability in ICS, none of them has thoroughly considered the real-time capability aspect when applying multiple antenna systems. This will be further discussed in Section 2.2.2 regarding a real-time transmit diversity technique.

To summarize the design of industrial wireless communications, while combination of mechanisms are required to achieve the satisfied reliability, additional methods for improving in real-time capability are still required. Table 2.1 summarizes the related works targeting sub-10ms cycle time in industrial wireless communications as references.

Table 2.1 Summary of related works targeting sub-10ms cycle time in industrial wireless communications.

	WISA [22]	**RT-WiFi [27]**	**MAC for real-time [28]**		**Wireless system design [29]**	**Industrial WLAN [30]**		**5G URLLC [31]**
Study method.	Experiment	Experiment	Experiment		Simulation	Simulation		Simulation
Based standard	Bluetooth	802.11n	802.11b		802.11ac/LTE	802.11ac		**5G**
Modulation	GFSK	OFDM	DSSS		OFDM	OFDM		OFDM
Coding	Repetition 1/3	Convolution 1/2	None		1/5	Convolution 1/2		Convolution 1/2
Equalization	No	Yes	Yes		Yes	Yes		Yes
Topology	Star	Star	Star		Star	Star		Star
Channel access	TDMA/FDD	TDMA/TDD	Polling	TDMA/ TDD	Improved TDMA /TDD	Polling	DL-Improved. TDMA, UL-FDMA (TDD)	OFDMA
Diversity	4 Freq, Ant	None	None		2 Freq, 4 Ant	None		~16 Ant
Retransmission	Yes	Yes	Yes		Yes	Yes		Yes
Interference avoidance	FH, Blacklist	None	None		None	None		-
@ SNR level	n/a	n/a	n/a		10 dB	16 dB		11 dB
Bandwidth	80 MHz	20 MHz	22 MHz		20 MHz	80 MHz		1.5 MHz
Data size	1 byte	200 bytes	40 bytes		20 bytes	32 bytes		10-20 bytes
Packet Error rate	1E-9	1E-3	1E-2		1E-8	1E-3		1E-9
Cycle time	2 ms	4 ms	25 ms	8 ms	2 ms	11.2 ms	2.4 ms	Latency 1ms
# devices	30	3	20		20	32		-

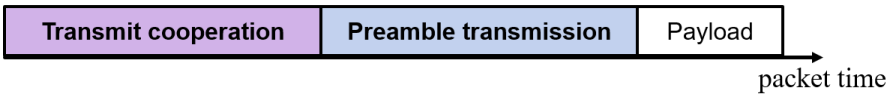

Fig. 2.3 Physical-layer transmission overhead.

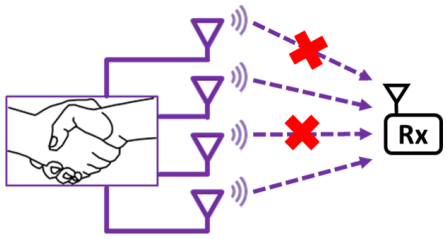

Fig. 2.4 Concept of transmit diversity.

2.2 Physical-layer Approaches

In this section, we explain the effect of physical-layer transmission overheads to the real-time capability and the reliability of wireless systems, and also methods to reduce the overheads in order to further improve the real-time capability. The transmission overhead is usually put before the transmission of informative data payload. Especially in ICS, it is essential to reduce this uninformative overhead that limit the real-time capability as the data exchanged between controllers and devices are on the scale of a few bytes, as depicted in Fig. 2.3. The overhead in physical layer can be grouped into two categories according to its functions.

The first transmission overhead is for transmitter-side cooperation. The cooperation is performed among transmitters such that the transmit diversity is obtained for better signal reception at a receiver. For example, when some of wireless links are not in good conditions such as when line-of-sight paths are blocked or shadowed by a moving machine, a good-quality link still exists and yields successful transmissions as shown in Fig. 2.4.

Another transmission overhead is for preamble transmission. A preamble is a reference signal known to both a transmitter and receivers. It is used for learning the state of channels and the information obtained at a receiver is called channel state information (CSI). The CSI is used for performing equalization in order to eliminate adverse effect of the wireless channel, as illustrated in Fig. 2.5. For example, this CSI is necessary in multi-carrier OFDM systems to compensate the effect of frequency-selective fading.

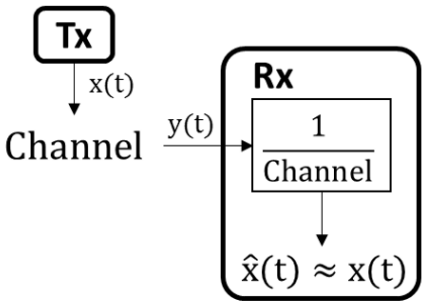

Fig. 2.5 Concept of equalization.

2.2.1 Shortening Preamble Transmission

Although preamble transmission should be reduced as much as possible to improve the real-time capability, it should be noted that reducing the preamble transmission could hurt the receiver performance. Thus, we need to reduce the preamble transmission while guaranteeing satisfactory reliability. Instead of totally removing the preambles, this thesis focuses on shortening the length of a preamble by exploiting time correlation among frequent transmissions in ICS to maintain the reliability. This section explains two general methods for shortening the preamble transmission.

One may consider totally removing the preamble, and adopt a blind estimation scheme or a scattered-pilot scheme. However, they cannot be adopted in ICS context because these schemes assume long packet transmissions in order to sufficiently collect statistical information for performing necessary equalization and synchronization. In [46, 47], the blind estimation schemes require the packet length to be at least several tens bytes to obtain reliable demodulation performance. On the other hand, the scattered-pilot scheme, e.g. [48], either needs similar long packet transmission or requires dense pilot signals inserted into data signals. The dense pilot pattern not only degrades the spectral efficiency, but also cannot fully serve all functions of preambles such as synchronization.

This thesis takes another class of methods, which shortens the length of the preamble itself. By doing this, the necessary information for equalization and synchronization can be estimated in short period of time. However, due to the shorter length, the estimated information is only partial to that of a full-length preamble, and this may degrade the reliability performance.

A key point of our short preamble design is to exploit frequency transmissions in ICS. Fig. 2.6 compares the packet traffic of wireless ICS and traditional wireless systems. Due

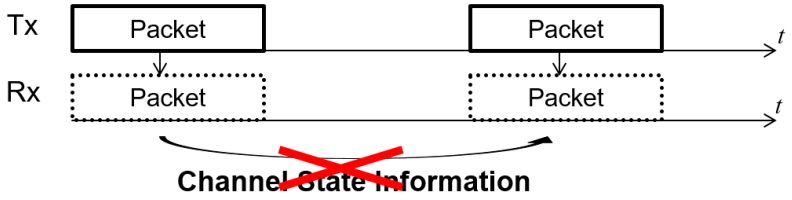

(a) Traditional wireless systems.

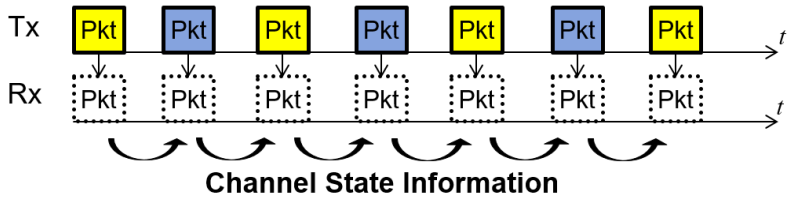

(b) Wireless ICS.

Fig. 2.6 Frequent packet transmission in ICS.

to the frequent transmissions, the inter-packet time correlation exists and can be adopted for assisting channel estimation and synchronization across the packets.

Chapter 3 discusses a short preamble called "subcarrier-*selectable* short preamble", which allows the use of the time correlation in preamble-aided channel estimation. The selectability of preamble patterns allows the short preambles to obtain different sets of information, which can be shared across packets. The preamble patterns are then changed every packet transmission in order to obtain a complete set of information within a short period of time.

2.2.2 Reducing Transmit Cooperation

While maintaining the reliability, it is necessary to reduce transmit cooperation in improve the real-time capability. This section introduces a real-time transmit cooperation schemes called "concurrent transmission (CT)".

First of all, an overview of transmit cooperation is given. Cooperation of multiple transmitters is adopted to improve the reliability with the merit of transmit diversity. As depicted in Fig. 2.7, the cooperation is performed in order to guarantee constructive combination of signals at a receiver. The cooperation can be in terms of timing t, frequency f, phase ϕ, and channel h.

Different levels of transmit cooperation yield different real-time capability. The more cooperation needed will result in worse real-time. The use of multiple transmit antennas

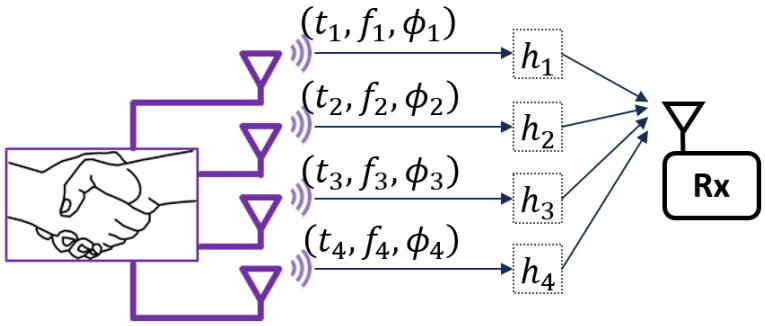

Fig. 2.7 Priori information in transmit cooperation.

Table 2.2 Long block length and low code rate of STBC with large numbers of antennas.

# antennas	# symbols	Block length	Rate
2	2	2	1
4	6	8	$\frac{3}{4}$
8	70	112	$\frac{5}{8}$
16	12870	22880	$\frac{9}{16}$

to perform beamforming as studied by [49] or requires high level of cooperation including the timing, frequency, phase as well as channel sounding in order to guarantee perfect constructive combination of signals at the receiver.

Without the necessity of channel sounding, an orthogonal precoding scheme such as space-time block coding (STBC) [50, 51] still require proper cooperation in timing, frequency and phase in order to realize analogously orthogonal channels, where the signals arriving at the receiver do not interfere destructively to each other. Moreover, a limited number of antennas can be applied because of two reasons. The first one is that the block length and the computation complexity grows enormously with a large number of antennas as demonstrated in Table 2.2 [51]. The second reason is that the code rate drops with more antennas. Therefore, STBC with a large number of antennas is not applicable in ICS.

Due to the stringent real-time requirements of ICS, this thesis focuses on concurrent transmission (CT), which performs transmissions of an identical baseband signal from several sources simultaneously. Notably, CT requires only cooperation in timing. CT, has been recently adopted in both single-hop distributed antenna systems [52] and multi-hop wireless sensor networks [53, 54] because of its simplicity and low latency. [52] has shown that CT with a large number of antennas has a good potential in ICS.

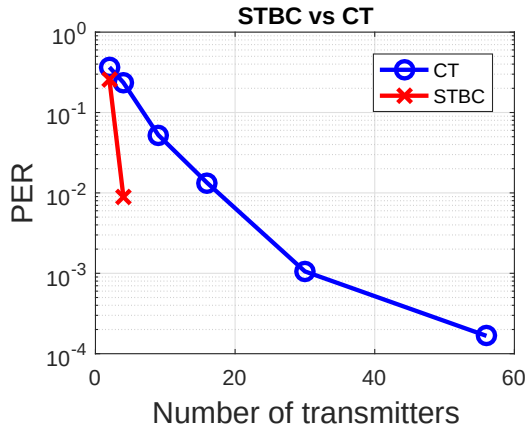

Fig. 2.8 STBC (ideal frequency and phase synchronizations) vs CT.

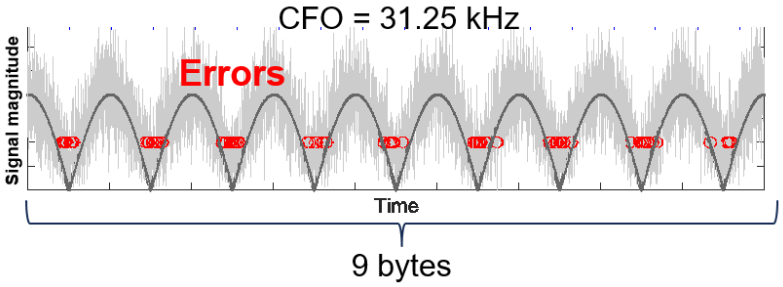

Fig. 2.9 Frequency errors caused by beating in IEEE 802.15.4 [6].

As a comparison to STBC, Fig. 2.8 shows that the reliability of the practical 4-antenna STBC system with ideal frequency and phase synchronizations falls behind that of the CT system with a sufficient number of antennas in a large factory. In practical aspect, this comparison suggests that investing in more number of antennas in the CT system may be more worthwhile than putting money in a radio-over-fiber system for perfect synchronizations in the unscalable STBC system.

In the physical-layer context, however, CT does not guarantee non-destructive signal combination which is still an issue that has not been addressed. When phase offset between signals exists, a complete signal cancellation occurs and causes dark spots at some of locations as studied in a physics' double slit experiment. With the presence of carrier frequency offsets (CFO) among transmitters, the phase of received signal continuously rotates and makes a periodic constructive and destructive combination of signals. This phenomenon is called "beating". This beat problem leads to frequency errors in a packet as shown by Fig. 2.9.

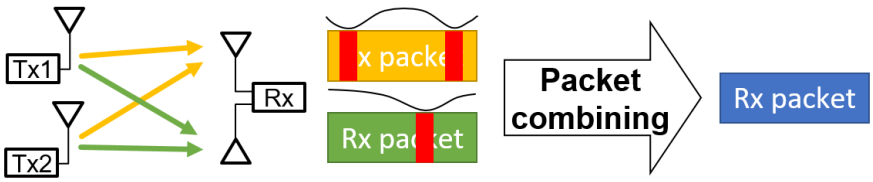

Fig. 2.10 Receive diversity for alleviating a beat problem.

In view of baseband signals, this small differences of carrier frequencies leads to fading-like signal amplitude fluctuation which leads to SNR degradation in the deep faded parts of the signal [6, 55, 56]. Compared to the fading caused by Doppler effect of mobility, the beat problem causes an extremely fast fading.

To cope with the beat problem, Chapter 4 introduces symbol-level packet combining using RSSI. As depicted by Fig. 2.10, the scheme combines multiple packets obtained by multiple receive antennas (receive diversity) at symbol level and use RSSI (received signal strength indicator) as a fading indicator. This approach does not incur additional transmit overhead, which is critical in ICS, and potentially enhances the reliability of CT-based transmit cooperation.

2.3 Summary

This section describes a design overview based on survey on related works and our approaches for realizing real-time and reliable wireless communications in ICS. In view of real-time capability, unlike the previous works, we focus on two physical-layer approaches: shortening preamble transmission and reducing transmit cooperation. In the former study, the time correlation among frequent transmissions in ICS is exploited to shorten the preamble length while maintain satisfactory reliability. In the latter one, we adopt CT as a transmit cooperation scheme for the sake of real-time capability. A packet combining is proposed to solve the beat problem and improve the reliability of CT. The detailed explanations, implementations and evaluations of both methods are further discussed in Chapter 3 and 4, respectively. Their relationship is illustrated by Fig. 2.11.

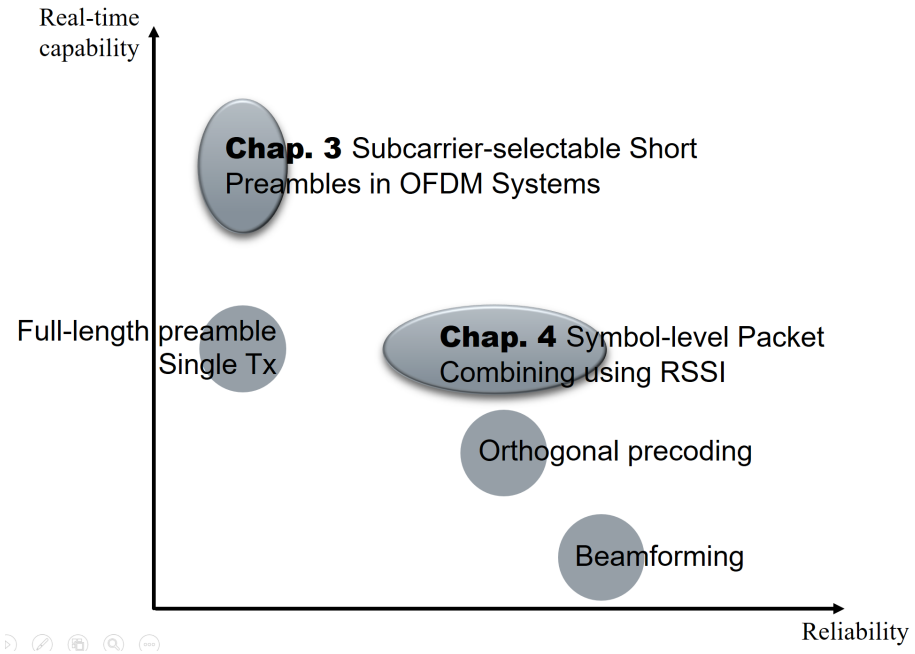

Fig. 2.11 Relationship between Chapter 3 and 4.

Chapter 3

Subcarrier-selectable Short Preambles in OFDM Systems

3.1 Background

This chapter aims to shorten the preamble transmission time of an orthogonal frequency division multiplexing (OFDM) system in order to improve real-time capability. Most closed-loop control applications such as motion control of machine tools [11] needs extremely low control cycle time in the order of few milliseconds to operate robustly. In addition, a centralized controller may also need to communicate with a large number (10 to 100) of slaves, as shown in Fig. 3.1, within such a limited cycle time. To satisfy these stringent requirements, an OFDM system is considered since it provides promisingly high throughput and supports low-complexity frequency-domain channel equalization.

This chapter describes short preambles for OFDM channel estimation. The overview of this chapter is given as follows.

To shorten the transmission time of the preamble, previous works have considered adopting either time-domain or frequency-domain channel correlation for channel estimation. However, this results in poor performance in fast fading channels and frequency-selective fading channels, respectively.

In this chapter, we propose a subcarrier-selectable short preamble (SSSP) by introducing selectability to subcarrier sampling patterns, in such a way that it can provide full sampling coverage of all subcarriers with only several preamble transmissions. The preamble shortening method performed at a transmitter as well as the preamble recovery method performed at a receiver are described accordingly.

In addition, we introduce adaptability to a channel estimation algorithm for the SSSP so that it conforms to both fast and frequency-selective channels. The proposed algorithm adopts the correlation of two preambles to determine the degree of channel variation in time, and select the operation for channel estimation of non-selected subcarriers.

The proposed short preamble and the channel estimation algorithm are evaluated by computer simulation based on IEEE 802.11 OFDM specifications [57]. Simulation results validate the feasibility of the proposed method in terms of the reliability and real-time capability. In particular, the SSSP scheme shows its advantage in flexibility as it can provide a low error rate and short communication time in various channel conditions.

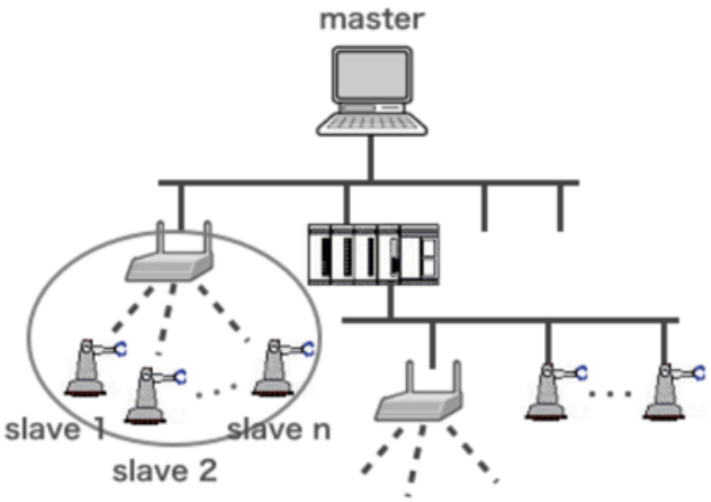

Fig. 3.1 Communication topology of closed-loop control in ICS.

3.2 Related Work

The great advantages that OFDM systems possess, such as high spectral efficiency and robustness to the inter-symbol interference (ISI) resulted from multipath channels, are desired for robust communications in ICS. To apply a packet-based OFDM system in an unlicensed band, preambles are needed for synchronizations, channel estimation, and equalization.

Although there are plenty of works studying joint time-frequency channel estimation in *pilot*-aided systems [48], few works have considered it in the context of *preamble*-aided systems. Since the pilot-aided systems still needs extra preambles for synchronization or relies on long transmission for blind or cyclic-prefix(CP)-based synchronizations [58], this work focuses on the preamble-aided schemes for real-time ICS.

Regarding channel estimation, existing preamble schemes are limited to either (1) time-direction extrapolation (TDE) or (2) frequency-direction interpolation (FDI) of wireless channels and are thus impaired in some wireless channel conditions.

(1) TDE: A transmitter could periodically omit the preamble transmission in some packets to reduce the preamble transmission overhead. Then, receivers buffer the channel estimation results in the previous packets and use TDE to predict the channel for the packets without the preamble. We refer to this method as intermittent full-length preambles (IFP). Compared to the traditional continual preambles, the reliability is similar in slow fading channels, but degrades significantly in fast fading ones.

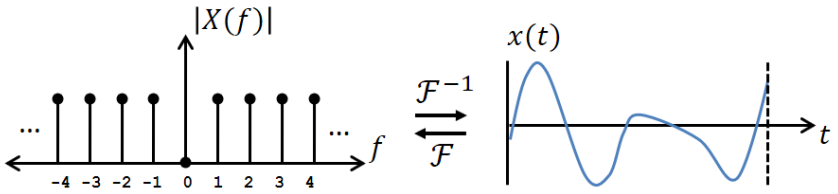

(a) Full-length preamble.

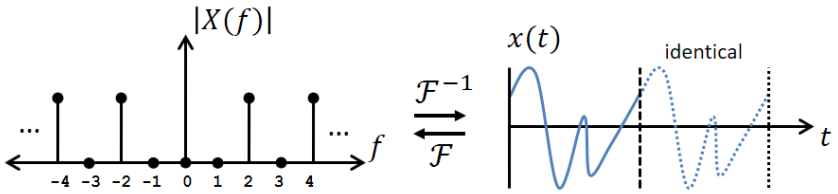

(b) Subcarrier-fixed short preamble (SFSP).

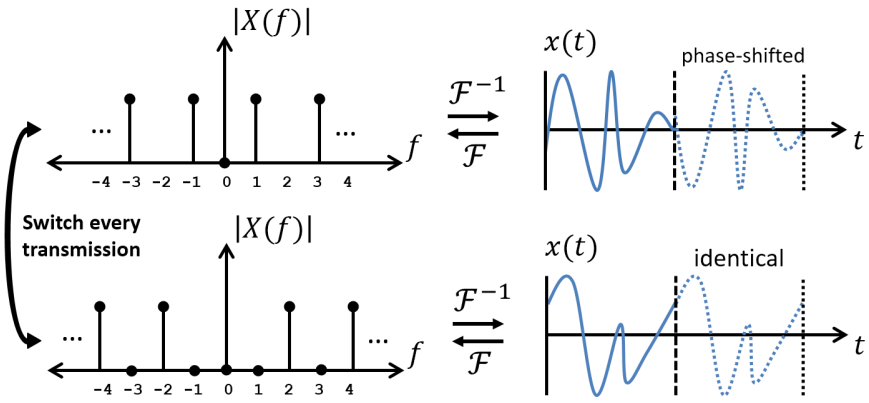

(c) Subcarrier-selectable short preamble (SSSP).

Fig. 3.2 Preamble shortening by subcarrier sampling.

(2) FDI: Another way of reducing the preamble transmission overhead is to shorten the preambles themselves by down-sampling the frequency domain subcarriers, i.e., by allocating the preamble pattern only on selected subcarriers, while keeping the others nulled. As an example illustrated in Fig. 3.2 (a) and 3.2 (b), if we select only the even-indexed subcarriers, the preamble signal in time domain will consist of two replicas aligned in series [59]. Then, the length of the preamble can be shortened by keeping only the first replica for the preamble transmission and removing the redundant replicas. Previous works [60,61] have considered repetitive short preamble signals formed by selecting a fixed set of subcarriers, thus we refer to it as subcarrier-*fixed* short preambles (SFSP). Since the channel of non-sampled subcarriers can only be estimated by FDI of the sampled ones, it performs poorly in multipath frequency-selective fading.

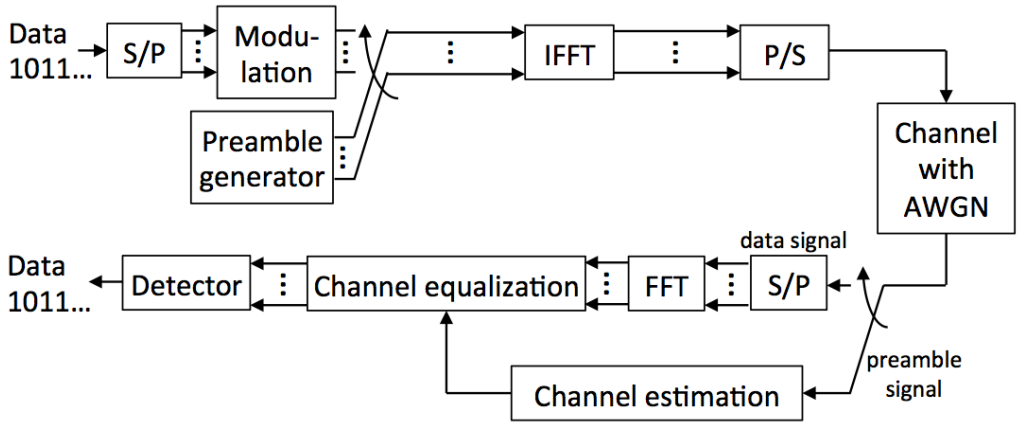

Fig. 3.3 OFDM system with full-length preambles.

In the next section, we describe a short preamble that is able to exploit not only FDI but also TDE for channel estimation by introducing *selectability* to the subcarrier sampling patterns. Instead of being fixed to a specific set of subcarriers, the subcarrier sampling set alters in every transmission, and therefore provides direct measurement to all subcarriers in the OFDM system, as illustrated in Fig. 3.2 (c).

In ICS, the preambles are also utilized for performing timing and frequency synchronization. The correlation-based methods using multiple preamble symbols in [60, 61] are fully compatible with the proposed SSSP and the synchronization performance has been already evaluated. Note that CP-based synchronizations, such as [62, 63], suffer from the inter-symbol interference (ISI) problem in multipath environments and require long acquisition time to improve the accuracy [58], and hence do not suit to ICS.

3.3 Subcarrier-selectable Short Preamble

In this section, we describe an OFDM system using short preambles schemes including both the SFSP and the proposed SSSP. As fundamental, we first describe a conventional preamble-aided OFDM System and a naive method for reducing preamble transmission by intermittently omitting preambles. Then, we discuss our proposed scheme regarding preamble shortening and preamble recovery. Note that since the SFSP is a special case of the SSSP, it will be discussed in terms of the SSSP.

Preamble-aided OFDM System

Consider a preamble-aided OFDM system with M subcarriers illustrated in Fig. 3.3. A preamble symbol is transmitted before the data symbols at the beginning of a packet.

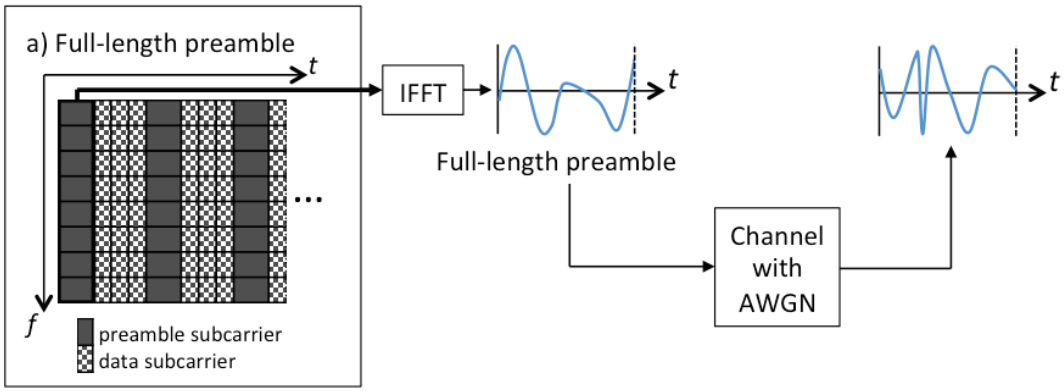

Fig. 3.4 Full-length preambles.

After being transmitted through a wireless fading channel and received by the receiver, the preamble symbol and the data symbols are separated. The frequency-domain channel estimation for each subcarrier is then obtained by dividing the frequency-domain response of the received preamble symbols with the known preamble pattern. By utilizing the channel estimation results, the data symbols are equalized by frequency-domain one-tap equalizers, and then demodulated to obtain the data bit stream.

Traditionally, the preamble transmission occupies all M OFDM subcarriers to allow channel estimation of all subcarriers, as shown by the time-frequency grid in Fig. 3.4. Let us denote the conventional full-length preamble pattern in frequency domain as

$$\underline{\mathbf{P}}_f = (P_m)_{1\times M}, \tag{3.1}$$

where the subcarrier index m satisfies $m \in \mathbb{Z}$ and $-\frac{M}{2} \leqslant m \leqslant \frac{M}{2}$, and P_m is the *non-zero* training signal except zero DC tone ($P_0 = 0$). After inserting guard band subcarriers to $\underline{\mathbf{P}}_f$, we obtain time samples $\underline{\mathbf{p}}_f = (p_n)_{1\times N}$ of a full-length preamble symbol by performing N-point inverse fast Fourier transform (FFT), where

$$p_n = \frac{1}{N} \sum_{m=-\frac{M}{2}}^{\frac{M}{2}} P_m \exp(j2\pi \frac{nm}{N}). \tag{3.2}$$

By using the full-length preamble, channel estimation $\hat{H}_m$ among communication cycles is performed independently by using the received preamble symbol P'_m and the known preamble pattern P_m. In particular, we consider least-square (LS) estimation algorithm for calculating channel estimation $\hat{H}_m$ as

$$\hat{H}_m = \frac{P'_m}{P_m}. \tag{3.3}$$

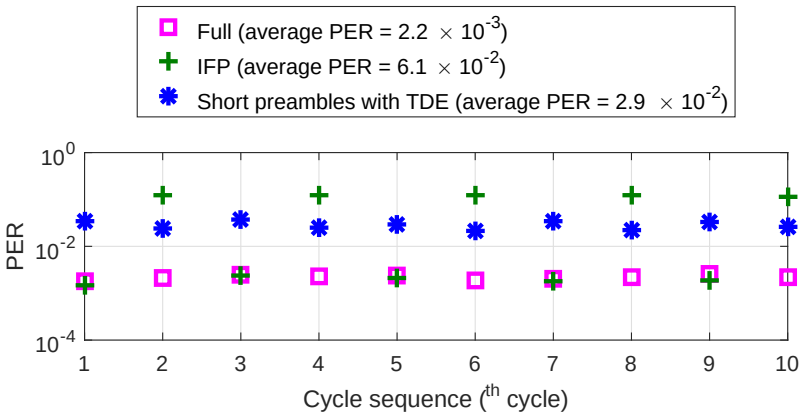

Fig. 3.5 Fluctuating PER of the IFP scheme among communication cycles.

Intermittent Full-Length Preamble

Methods for reducing preamble transmission time can be categorized into 2 main approaches: omitting some preamble transmissions and shortening a preamble length. We refer to them as intermittent full-length preambles (IFP) and short preambles, respectively. In this section, we describe the concept, a channel estimation method and a drawback of the IFP scheme.

By taking advantage of the short and frequent transmission in ICS, the IFP scheme makes a transmitter simply omit some preamble transmissions, in other words, intermittently transmit preambles. For example, a preamble is transmitted in every other packet, hence the preamble transmission time is reduced by half, i.e., $C = 2$ where C is the reduction rate of preamble transmission.

At a receiver, the channel estimation of the packet without the preamble adopts a TDE algorithm to predict the channel based on the previous packet with the preamble. That is, $\hat{H}_m$ of the IFP scheme can be written as

$$\text{packet w/ preamble}: \quad \hat{H}_m = \frac{P'_m}{P_m}, \tag{3.4}$$

$$\text{packet w/o preamble}: \quad \hat{H}_m = \hat{H}_{m,\text{time}}, \tag{3.5}$$

where $\hat{H}_{m,\text{time}}$ is the estimate obtained by TDE.

Since the packet using outdated preambles is greatly affected by the channel variation, the IFP scheme degrades significantly in fast fading channels and also causes fluctuating

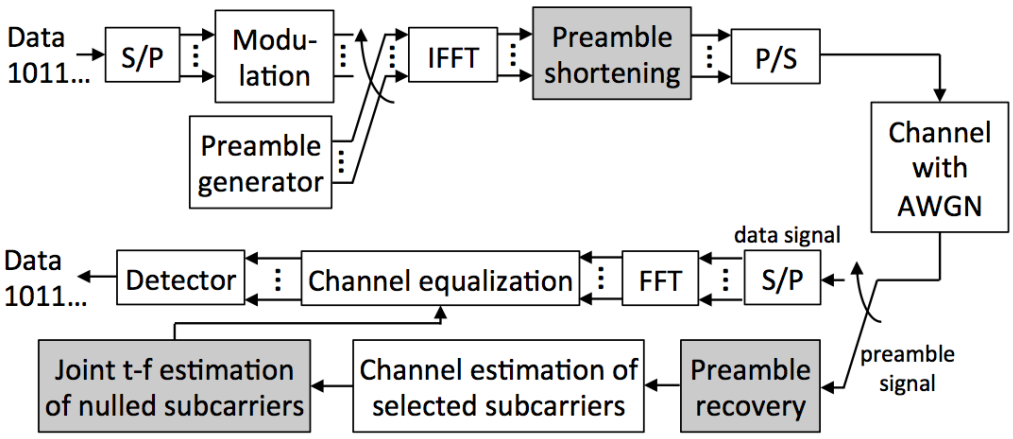

Fig. 3.6 OFDM system with SSSP.

packet error rate (PER) as illustrated in Fig. 3.5 [*1]. Compared to the continual full-length preamble, the PER of the IFP scheme might be worse by two orders in the cycle using outdated preambles.

3.3.1 Preamble Shortening

An OFDM system using the SSSP is shown in Fig. 3.6. In addition to the modules used in the conventional OFDM system with full-length preambles (marked as white blocks), additional modules (marked as shaded blocks) are required by the SSSP, including preamble shortening, preamble recovery, and channel estimation for the SSSP which performs adaptive joint time-frequency channel estimation for nulled subcarriers.

To obtain the frequency-domain preamble pattern of the SSSP, we deliberately select one subcarrier out of every C subcarriers to carry a preamble pattern as shown by the time-frequency grid in Fig. 3.7. Specifically, at an arbitrary i^{th} packet transmission, the frequency-domain SSSP pattern $\underline{\mathbf{P}}_{s,i}$ is written as

$$\underline{\mathbf{P}}_{s,i} = [P_{-\frac{M}{2}+\alpha}, P_{-\frac{M}{2}+\alpha+C}, P_{-\frac{M}{2}+\alpha+2C}, \cdots], \tag{3.6}$$

where $\underline{\mathbf{P}}_{s,i} \subset \underline{\mathbf{P}}_f$ and contains non-zero training signals, and $\alpha \in \{0, 1, ..., C-1\}$. By selecting different α, a total of C sets of the SSSP can be obtained. Therefore, all subcarriers can be sampled after at least C packet transmissions by sequentially adopting the

[*1] Simulated with $C = 2$, $f_{D,max} \cdot T_p = 100$ Hz $\cdot$ ms, channel HiperLAN/2 model C, CNR = 15 dB, and the parameters in Table 3.1

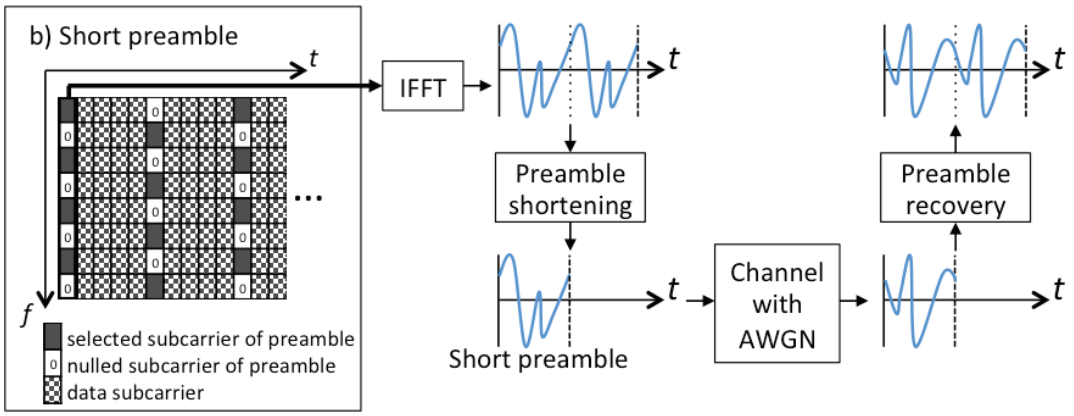

Fig. 3.7 SSSP with $C = 2$ (half-length preambles).

SSSP of different α. As a special case of the SSSP, the SFSP can be obtained when α is always set to 0.

To obtain time samples of an SSSP symbol, there are two implementations: using N-point FFT and using $\frac{N}{C}$-point shifted discrete Fourier transform (SDFT). They provides an identical outcome and their overviews are illustrated in Fig. 3.8.

N-point FFT: After performing the subcarrier selection in Eq. (3.6), the non-selected subcarriers are all nulled to be zeros. By using N-point inverse FFT, the time samples will consist of contiguous phase-rotated replicas. Specifically, the repeating time samples with phase shift can be written as

$$\underline{\mathbf{p}}_{f,i} = [\underline{\mathbf{p}}_{s,i}, \varphi_1 \underline{\mathbf{p}}_{s,i}, \varphi_2 \underline{\mathbf{p}}_{s,i}, \cdots, \varphi_a \underline{\mathbf{p}}_{s,i}, \cdots, \varphi_{C-1} \underline{\mathbf{p}}_{s,i}]. \tag{3.7}$$

where $\underline{\mathbf{p}}_{s,i}$ is the first $\frac{N}{C}$ samples of $\underline{\mathbf{p}}_{f,i}$ and the phase shift factor φ_a is represented by

$$\varphi_a = e^{-j2\pi \frac{a\alpha}{C}}, a \in \mathbb{Z}, 0 \leqslant a \leqslant C-1. \tag{3.8}$$

Finally, the SSSP symbol is obtained by taking only an arbitrary part of Eq. (3.7), $\varphi_a \underline{\mathbf{p}}_{s,i}$, and all the other phase-rotated replicas are removed out.

$\frac{N}{C}$-point SDFT: The $\frac{N}{C}$ selected subcarriers described by $\underline{\mathbf{P}}_{s,i}$ are sampled from the length-N OFDM symbol. By this way, we obtain a length-$\frac{N}{C}$ OFDM symbol where the non-selected subcarriers are removed out. Then, the $\frac{N}{C}$-point inverse SDFT with frequency shift $\frac{\alpha}{C}$ is performed to obtain $\underline{\mathbf{p}}_{s,i}$ [64]. Any phase-rotated replica $\varphi_a \underline{\mathbf{p}}_{s,i}$ can be adopted as the SSSP symbol.

Similar to the full-length preamble, multiple symbols of the SSSP can be adopted to reduce the effect of noise in the channel estimation and perform frequency synchronization.

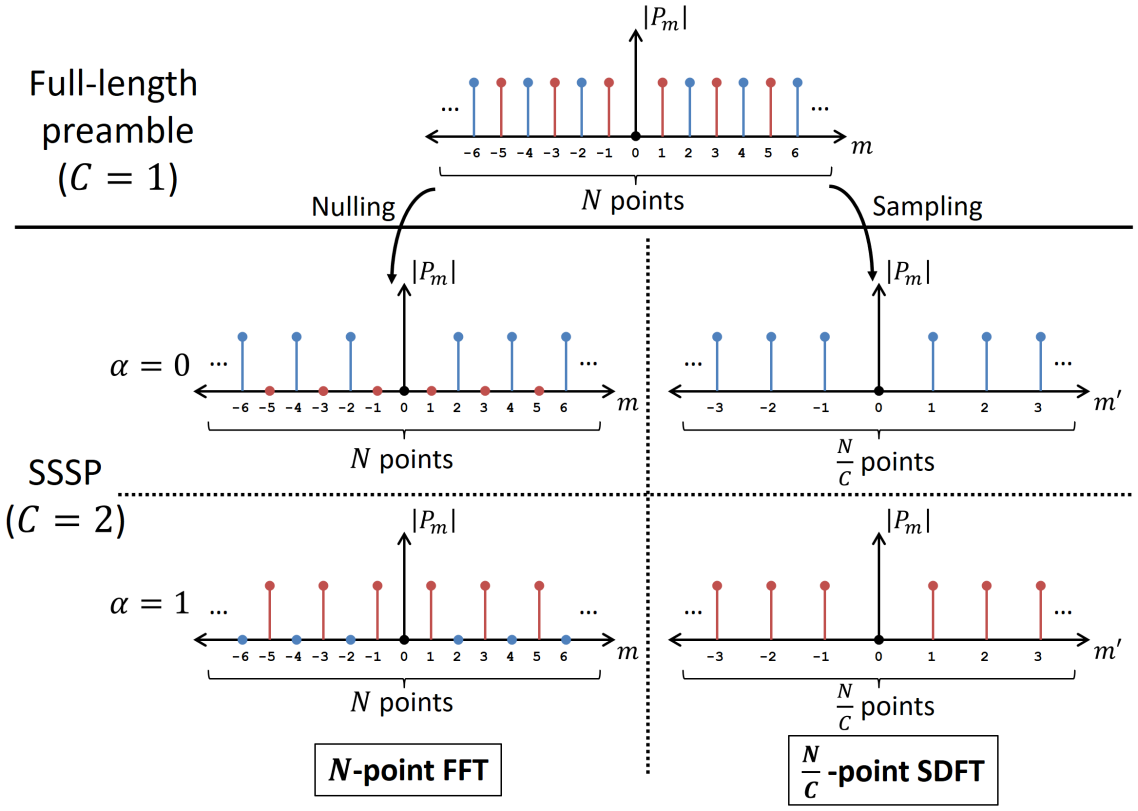

Fig. 3.8 Two implementations of preamble shortening.

To make the multiple SSSP symbols robust to the ISI in multipath environments, the order of a of the phase shift factor φ_a among the multiple SSSP symbols must be maintained. For example, the time samples of the SSSP can be written as $[\varphi_a \underline{\mathbf{p}}_{s,i}, \varphi_{a+1} \underline{\mathbf{p}}_{s,i}]$, when the number of symbols is set to be a typical number, 2.

Also, to avoid the ISI being influenced by the previous symbol, a proper guard interval (GI) must be prepended before the beginning of the SSSP. Given that the SSSP starts with $\varphi_a \underline{\mathbf{p}}_{s,i}$, the GI is obtained from the left adjacent time samples located before $\varphi_a \underline{\mathbf{p}}_{s,i}$ in Eq. (3.7). If the SSSP starts with $\underline{\mathbf{p}}_{s,i}$, then the GI is obtained from cyclic shift of $\underline{\mathbf{p}}_{f,i}$.

Note that the preamble reduction rate C for the SSSP must be an exponential of the number 2 to preserve the FFT length property. In a particular case of $C = 2$ or when the preamble is shortened by half, we can obtain even-indexed and odd-indexed set of selected subcarriers as $\underline{\mathbf{P}}_{s,i|C=2,\alpha=0} = [\cdots, P_{-4}, P_{-2}, P_2, P_4, \cdots]$ and $\underline{\mathbf{P}}_{s,i|C=2,\alpha=1} = [\cdots, P_{-3}, P_{-1}, P_1, P_3, \cdots]$, respectively. When the even-indexed subcarriers are being selected, the time-domain preamble is consisted of two identical copies repeating in series ($\varphi_1 = 1$); if the odd-indexed subcarriers are being selected, the second half of the time-

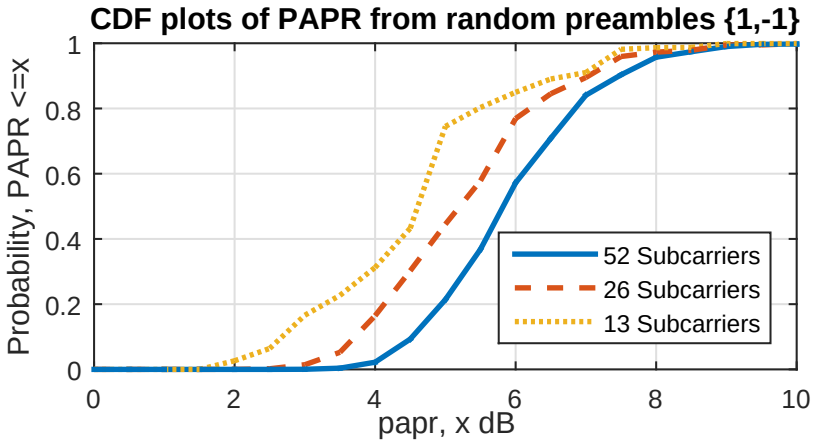

Fig. 3.9 CDF of the PAPR when the number of activated subcarriers is 13, 26, and 52.

domain preamble is a sign inverse version of the first half ($\varphi_1 = -1$). The allocation of preamble subcarriers is shown by on the time-frequency grid demonstrated in Fig. 3.7, where the shaded, zero-marked, and patterned grids represent selected subcarriers, nulled subcarriers, and data, respectively.

In addition, preamble shortening by nulling out some subcarriers has no adverse effect on peak-to-average power ratio (PAPR), because it is similar to when the number of subcarriers in a system decreases [65]. To verify this, we study the distribution of the PAPR of random preamble patterns. PAPR which is the ratio of the highest signal peak power to its average power is defined as $\text{PAPR}_{\text{dB}} = 10\log_{10}\frac{\max|\underline{\mathbf{p}}_s|^2}{\|\underline{\mathbf{p}}_s\|^2}$ dB. Fig. 3.9 shows the simulated cumulative distribution function (CDF) plots of PAPR, where the preamble symbols are {1,-1}-BPSK random. The SSSP which activates less number of subcarriers causes no concern on the PAPR issue. In practice, the preamble pattern is deterministic and well designed such that the PAPR is low. For instance, the PAPR of the legacy long training field (L-LTF) defined in IEEE 802.11 OFDM standards which adopts 52 subcarriers is 3.17 dB. In this work, we consider random preamble patterns of both the full-length and the short preambles for generality.

3.3.2 Preamble Recovery

At the receiver, the preamble recovery is performed to reconstruct the full-length received preamble $\underline{\mathbf{p}'}_{f,i}$ by removing the GI and extracting the received SSSP symbol $\varphi_a\underline{\mathbf{p}'}_{s,i}$. Since the proper GI is added to avoid the ISI problem and assuming that the wireless channel is quasi-static during the preamble, $\varphi_a\underline{\mathbf{p}'}_{s,i}$ with the other phase-rotated versions are

serially connected to obtain $\underline{\mathbf{p}'}_{f,i}$ as

$$\underline{\mathbf{p}'}_{f,i} = [\underline{\mathbf{p}'}_{s,i}, \varphi_1 \underline{\mathbf{p}'}_{s,i}, \varphi_2 \underline{\mathbf{p}'}_{s,i}, \cdots, \varphi_a \underline{\mathbf{p}'}_{s,i}, \cdots, \varphi_{C-1} \underline{\mathbf{p}'}_{s,i}], \tag{3.9}$$

similar to Eq. (3.7). Then, the received SSSP $\underline{\mathbf{P}'}_{s,i}$ containing received training signals P'_m are obtained by performing N-point FFT to $\underline{\mathbf{p}'}_{f,i}$. It should be noted that, similar to the two implementations in preamble shortening, instead of following Eq. (3.9) and performing N-point FFT, one may perform $\frac{N}{C}$-point SDFT with frequency shift $\frac{\alpha}{C}$ to $\underline{\mathbf{p}'}_{s,i}$ in order to obtain $\underline{\mathbf{P}'}_{s,i}$ and P'_m accordingly.

3.4 Channel Estimation for SSSP

While the channel estimation results of the selected subcarriers can be calculated directly, we apply joint time-frequency channel interpolation/extrapolation for the SSSP to complement the channel estimation on the nulled subcarriers. The joint estimation between time and frequency domain is calculated by using a weighted sum technique. Thus, $\hat{H}_m$ of the SSSP scheme can be written as

$$\text{selected subcarrier}: \quad \hat{H}_m = \frac{P'_m}{P_m}, \tag{3.10}$$

$$\text{nulled subcarrier}: \quad \hat{H}_m = (1-w)\hat{H}_{m,\text{freq}} + w\hat{H}_{m,\text{time}}, \quad 0 \le w \le 1, \tag{3.11}$$

where w is the weighting factor, and $\hat{H}_{m,\text{freq}}$ is the estimate obtained by FDI. Unlike a 2D channel estimation designed for pilot-aided schemes [48, 66], this estimation algorithm does not require future channel samples and is also computationally lightweight in order to satisfy the real-time requirement of ICS. In particular, this algorithm acts as a causal fixed-coefficient interpolation filter.

In two special cases where $w = 0$ and $w = 1$, the joint time-frequency channel estimation becomes channel estimation with pure FDI and TDE, respectively. The FDI provides the estimation at the nulled subcarriers by interpolating the estimates of neighbor selected subcarriers. Various interpolation methods such as linear and spline interpolation can be applied for the estimation in the frequency direction [67]. The TDE utilizes the channel estimate of the selected subcarrier from previous cycles to obtain the estimate of the nulled subcarrier in the current cycle.

The weighting factor w can be adaptively selected according to channel conditions, i.e., how fast and how frequency-selective the channel fading is. In particular, when the channel

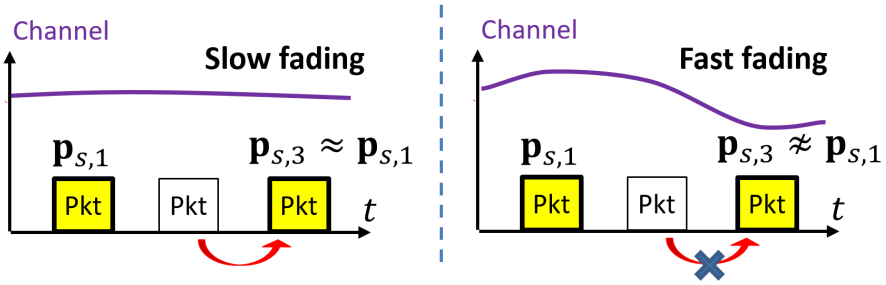

Fig. 3.10 Adaptive algorithm based on the correlation between time-domain preamble signals.

varies quickly in time due to mobility, the estimation at the nulled subcarrier should rely on the estimate from FDI. On the other hand, the estimation from the previous cycle should be used for a slow fading channel. Fig. 3.10 illustrates the adaptive algorithm, which adjust itself according to the channel condition based on the correlation between time-domain preamble signals. In this work, the weighting factor w is simplified as a selection from 0 or 1 by thresholding, because the weighting factors between 0 and 1 do not provide significant gain as shown in Section 3.5.1. Let us define the channel varying indicator K as

$$K = \mathrm{corr}(\varphi_a \underline{\mathbf{p}'}_{s,i}, \varphi_a \underline{\mathbf{p}'}_{s,i-C}) + \frac{1}{1+\mathrm{SNR}}, \tag{3.12}$$

where K is the correlation between time-domain preamble signals of two recent packet transmissions with an identical α biased by the SNR [68]. The SNR can be estimated by exploiting the repetition of identical preambles signals or the noise appearing in the nulled subcarriers and guard band. The thresholding is performed as follows. If K is smaller than a threshold k, then the weighting factor w is set to 0. Otherwise, it is set to 1. The setting of k relies on the preamble shortening rate C and a Doppler spectrum due to the difference in subcarrier selection pattern and fast fading characteristic, respectively. In this study, we assume the Doppler spectrum to be the prevalent Jakes' model with various maximum Doppler frequency $f_{D,max}$.

3.5 Evaluation

We convey extensive simulations to validate the feasibility of the SSSP. Firstly, the error rate performance is evaluated in a common transmitter-to-receiver model in Section 3.5.1 and 3.5.2. Various channel conditions including both fast and frequency-selective fading as

Table 3.1 Simulation parameters based on IEEE 802.11 OFDM standards.

Subcarrier modulation	BPSK (coding rate 1/2)
Sampling rate	20 MHz
Bandwidth	16.25 MHz
Number of subcarriers	52
(data/pilot)	(48/4)
IFFT/FFT period	3.2 μs
Guard interval of data symbols	0.8 μs
Decoder	Hard-decision Viterbi
Equalizer	Zero forcing

well as varying carrier-to-noise ratio (CNR) are tested. The improved performance of the SSSP in the frequency-selective fading channels is verified. The adaptive algorithm also shows the improved flexibility in the fading channels. Secondly, the real-time capability is evaluated in an ICS communication model consisting of one controller and many slaves in Section 3.5.3. Within a limited cycle time, an ACK mechanism and retransmission are performed to enhance the success rate of packet delivery. The overall efficiency of different preamble schemes is evaluated in terms of the total communication time required by the ICS to successfully finish all transmissions. We show that the SSSP scheme with adaptive channel estimation provides good real-time capability in various channel conditions.

Table 3.1 shows the major simulation parameters based on the lowest rate of IEEE 802.11 OFDM standards. The performance of the SFSP scheme is studied in terms of the SSSP scheme with $w = 0$. Similar to the standards, two symbols of preambles are transmitted at the beginning of each packet for channel estimation. A fixed-length GI of 1.6 μs is prepended to preambles. The OFDM symbol error rate (SER) is measured and the OFDM symbol is counted as success only if all bits in the symbol are decoded correctly. The SER is equivalent to PER by assuming that the packet contains 1 OFDM data symbol, which is equivalent to 3 bytes. To represent the degree of frequency-selective and fast fading quantitatively, we adopt multipath root-mean-square (rms) delay spread, and a product of maximum Doppler frequency and time between two packets $f_{D,max} \cdot T_p$ as the metrics, respectively. To evaluate the channel estimation performance, the timing and frequency synchronization are assumed to be perfect. The numerical results of the synchronization methods based on shortened preambles [60, 61] show that the synchronization errors are negligibly small, especially in high-CNR environments.

3.5.1 Effect of Fast Frequency-selective Fading

In this section, we study the adverse effects caused by the joint time-frequency estimation at the nulled subcarriers by assuming a noise-less environment and perfect channel estimation at selected subcarriers. The multipath channel is modeled as two-ray Rayleigh fading channel in order to investigate the worst-case performance when forward error correction (FEC) is applied [69].

We evaluate the SER performance in fast frequency-selective fading conditions. The simulation results are shown in terms of contour plots in Fig. 3.11 and 3.12.

Fig. 3.11 (a) and 3.11 (b) show the SER of the full-length preamble and the IFP as references, while Fig. 3.11 (c), 3.11 (d), and 3.11 (e) show the SER of the SSSP scheme with $C = 2$ and $w = 0$ (SFSP), $w = 1$, and adaptive w ($k = 0.98$), respectively. The filled intensity depicts the SER in a channel fading condition and the bold line represents the interested SER bound = 10^{-3}.

To evaluate the joint time-frequency channel estimation with weighted sum technique, we vary w from 0 to 1 with 0.2 increment. Fig. 3.12 (a) shows the interested SER bound = 10^{-3} of the full-length preamble, the IFP, and the SSSP with $C = 2$. Each line represents the interested SER bound = 10^{-3} of each scheme. The threshold k is selected to give a good balance between time and frequency fading characteristics based on this evaluation and is used throughout this chapter.

While the full-length preamble provides low SER in both fast and frequency-selective fading channel, the SSSP scheme with $w = 0$ (SFSP) can provide good performance only in relatively flat fading. On the other hand, the SSSP with $w = 1$ is verified to be good in relatively slow fading. In particular, the SSSP with $C = 2$ and $w = 0$ (SFSP) provides SER $< 10^{-3}$ when the rms delay is less than 275 ns. The SSSP with $C = 2$ and $w = 1$ provides the same performance when $f_{D,max} \cdot T_p < 20$ Hz $\cdot$ ms. The adaptive algorithm can moderately combine the effectiveness of the algorithms with fixed $w = 0$ and $w = 1$ altogether. Sub-optimal combination can be investigated because of occasional misestimation of channel time variation by K.

The weighting factor w can adjust the characteristic of the channel estimation. Increasing the weighting factor degrades the performance in fast fading region but makes the system perform better in frequency-selective fading, and vice versa. However, varying the weight factor between 0 and 1 provides a small extra region in addition to the two special cases due to the Nyquist rate constraint.

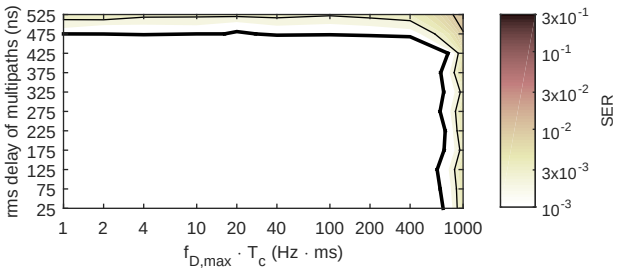

(a) Full-length preamble.

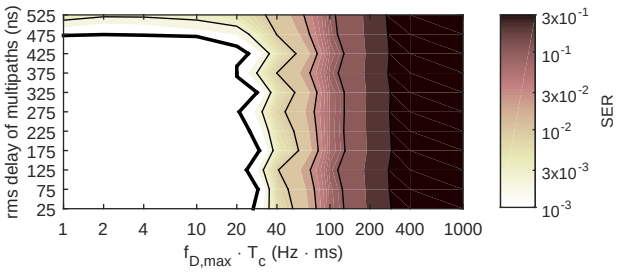

(b) IFP.

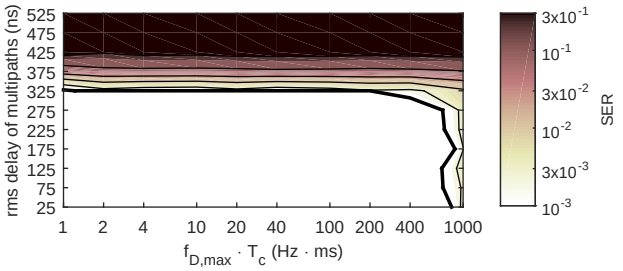

(c) SSSP with $C = 2$ and $w = 0$ (SFSP).

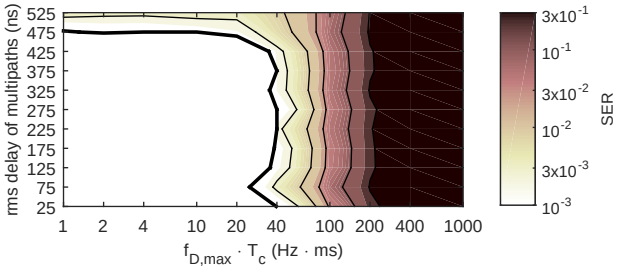

(d) SSSP with $C = 2$ and $w = 1$.

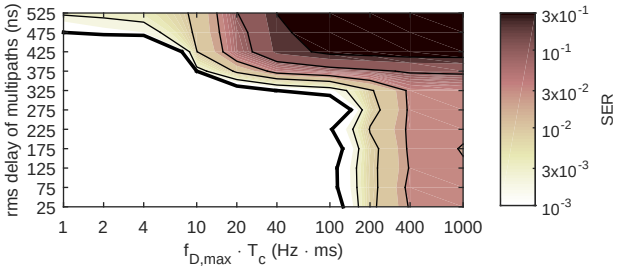

(e) SSSP with $C = 2$ and adaptive w ($k = 0.98$).

Fig. 3.11 SER in various wireless environments.

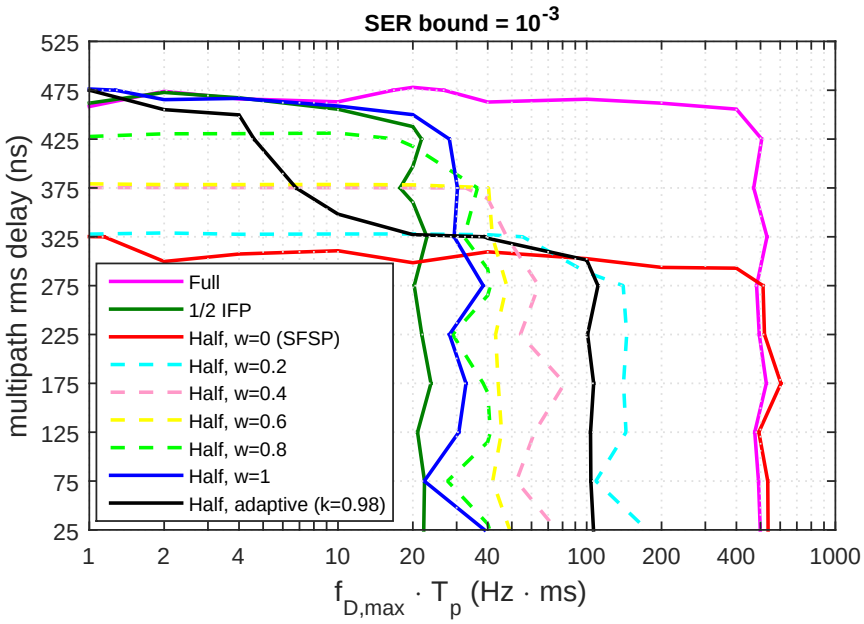

(a) SSSP with $C = 2$.

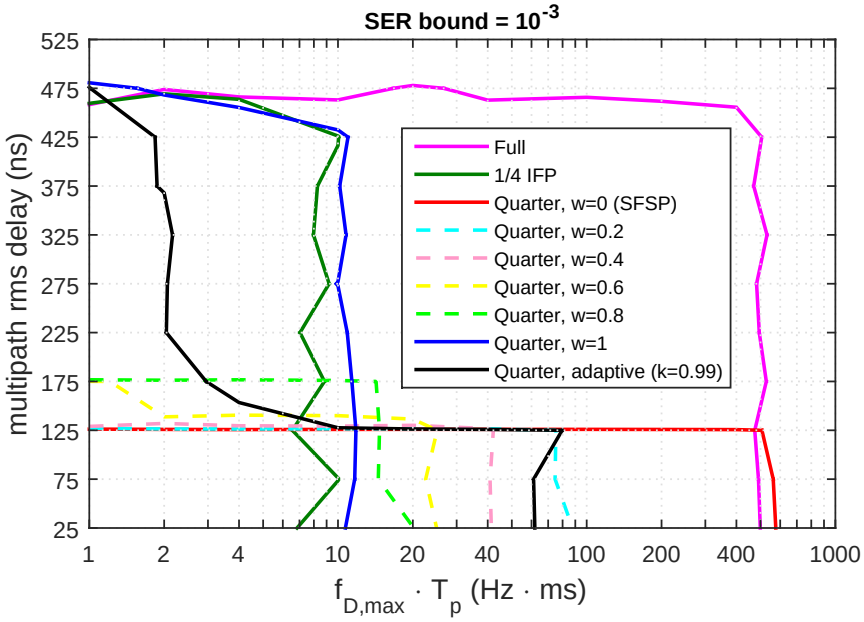

(b) SSSP with $C = 4$.

Fig. 3.12 SER bound $= 10^{-3}$ (equivalent to PER where a packet contains 1 OFDM symbol.

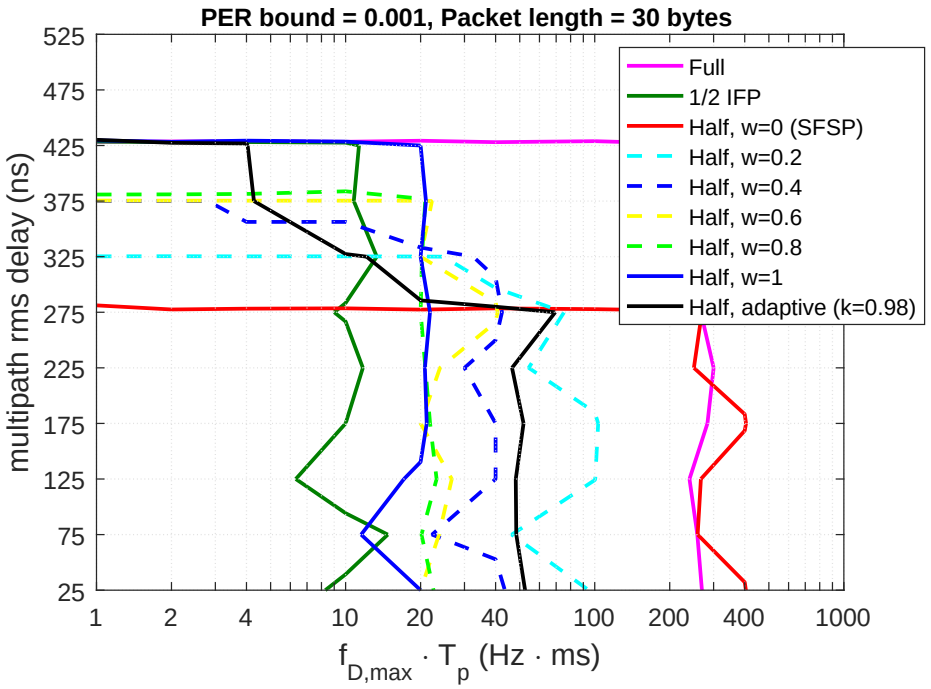

(a) SSSP with $C = 2$.

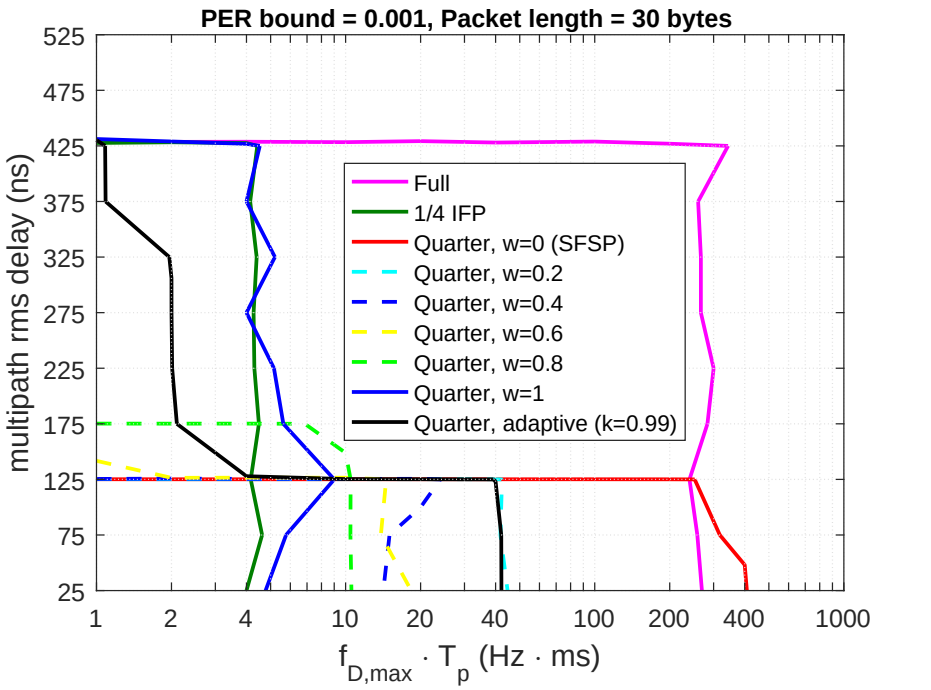

(b) SSSP with $C = 4$.

Fig. 3.13 PER bound = 10^{-3}, where a packet contains 10 OFDM symbols.

Furthermore, the SER bound of the SSSP with $C = 4$ is shown in Fig. 3.12 (b). While the preamble is shortened by 4 times, the good SER area becomes significantly smaller, hence it performs well in very slow fading ($f_{D,max} \cdot T_p < 10$ Hz $\cdot$ ms) or relatively flat fading (rms delay < 125 ns).

Note that the results for longer packets cases show the identical insight about the weighting factor w, as illustrated in Fig. 3.13 where a packet contains 10 OFDM symbols (30 bytes). Naturally, the PER with the longer packet length is worse than that of shorter packet length.

3.5.2 Effect of CNR

In this simulation, we evaluate the effect of CNR in a practical setting for the SSSP with $C = 2$. The practical LS channel estimation algorithm is adopted at the selected subcarriers. The channel models are HiperLAN/2 model C and E, which emulate non line-of-sight environments with rms delay 150 and 250 ns, respectively. We consider two cases of channel variation in time as $f_{D,max} \cdot T_p = 10$ and 200 Hz $\cdot$ ms. In this section, we evaluate the SSSP scheme with adaptive w ($k = 0.98$) and only two special cases of $w = 0$ (SFSP) and $w = 1$, because the two extreme cases can cover most of channel conditions supported by the SSSP with $C = 2$ as observed in Section 3.5.1. The performances of the full-length preamble and the IFP are also given as references.

Fig. 3.14 (a) shows the SER in varying CNR for $f_{D,max} \cdot T_p = 10$ Hz $\cdot$ ms (slow fading). In comparison with the SFSP, the SSSP with adaptive w presents the significant improvement in highly frequency-selective fading of channel model E, especially in high CNR region. However, it provides marginal improvement over the SFSP in the channel model C. Fig. 3.14 (b) shows the SER evaluation when $f_{D,max} \cdot T_p = 200$ Hz $\cdot$ ms (fast fading). In this situation, the SFSP and the SSSP with adaptive w perform similarly.

The comparison with the full-length preamble is given as follows. In the slow fading, although the adaptive scheme causes almost no degradation in the channel model C, it causes approximately 5-dB degradation in the channel model E. In the fast fading, both SFSP and the SSSP with adaptive w cause degradation of 2 dB in the channel model C at SER $= 10^{-3}$, and 8 dB in the channel model E at SER $= 10^{-2}$. Regarding the SSSP with $w = 1$, in the slow fading regardless of the frequency-selective fading, it can provide comparable SER performance to that of the full-length preamble in all CNR conditions. However, in the fast fading it causes deficient performance in the fast fading condition

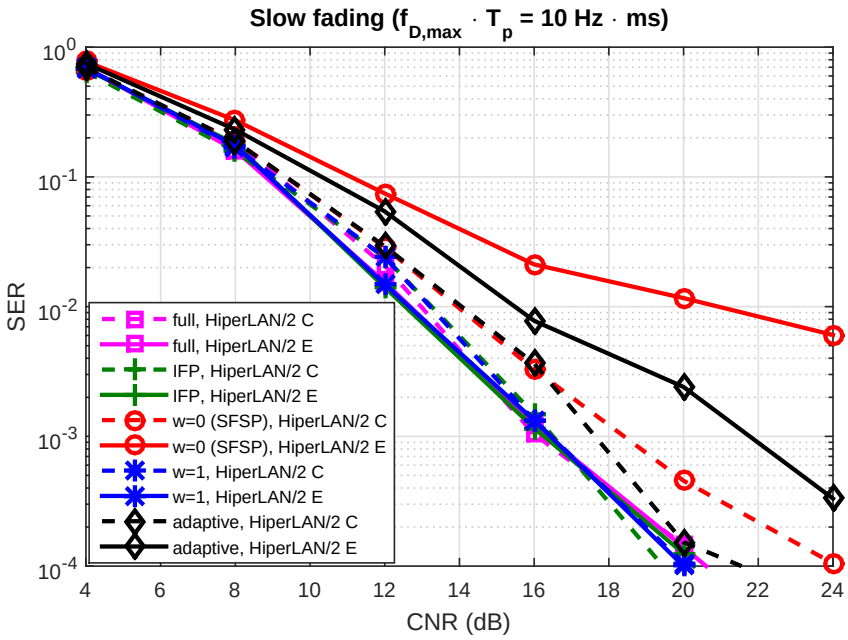

(a) Slow fading channel $f_{D,max} \cdot T_p = 10$ Hz $\cdot$ ms.

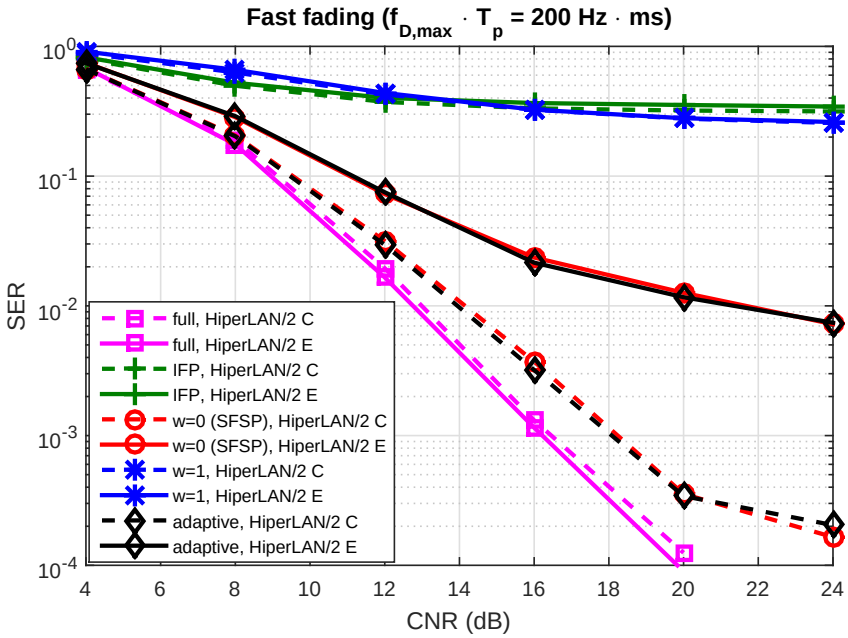

(b) Fast fading channel $f_{D,max} \cdot T_p = 200$ Hz $\cdot$ ms.

Fig. 3.14 SER in noisy environments.

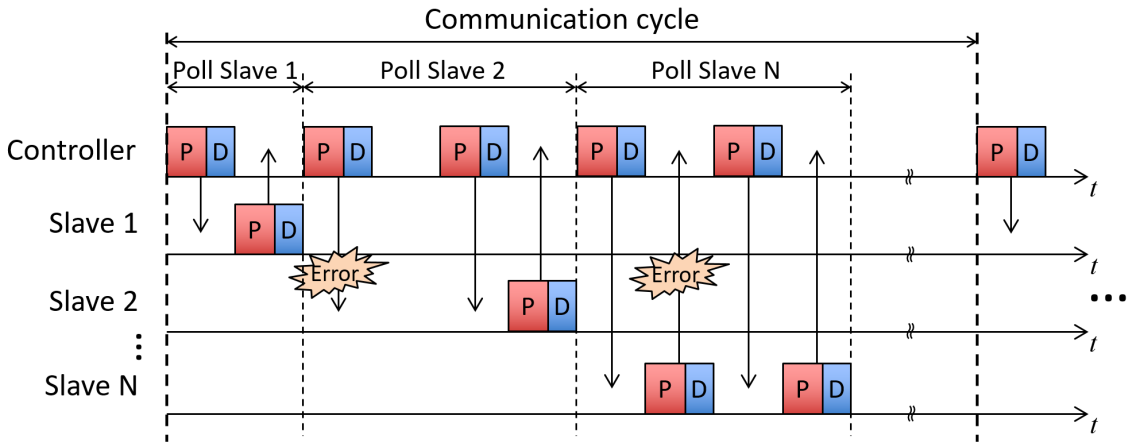

Fig. 3.15 Communication process in polling-based MAC.

independently of CNR. In general, the adaptive SSSP scheme can achieve reasonable performance in both slow and fast fading among the short preamble schemes.

3.5.3 Real-time Capability

Unlike the common transmitter-to-receiver model in Section 3.5.1 and 3.5.2, we study the real-time capability with a complete ICS model consisting of a controller and many slaves in this section. The real-time capability is evaluated in terms of the transmission time required to reliably complete a communication process. We consider the satisfied success rate to be 99.9% and compare the preamble transmission schemes in various channel conditions. We consider four channel models: (a) $f_{D,max} = 10$ Hz, HiperLAN/2 model C as slow flat fading, (b) $f_{D,max} = 200$ Hz, HiperLAN/2 model C as fast flat fading, (c) $f_{D,max} = 10$ Hz, HiperLAN/2 model E as slow frequency-selective fading, and (d) $f_{D,max} = 200$ Hz, HiperLAN/2 model E as fast frequency-selective fading. CNR is set to be 20 dB. We investigate two deterministic MAC protocols that are polling and TDMA protocols.

(a) Evaluation Model 1: Polling

In this section, a simple polling-based MAC scheme is considered. As shown in Fig. 3.15, the medium access in one communication cycle is completely organized by the master. The master sends downlink control data together with a request to a slave and the slave replies back with uplink state data and ACK to the downlink. If downlink data is lost, there will be no reply from the slave and the master will then retransmit the downlink data. In case

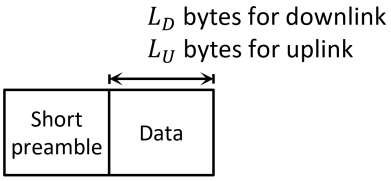

Fig. 3.16 Frame format in polling-based MAC.

of error in downlink, the master retransmits according to the received ACK. If uplink data is lost or error, the master will send the request to the slave again.

As shown in Fig. 3.16, the frame formats of both downlink and uplink traffic begins with a preamble followed by data L_D bytes for downlink or L_U bytes for uplink. These data include either control data or state data, and request message or piggybacked ACK.

In this evaluation, the total communication time required to reliably complete a data exchange with 1 slave is measured. The number of slaves supported by this system can be further estimated by dividing the communication cycle time T_c with the communication time per slave. We evaluate two cases of packet length: (1) The data length is 1 OFDM symbol long and (2) The data length is 5 OFDM symbols long.

Evaluation Results

(1) 1-symbol data length

Fig. 3.17 shows the total time required to complete the data exchange with the corresponding success rate. In general, the short preambles can improve the real-time capability by approximately 25% when the channel correlation exists. In particular, the adaptive SSSP can provide relatively good performance in most channel conditions. The detailed explanation in each channel condition is given as follows.

As shown in Fig. 3.17 (a), the short preambles requires 0.048 ms to obtain 99.9% successful communication, which is reduced by 28% compared to the full-length preamble, in the slow and flat channel fading. Based on this result, ICS should be able to support up to 20 devices by using the polling-based MAC protocol.

Fig. 3.17 (b) shows the results in the fast and flat channel fading. The SSSP with $w = 0$ (SFSP) and the adaptive SSSP provide two best real-time capability in this channel condition. They can reduce the communication time by approximately 25%.

For the slow and frequency-selective channel fading as Fig. 3.17 (c), the SSSP with $w = 1$ and the IFP provides the shortest communication time at 0.050 ms, while the adaptive

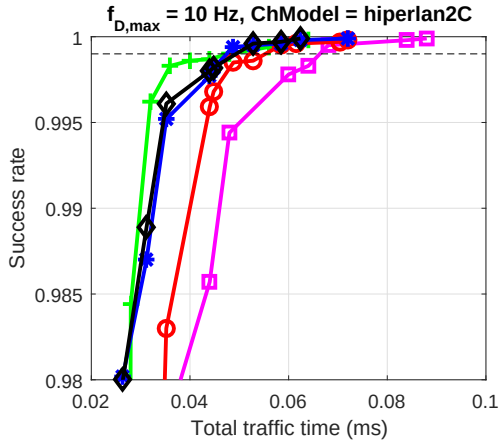

(a) Slow fading ($f_{D,max} = 10$ Hz) and flat fading (HiperLAN/2 model C).

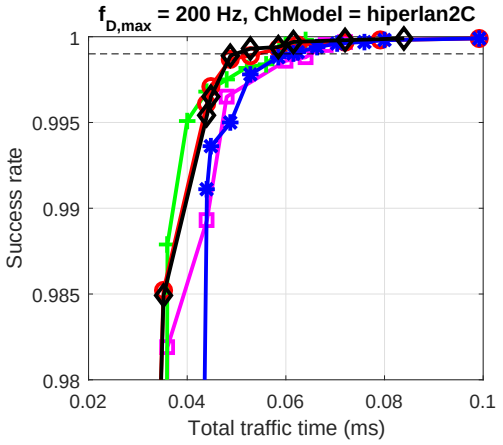

(b) Fast fading ($f_{D,max} = 200$ Hz) and flat fading (HiperLAN/2 model C).

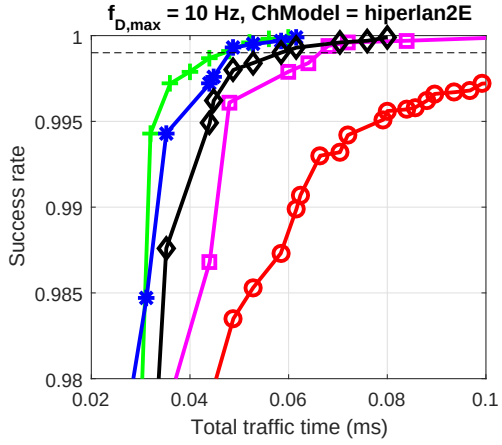

(c) Slow fading ($f_{D,max} = 10$ Hz) and frequency-selective fading (HiperLAN/2 model E).

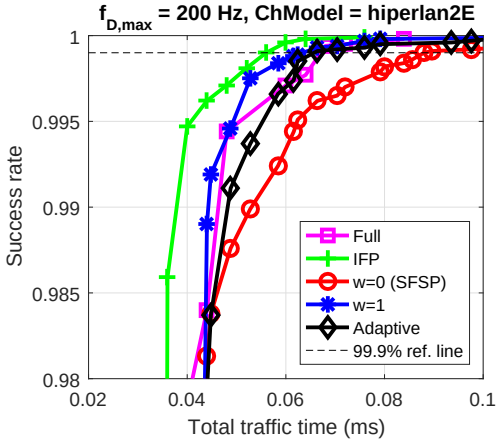

(d) Fast fading ($f_{D,max} = 200$ Hz) and frequency-selective fading (HiperLAN/2 model E).

Fig. 3.17 Polling: Total communication time per 1 slave for 1 OFDM data symbol.

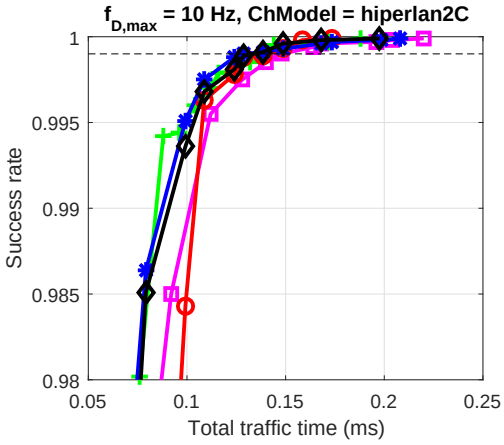

(a) Slow fading ($f_{D,max} = 10$ Hz) and flat fading (HiperLAN/2 model C).

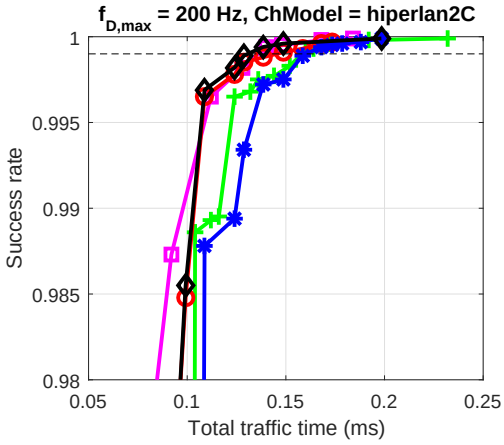

(b) Fast fading ($f_{D,max} = 200$ Hz) and flat fading (HiperLAN/2 model C).

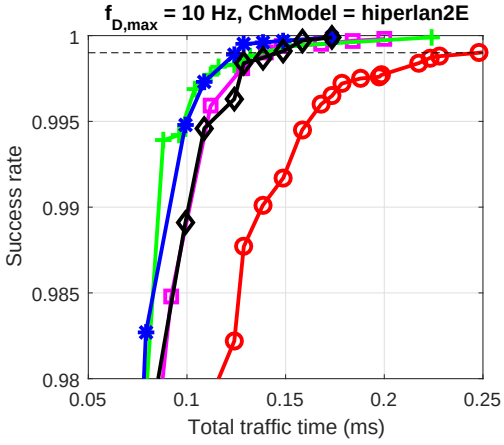

(c) Slow fading ($f_{D,max} = 10$ Hz) and frequency-selective fading (HiperLAN/2 model E).

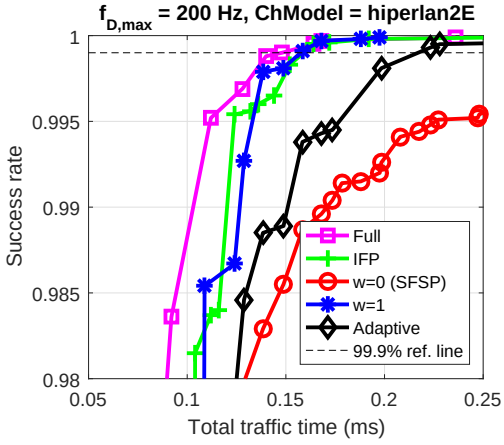

(d) Fast fading ($f_{D,max} = 200$ Hz) and frequency-selective fading (HiperLAN/2 model E).

Fig. 3.18 Polling: Total communication time per 1 slave for 5 OFDM data symbols.

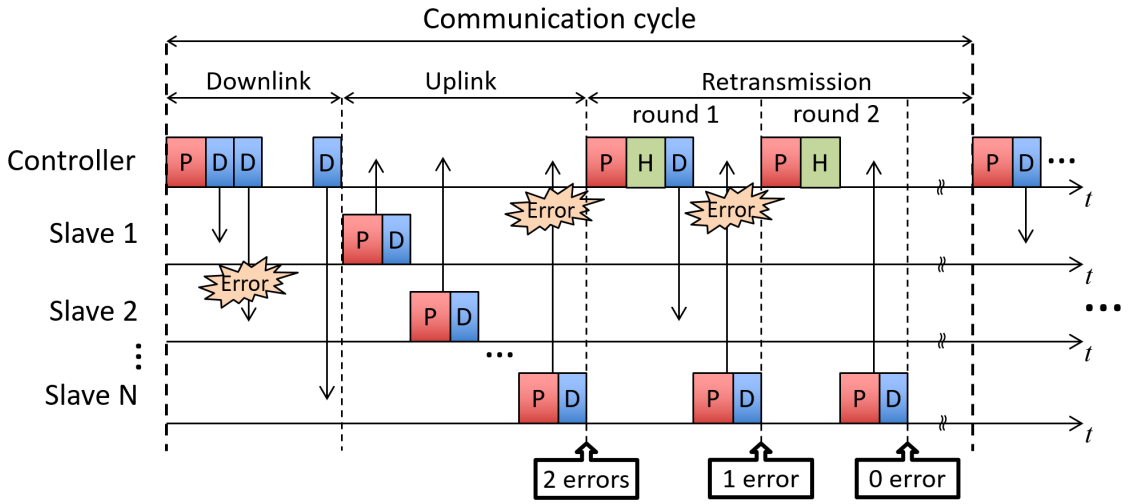

Fig. 3.19 Communication process in TDMA-based MAC.

SSSP can still give relatively good performance. The communication time is reduced 26% and 11% by the SSSP with $w = 1$ and the adaptive SSSP, respectively.

Fig. 3.17 (d) shows the results in the fast and frequency-selective channel fading. The results show that the IFP reveals the best real-time capability at 19% improvement, while the SSSP with $w = 1$ and the adaptive SSSP cannot provide significant improvement over the full-length preamble.

(2) 5-symbol data length

Fig. 3.18 show the communication time when the packet contains 5 OFDM data symbols. The short preamble schemes provide significantly less real-time capability improvement in this long-packet case. Such a long packet transmission time degrades the inter-packet correlation, which is an important prerequisite of the short preamble design.

In addition, the results show that the communication time per 1 slave takes 0.15 ms even with the optimal preamble scheme. Given $T_c = 1$ ms, this polling-based MAC protocol can support up to 7 devices per one system, which is however considered far too small for applications in ICS.

(b) Evaluation Model 2: TDMA

In this evaluation, we consider a time-efficient TDMA scheme. Compared to the polling protocol, the TDMA scheme is more efficient since only one downlink preamble can be transmitted and used by all slaves, as proposed in [30]. As illustrated in Fig. 3.19, a communication cycle is divided into 3 stages as follows.

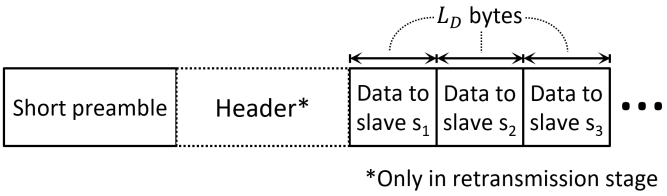

(a) Downlink traffic.

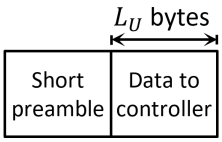

(b) Uplink traffic.

Fig. 3.20 Frame format in TDMA-based MAC.

- **Downlink**: At the beginning of each cycle, the controller transmits a preamble which will be received by all slaves for channel estimation. Then, the controller transmits a control data of each slave to every slave consecutively based on a predefined order. Each control data is L_D bytes in length.
- **Uplink**: After the downlink stage, every slave transmits a preamble and its state data consecutively based on a predefined order. The ACK to the downlink message is also piggybacked in the uplink data. Each state data is L_U bytes in length.
- **Retransmission**: After the downlink and uplink stages, there might be a time interval for retransmission. The available time depends on a preamble reduction scheme and the number of slaves. Unlike the downlink, after transmitting the preamble the controller also transmits a slot control header which describes downlink sequence and uplink data request. Then, the retransmission including both downlink and uplink traffic follows as the controller has specified for that round. The retransmission stage can last several rounds until all transmissions are successful or the cycle time T_c is over. A communication cycle is forced to start every T_c to guarantee the freshness of control and state data.

In view of traffic direction, there are controller-to-slave downlink and slave-to-controller uplink traffic. The frame format of the downlink traffic and the uplink traffic are shown in Fig. 3.20 (a) and 3.20 (b), respectively.

The cycle is counted as failed if the communication process is not finished within the cycle time T_c. In particular, the cycle time T_c is set to be 1 ms. Both control and state

data payloads including an error-detecting code occupy one OFDM symbol, and the retransmission header occupies two OFDM symbols. We separately measure the downlink traffic time and the uplink traffic time required to obtain the corresponding success rate, since the downlink and uplink traffic have different frame formats which may result in different optimal preamble shortening scheme. In this evaluation, we evaluate two parameter settings: (1) The data length is 1 OFDM symbol long and ICS has 30 slaves, and (2) The data length is 5 OFDM symbols long and ICS has 6 slaves.

Evaluation Results

(1) 1-symbol data length, 30 slaves

The downlink and uplink traffic time with the corresponding success rate are evaluated as shown in Fig. 3.21 and 3.22, respectively. In general, the SSSP can shorten the uplink traffic time, while the full-length preamble should be applied in the downlink. This is because the downlink traffic includes only a small portion of preamble transmission and shortening the preamble is not worth to sacrifice the reliability.

In addition, for the uplink traffic, the adaptive SSSP provides relatively good real-time capability in all channel conditions. The uplink traffic time is explained in detail to emphasize the essential benefit of the short preambles for each channel condition as follows.

Fig. 3.22 (a) shows the results in the slow and flat channel fading. In this channel condition, the SSSP with $w = 1$ and adaptive w achieve the best real-time capability. In particular, they perform uplink transmissions for 0.35 ms. Since the full-length preamble scheme needs 0.47 ms for uplink, they can reduce the uplink time by 25.5%.

Fig. 3.22 (b) shows the results in the fast and flat channel fading. Because of the flat but fast fading, the SSSP with $w = 0$ (SFSP) reveals the best real-time capability, while the adaptive SSSP provides comparably good outcome. Specifically, the SSSP with $w = 0$ (SFSP) and the adaptive SSSP can reduce the uplink time by 17.8% and 11.1%, respectively.

Fig. 3.22 (c) shows the results in the slow and frequency-selective channel fading. In this environment, the SSSP with $w = 1$ is the most favored, while the adaptive SSSP can still come in the second place. Compared to the full-length preamble scheme, they can decrease the uplink time by 24.4% and 17.8%, respectively.

Fig. 3.22 (d) shows the results in the fast and frequency-selective channel fading. In this harsh conditions, all short preamble schemes including the adaptive SSSP cannot

Table 3.2 Upper-limit number of slaves achieving 99.9% success rate within 1-ms cycle time.

Preamble scheme	**# slaves**
Full	49
IFP	50
$w = 0$ (SFSP)	59
$w = 1$	61
Adaptive	61

provide an improvement over the full-length preamble, since they need to perform a lot of retransmissions to complete the communication process. Essentially, the adaptive SSSP does not degrade the real-time capability.

Moreover, we evaluate an upper-limit number of slaves that can be supported 1-ms cycle time. Table 3.2 shows the maximum number of slaves achieving 99.9% success rate in the slow and flat channel fading. By using the proposed short preambles, the upper-bound number of slaves can be increased from 49 slaves to 61 slaves or by 24.5%.

In summary, we verify that without the knowledge of channel condition, the adaptive SSSP is recommended as it can generally achieve good real-time capability. With a prior knowledge, a system designer may choose the SSSP with $w = 0$ or $w = 1$ to obtain the optimal performance.

(2) 5-symbol data length, 6 slaves

Fig. 3.23 and 3.24 shows the downlink and uplink traffic time when a packet contains 5 OFDM data symbols. Overall, the short preambles provide comparable real-time capability in slow fading, but increase the traffic times in fast fading. The longer packet length causes the lower channel correlation in time domain, and this makes the short preambles perform worse. Therefore, the full-length preamble should be rather adopted than the short preambles, when the packet is long, e.g., 20 μs in this case.

However, the results also show that the long packet transmission time makes the system be able to support less than 10 devices within 1-ms cycle time even with the full-length preamble. Instead of increasing a number of OFDM data symbols, a high data rate setting should be adopted in order to put more data into the packet. For example, with higher modulation levels such as 64-QAM and lower code rates, 5 OFDM data symbols may carry up to hundreds of bytes, which is larger than most situations in ICS.

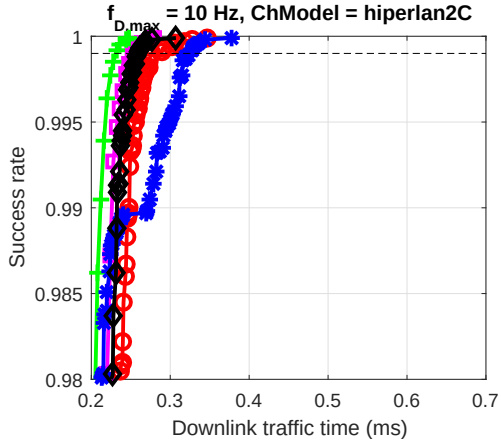

(a) Slow fading ($f_{D,max} = 10$ Hz) and flat fading (HiperLAN/2 model C).

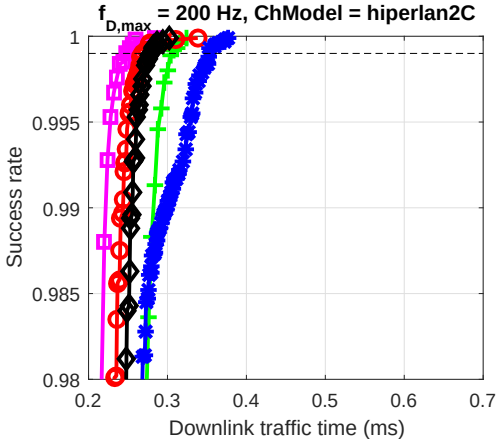

(b) Fast fading ($f_{D,max} = 200$ Hz) and flat fading (HiperLAN/2 model C).

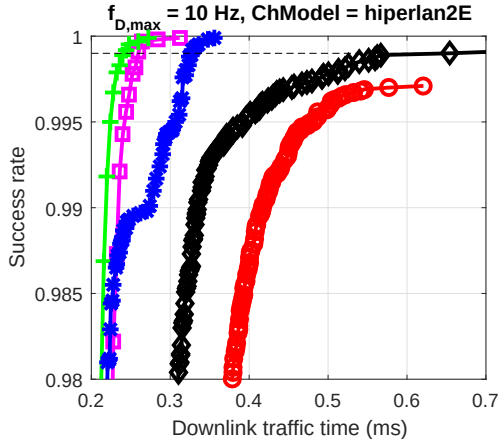

(c) Slow fading ($f_{D,max} = 10$ Hz) and frequency-selective fading (HiperLAN/2 model E).

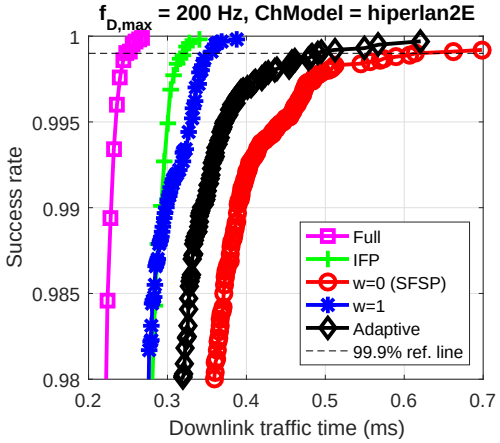

(d) Fast fading ($f_{D,max} = 200$ Hz) and frequency-selective fading (HiperLAN/2 model E).

Fig. 3.21 TDMA: Downlink traffic time of ICS with 30 slaves and 1 OFDM data symbol per slave.

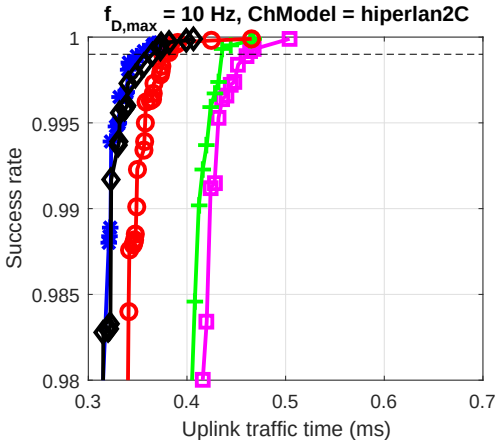

(a) Slow fading ($f_{D,max} = 10$ Hz) and flat fading (HiperLAN/2 model C).

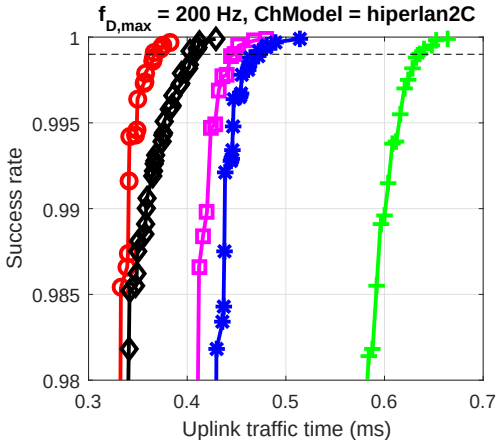

(b) Fast fading ($f_{D,max} = 200$ Hz) and flat fading (HiperLAN/2 model C).

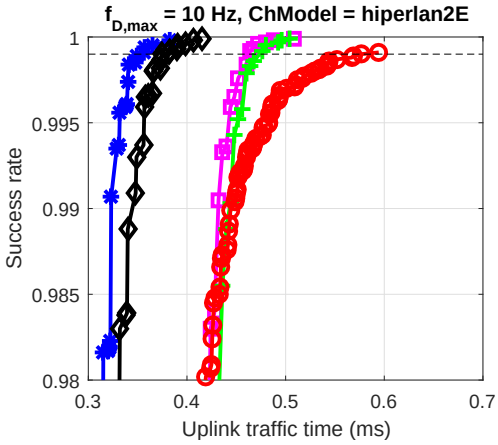

(c) Slow fading ($f_{D,max} = 10$ Hz) and frequency-selective fading (HiperLAN/2 model E).

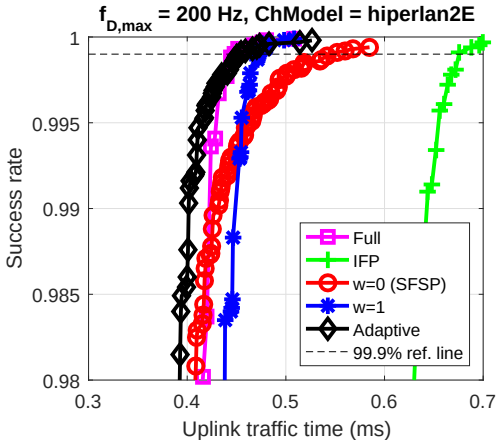

(d) Fast fading ($f_{D,max} = 200$ Hz) and frequency-selective fading (HiperLAN/2 model E).

Fig. 3.22 TDMA: Uplink traffic time of ICS with 30 slaves and 1 OFDM data symbol per slave.

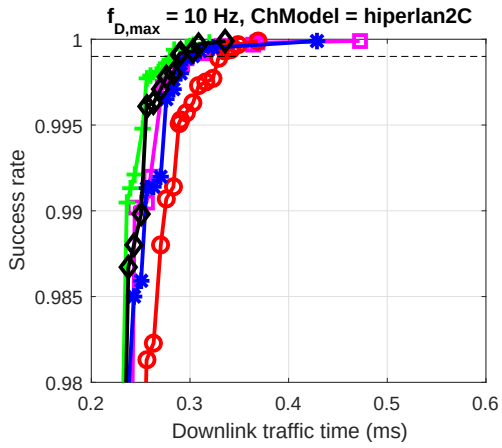

(a) Slow fading ($f_{D,max} = 10$ Hz) and flat fading (HiperLAN/2 model C).

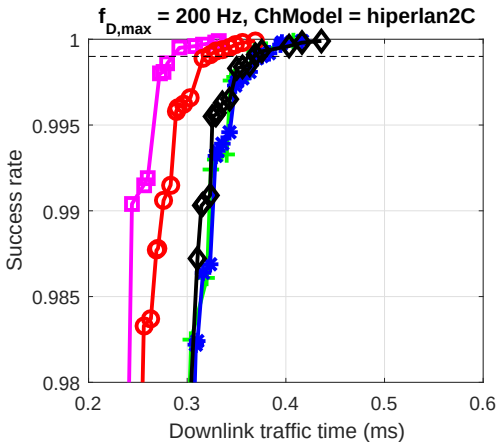

(b) Fast fading ($f_{D,max} = 200$ Hz) and flat fading (HiperLAN/2 model C).

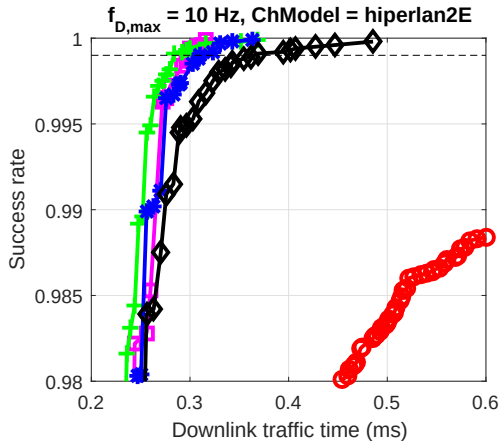

(c) Slow fading ($f_{D,max} = 10$ Hz) and frequency-selective fading (HiperLAN/2 model E).

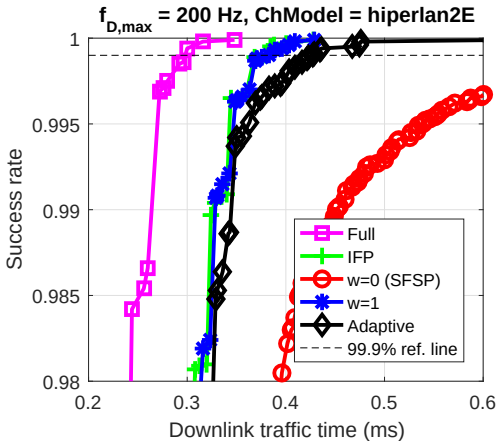

(d) Fast fading ($f_{D,max} = 200$ Hz) and frequency-selective fading (HiperLAN/2 model E).

Fig. 3.23 TDMA: Downlink traffic time of ICS with 6 slaves and 5 OFDM data symbols per slave.

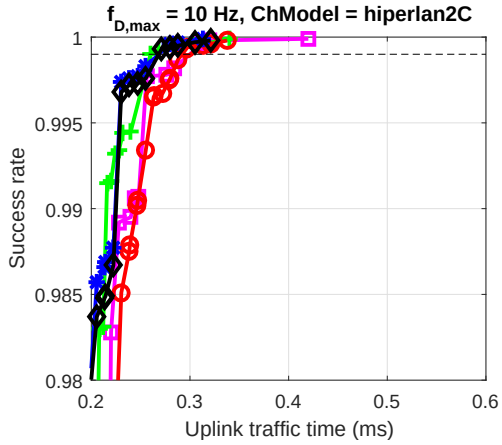

(a) Slow fading ($f_{D,max} = 10$ Hz) and flat fading (HiperLAN/2 model C).

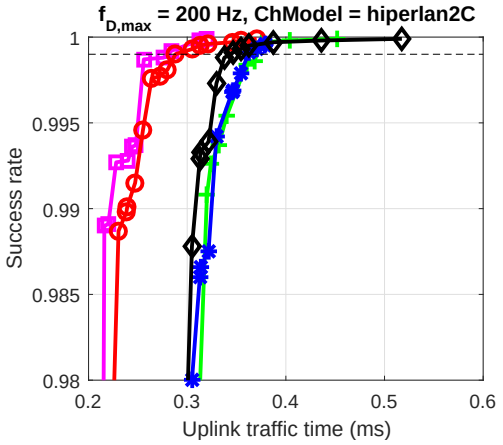

(b) Fast fading ($f_{D,max} = 200$ Hz) and flat fading (HiperLAN/2 model C).

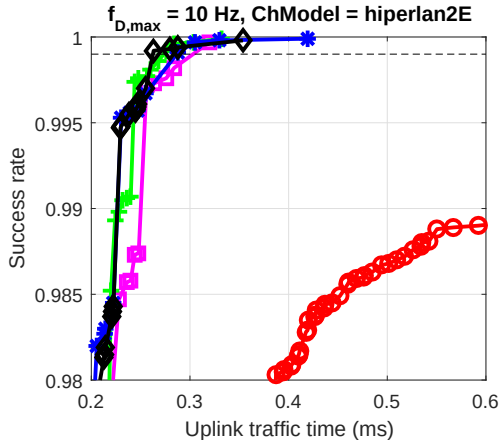

(c) Slow fading ($f_{D,max} = 10$ Hz) and frequency-selective fading (HiperLAN/2 model E).

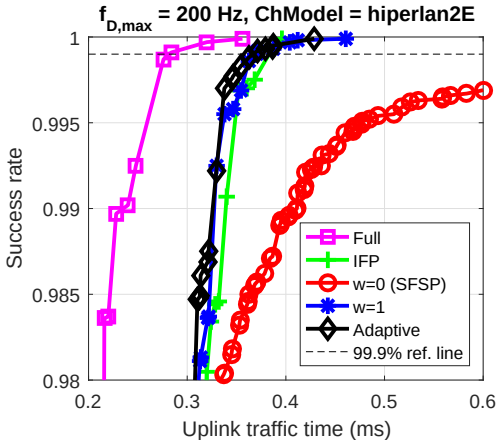

(d) Fast fading ($f_{D,max} = 200$ Hz) and frequency-selective fading (HiperLAN/2 model E).

Fig. 3.24 TDMA: Uplink traffic time of ICS with 6 slaves and 5 OFDM data symbols per slave.

3.6 Summary

This chapter proposes an SSSP scheme with a corresponding channel estimation for real-time and reliable ICS. We introduce subcarrier selectability and algorithm adaptability to the OFDM short preamble design and the channel estimation, respectively. Unlike IFP and SFSP, the selectability of the SSSP allows full sampling coverage of all OFDM subcarriers with several preamble transmissions by exploiting frequent transmissions in ICS, and thus enables the usage of channel correlation in time domain with consistently reliable performance. On the other hand, the adaptability makes the channel estimation take the advantage of the selectability and achieve all-round performance in various wireless channel conditions including both fast and frequency-selective fading. The comparison between the full-length preamble and the preamble reduction schemes verifies that the adaptive SSSP scheme can achieve improved real-time capability in time and frequency correlated channels, thus is promising for ICS.

Chapter 4

Symbol-level Packet Combining using RSSI

4.1 Background

This chapter aims to alleviate the beat problem in concurrent transmission (CT) in order to realize not only real-time but also reliable transmit cooperation. To achieve this, an approach should satisfy two constraints posed by the low-latency characteristic of CT. The first one is that only timing synchronization is available in CT. The solution should not exploit other transmitter coordination such as phase and frequency synchronization, or transmitters' gain control which may cause latency to CT. The second one is that the process should be lightweight. Not only the coordination before the transmission, but also the process after the reception should be minimized so that it does not affect the low-latency characteristic.

In this chapter, by exploiting receive diversity, we propose symbol-level packet combining (PC) which adopts RSSI (Received Signal Strength Indication) values for post-detection selection combining. The use of RSSI differentiates our PC from other PC, thus our proposal can be also named as RSSI-based PC. The proposal can be viewed as a receiver-side error correction algorithm which exploits RSSI as SNR indicators to perform selection combining of decoded data. The use of RSSI values allows us to locate low-SNR data and implement on-the-fly combining process in order to recover the erroneous decoded data while still maintaining lightweight process at the end of the reception.

In the evaluation, simulation results verify the feasibility of RSSI-based PC based on the IEEE 802.15.4 [70] and IEEE 802.11 DSSS standards [71]. In addition, over-the-air experiments using off-the-shelf resource-constrained Tmote Sky sensor nodes (TelosB) nodes confirm the simulation results and show an improvement in reception reliability for proof of concept.

4.2 Related Work

In this section, we overview the related works on transmitter coordination for mitigating the beat problem and receiver-side error correction by PC. After the discussions, we show that to deal with the beat problem, neither of them can satisfy the two constraints including no transmitter coordination except timing synchronization and lightweight.

To avoid the degradation due to the beat, some studies has required precise coordination among the cooperating transmitters. Kubo et al. [72] have introduced strict control of symbol-level transmission timing offset to avoid the transmission of duplicated waveforms,

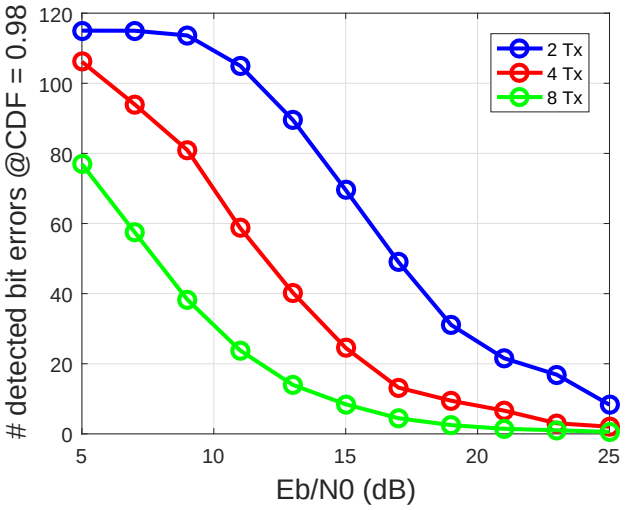

Fig. 4.1 Numbers of detectable bit errors by bit-wise comparison in CT environments.

and performed inter symbol interference (ISI) cancellation at the receiver. [73] and [74] have shown that the beat problem can be mitigated with an optimum carrier frequency allocation. However, such a precise coordination in either timing and carrier frequency can cause a synchronization delay weakening the main strong point of CT towards recent applications.

In contrast to the transmitter-side approaches, the receiver can also correct errors by combining multiple failed packets received by using a diversity. Since state-of-the-art PC techniques have been introduced for general purposes to improve packet reception reliability, they incur high complexity for correcting beat-induced frequent errors in time-sensitive CT systems. The simplest PC scheme adopts a majority voting method [75], which requires at least 3 branches of diversity.

The more sophisticated PC schemes adopt coding-based [76] and search-based [75–78] algorithms, which can work with 2-branch diversity. However, these works do not suit to the real-time CT. The coding-based algorithm put an extra overhead into coded packets, which take longer transmission time and degrade the real-time capability. On the other hand, the search-based algorithm detects the bit-wise difference between multiple received packets, and performs combinatorial testing in order to obtain the correct packet. This method can theoretically correct all errors except *hidden errors*, where the error bits appear to be the same in all received packets. To correct the frequent errors caused by the beat problem, the complexity of the exhaustive search grows excessively with the number of errors and makes them not lightweight enough in practice. Fig. 4.1 shows numbers of

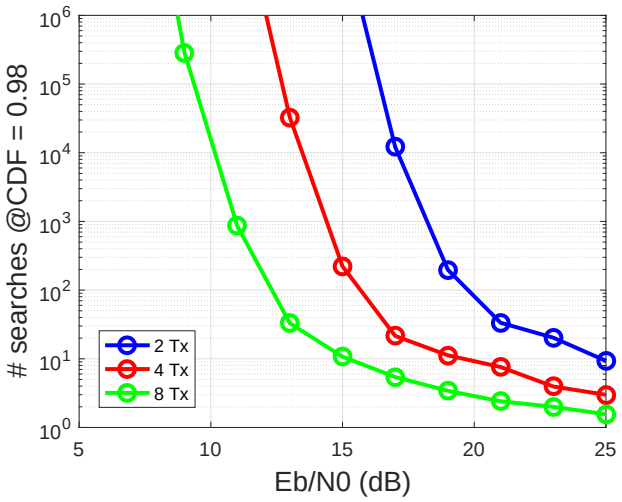

Fig. 4.2 Excessive numbers of searches of the search-based PC

detectable bit errors by bit-wise comparison in CT environments [*1]. Consequently, the corresponding numbers of searches are shown in Fig. 4.2, as the search count increases exponentially with a number of errors ($2^{\#errors}$). The huge numbers of searches can be inferred that this algorithm requires high computation power and time, and also a large amount of memory to buffer all packet combinations.

4.3 Proposed Packet Combining

Fig. 4.3 shows the system diagram of RSSI-based PC with D branches of receive diversity. Baseband signals from each d-th branch are separately decoded to output binary data. These binary data together with RSSI values outputted from an RSSI estimator are fed into RSSI-based PC to form a combined packet. Finally, a CRC checker confirms the validity of all packets from both all diversity branches and RSSI-based PC, and selects one correct data packet.

RSSI-based PC has three key points. Firstly, it adopts receive antenna diversity to obtain multiple packets, and therefore there is no additional transmit overhead. Secondly, it combines packets at symbol level, hence it is capable of correcting beat-induced errors,

[*1] Simulated in Rayleigh fading channel, random carrier frequency by normal distribution with standard deviation of 19.2 kHz, and IEEE 802.15.4 physical-layer standard with packet length of 20 bytes.

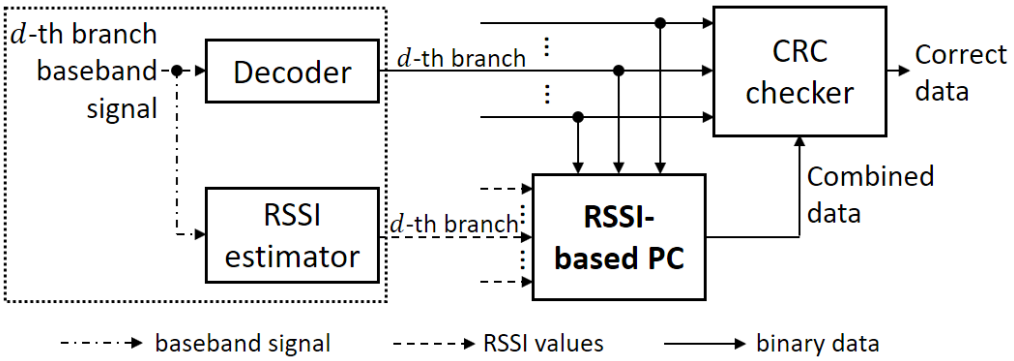

Fig. 4.3 Overview of systems with RSSI-based PC.

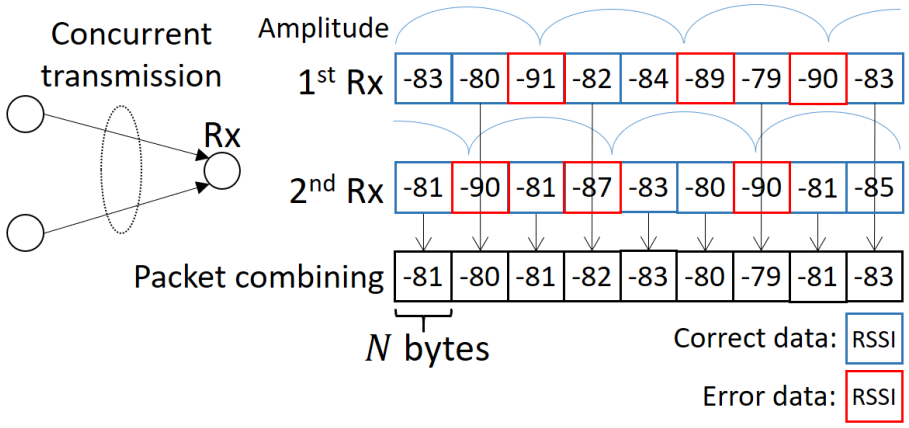

Fig. 4.4 Symbol-level selection combining using RSSI in CT environments.

which behaves like extremely fast fading. Lastly, it utilizes RSSI values as fading indicator, so it can easily locate and avoid error-sensitive errors for simple post processing. This section discusses RSSI-based PC about the symbol-level selection combining method, effects of combining cycle period and RSSI averaging period as well as the implementation aspect.

4.3.1 Symbol-level Selection Combining Method

RSSI-based PC exploits multiple receptions of an identical packet to perform selection combining using RSSI values, as shown in Fig. 4.4. The diversity can be exploited for reducing the effect of the beat as a phase of the beat differs among multiple branches of reception. The beat can be observed by monitoring the RSSI values. To combine the packets, the post-detection selection combining simply selects the demodulated data with the corresponding higher RSSI value from multiple failed packets to form a new packet.

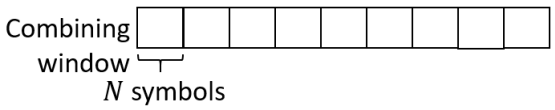

Fig. 4.5 Combining cycle period of N symbols.

Ideally, an instantaneous SNR [79] should be adopted to perform continuous selection combining; however, in practice, the combining is performed in cycles and the RSSI values is averaged.

4.3.2 Combining Cycle Period

As shown in Fig. 4.5, the combining are performed periodically every N symbols or, in other words, at the frequency $f_S = \frac{R}{N}$ Hz, where R is transmission symbol rate.

Similar to the sampling theory, the combining frequency f_S must satisfy $f_S > 2f_B$, where f_B is the maximum frequency of an interested beat, for effective combining. In practice, f_S depends on SPI bus and MCU speed. The beat pattern is influenced by CFO between transmitters participating in CT. In two-transmitter case, f_B depends solely on CFO.

4.3.3 RSSI Averaging Period

The output of the RSSI estimator is not only sampled but also statistically averaged over a time window M symbols, as illustrated in Fig. 4.6. This RSSI averaging acts as a filter, which distorts the magnitude of the observed beat. Fig. 4.7 shows the low-pass filter effect in terms of frequency response, when the filter is a moving average filter with 128-μs window size ($M = 8$ symbols based on IEEE 802.15.4). Note that the red line denotes the negative-gain region, where the beat is observed in an inverse sign to the real beat. We defines zero-gain frequency to be the gain turning zero, and it can be calculated as $\frac{R}{M}$ Hz.

As illustrated in Fig. 4.8, the selection combining may mistakenly choose the low-SNR decoded data since the deep faded signals can be overlooked. Dotted rectangles locate bit errors which are mistakenly combined.

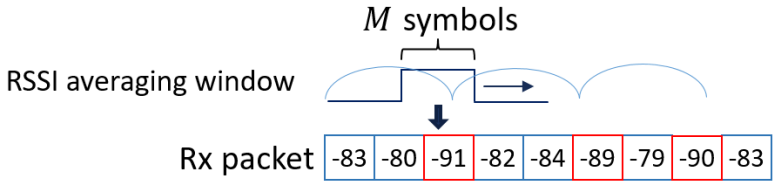

Fig. 4.6 RSSI average period of M symbols.

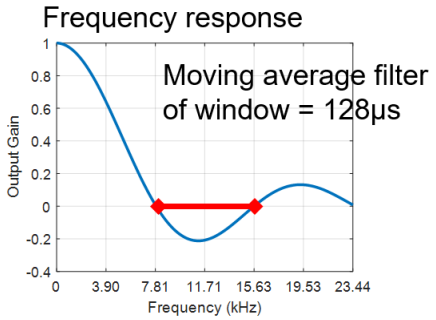

Fig. 4.7 Frequency response of moving average filter with 128-μs window size.

4.3.4 Implementation

In this section, we discuss the implementation aspects of RSSI-based PC. On-the-fly combining process is implemented to achieve low-latency PC. It has been ported to off-the-shelf sensor nodes, namely TelosB.

(a) On-the-fly Combining Process

We extend packet reception process of a CT scheme [53] such that it performs RSSI-based PC while a packet is being received. This reduces the computation time at the

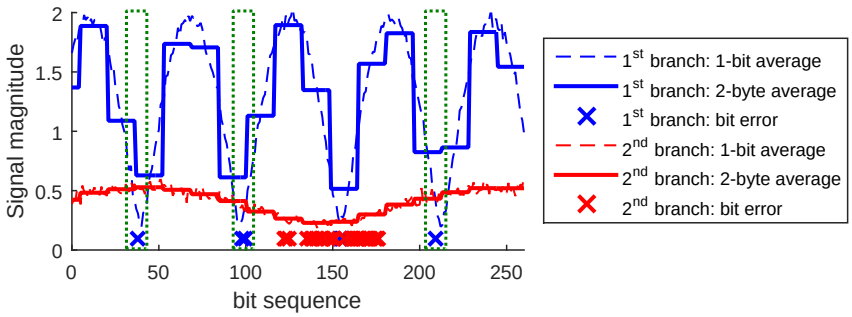

Fig. 4.8 Illustration of erroneous combining due to averaging of RSSI values.

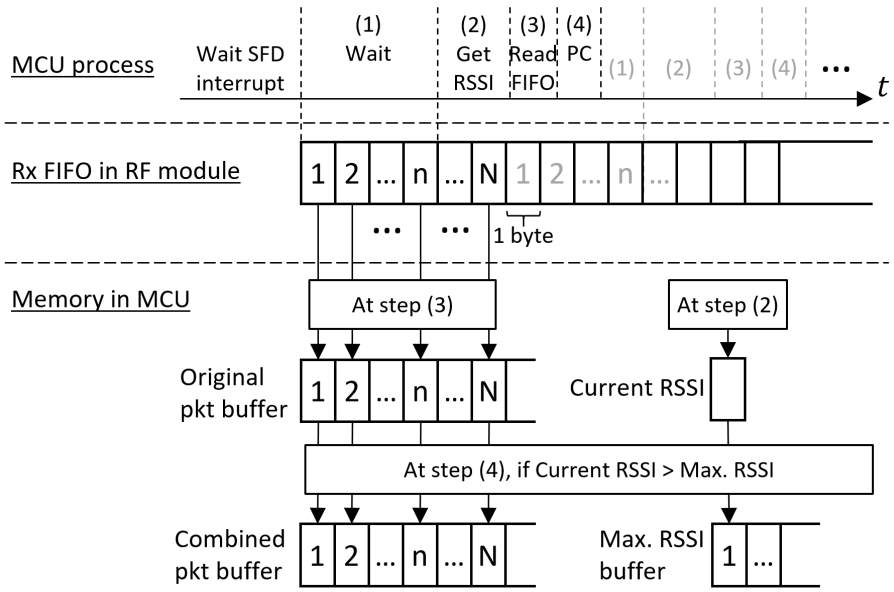

Fig. 4.9 Packet reception process with RSSS-based PC.

end of packet reception and causes no additional delay in the reception. As illustrated in Fig. 4.9, the reception process with RSSI-based PC follows these steps:

（1） Wait until there are n symbols inside the RX-FIFO. This step is required for compensating the execution delay of the next step.

（2） Acquire RSSI measurement.

（3） Read N symbols from the RX-FIFO into an original packet buffer.

（4） Perform RSSI-based combining.

In step (4), if the RSSI value measured in (2) is higher than the value in a maximum RSSI buffer at the corresponding symbols, the new maximum RSSI value and the N-symbol data read in (3) are stored into the maximum RSSI buffer and a combined packet buffer, respectively. At the end of packet reception, either the original packet buffer or the combined packet buffer will be copied to TX-FIFO for the transmission based on error check results. In contrast, the traditional process simply follows step (1) and (3) and needs only the original packet buffer.

(b) Proof-of-concept in TelosB

The CT scheme with RSSI-based PC is implemented on TelosB sensor nodes. Based on the timing verification, n and N are set to be 12 and 16, respectively. As $N = 16$ in IEEE 802.15.4, combining is performed at $f_S = 3.9$ kHz, and thus it is effective when $f_B < 2$ kHz.

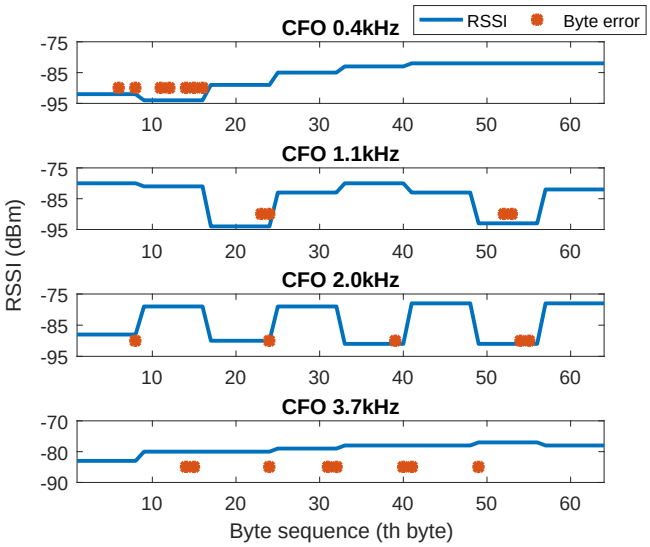

Fig. 4.10 Real-world examples of the beats observed by RSSI and the corresponding byte errors when $N = 16$.

By delaying the step (4) to the end of the reception, N can be reduced to 4. This is because the current implementation of the step (4) PC in TelosB involves in computation-heavy CRC calculation. With $N = 4$, the combining frequency f_S becomes $f_S = 15.6$ kHz.

Fig. 4.10 shows examples of the beat observed by RSSI values from TelosB in two-transmitter CT case when $N = 16$. As shown in Fig. 4.10, the beat with the corresponding CFO and the errors in low RSSI region can be verified. When CFO = 3.7 kHz, the beat is under sampled.

4.4 Evaluation

In this section, we first explain the simulation model, and then we discuss the evaluation results, which can be divided into 4 items.

（1） **Combining cycle period**: The relationship between the combining cycle period and the beat frequency is verified.

（2） **RSSI averaging period**: The relationship between the RSSI averaging period and the beat frequency is verified.

（3） **Performance in IEEE 802.15.4**: The reliability improvement provided by CT with RSSI-based PC is verified.

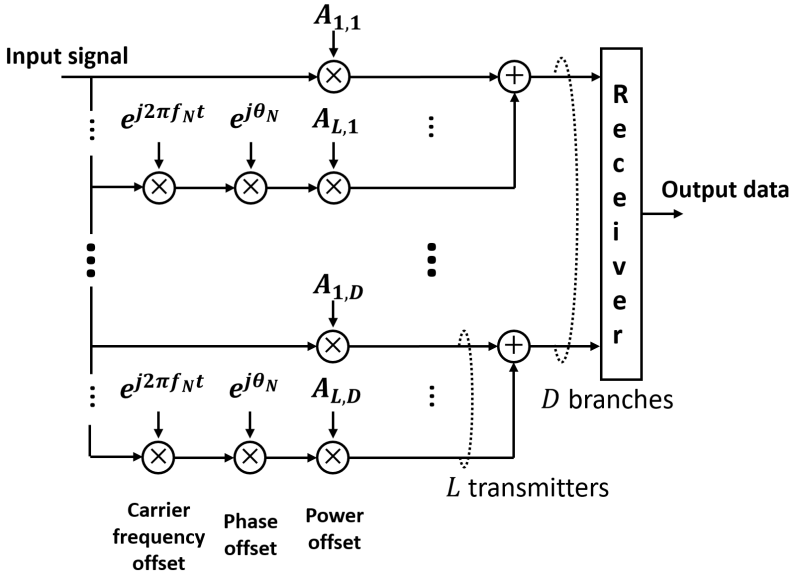

Fig. 4.11 Channel impairment model of CT with L transmitters and D branches of receive diversity.

(4) **Performance in IEEE 802.11 DSSS**: The necessity of RSSI-based PC for enabling CT in this standard is verified.

4.4.1 Simulation Model

We evaluate our proposal in CT environment in by simulation using MATLAB. The evaluation metric is packet error rate (PER). A packet which is received by multiple branches of diversity and also by PC is counted as success if at least one branch or the combining is successful. Throughout the evaluation, the packet length is set to be 20 and 64 bytes for IEEE 802.15.4 and IEEE 802.11 DSSS, respectively. With different packet lengths, the effect of evaluated parameters does not change significantly.

Note that the packet length is set to be longer in IEEE 802.11 DSSS due to its higher bit rate. IEEE 802.11 DSSS contains 4 levels of bit rates: 1, 2, 5.5, and 11 Mbps. The 1 and 2 Mbps physical-layer specifications are based on DSSS modulation using Barker code with the DSSS symbol rate of 1 mega symbols per second. On the other hand, the 5.5 and 11 Mbps standard uses complementary code keying (CCK) as its modulation technique which gives the symbol rate of 1.375 mega symbols per second. Without loss of generality, 2 and 11 Mbps standards can be representative of each modulation type and they will be adopted in this evaluation.

The simulation is based on the channel impairment model as shown in Fig. 4.11. To understand the effect of CT parameters on RSSI-based PC, we consider the two-transmitter ($L = 2$) CT model in Section 4.4.2 and 4.4.3. In Section 4.4.4 and 4.4.5, multiple-transmitter cases of CT are considered.

We sweep $\frac{E_B}{N_0}$ which is signal-to-noise ratio of the 1st-branch ($d = 1$) 1st-transmitter received signal to change the channel quality. The noise is modelled as additive white Gaussian noise (AWGN). In this simulation, the timing offset is assumed to zero. Timing and frequency synchronization of each branch's radio module are perfectly locked to the strongest 1st-transmitter signal.

4.4.2 Combining Cycle Period

In this section, we evaluate the effect of combining cycle period N in both IEEE 802.15.4 and IEEE 802.11 DSSS. This evaluation also reveals the effect of CFO to the performance of CT in both standards. Especially, in IEEE 802.11 DSSS, this CFO characteristic has not been studied before.

(a) IEEE 802.15.4

For evaluating the effect of combining cycle period N in IEEE 802.15.4, N is set to be 16, 8, 4, 2 and 1. Table 4.1 shows the relationship between N and corresponding combining frequencies and CFO limits. The beat frequency is varied in terms of CFO between two transmitters from 0.1 kHz to 100 kHz.

Fig. 4.12 shows the comparison of PER of a receiver with $D = 1$ and $D = 4$. When $D = 4$, "No combining" represents a receiver that does not perform RSSI-based PC. The $\frac{E_B}{N_0}$ and M are set to be 20 dB and 1, respectively.

The results verify the relationship between the corresponding combining frequencies and the CFO limits. In each case of N, when CFO reaches the limit, the improvement of PER disappears. In addition, N should be set as low as possible for obtaining the most desired performance; however, the lowest value of N in practice is constrained by the hardware performance as discussed in Section 4.3.4. Note that the $D = 1$ curve matches the previous study of CT in IEEE 802.15.4 [6].

Table 4.1 Relationship between combining cycle periods, corresponding combining frequencies, and CFO limits in IEEE 802.15.4.

N	f_S	CFO limit
16	3.9 kHz	2.0 kHz
8	7.8 kHz	3.9 kHz
4	15.6 kHz	7.8 kHz
2	31.3 kHz	15.6 kHz
1	62.5 kHz	31.3 kHz

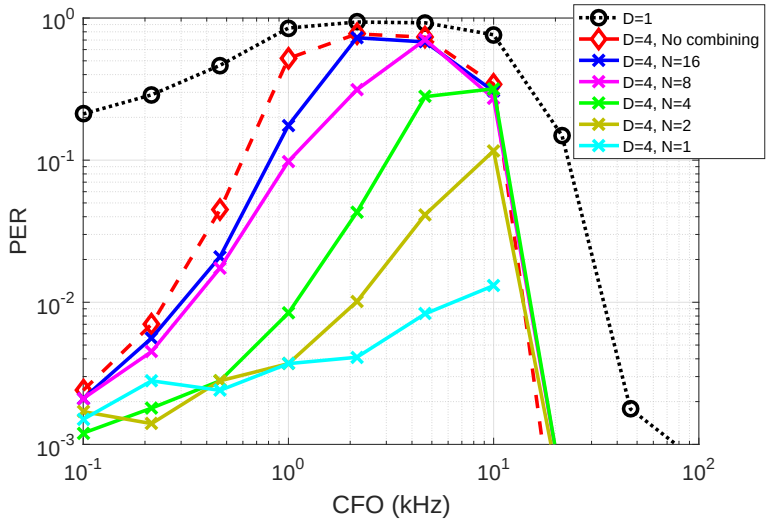

Fig. 4.12 Effects of combining period in IEEE 802.15.4.

(b) IEEE 802.11 DSSS

This section evaluates the effect of combining period and the CFO to the performance of CT with RSSI-based PC. We set the simulation as follows: the RSSI averaging period $M = 2$, $\frac{E_B}{N_0} = 12$ dB, and $D = 4$. Fig. 4.13 and 4.14 shows PER in each corresponding CFO of CT using 2 Mbps and 11 Mbps of IEEE 802.11, respectively. The effect of CFO is first discussed, then followed by the effect of combining period.

The results show that the CT without diversity (black dotted line) cannot survive in both cases. This is because the deep faded duration caused by a typical value of CFO is relative large compared the short symbol length of IEEE 802.11 DSSS. IEEE 802.11 allows the maximum frequency deviation to be ±25 ppm or approximately ±60 kHz, which gives the maximum CFO of 120 kHz. As observed by [6], the reciprocal of CFO, which represents the beating period, should be smaller than the symbol length to guarantee that most of

Table 4.2 Relationship between combining cycle periods, corresponding combining frequencies, and CFO limits in 1 and 2 Mbps of IEEE 802.11.

N	f_S	CFO limit
16	62.5 kHz	31.25 kHz
8	125 kHz	62.5 kHz
4	250 kHz	125 kHz
2	500 MHz	250 kHz
1	1000 kHz	500 kHz

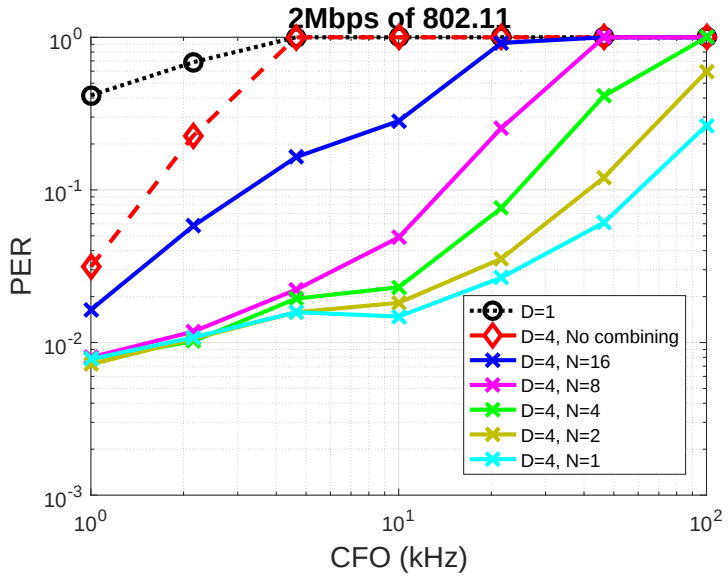

Fig. 4.13 Effects of combining period in 2 Mbps of IEEE 802.11 .

symbol time enjoys a non-faded signal. In particular, $\frac{1}{120kHz} = 8.3$ μs is far too large compared to 1-μs symbol length.

Moreover, the results show that even with 4 receiving branches ($D = 4$), the CT without RSSI-based PC still cannot provide low PER in high CFO region. This is because all received packets contain at least one error that makes the packet become error. In low CFO region, i.e., the beating period is longer than packet transmission time, the beat problem acts similar to slow fading where the packet-level diversity can help improving the performance.

With the help of RSSI-based PC, the improvement of PER can be clearly observed, where the smaller combining period N gives the bigger improvement. We set the combining

Table 4.3 Relationship between combining cycle periods, corresponding combining frequencies, and CFO limits in 5.5 and 11 Mbps of IEEE 802.11.

N	f_S	CFO limit
16	86 kHz	43 kHz
8	172 kHz	85.9 kHz
4	344 kHz	172 kHz
2	688 kHz	344 kHz
1	1375 kHz	688 kHz

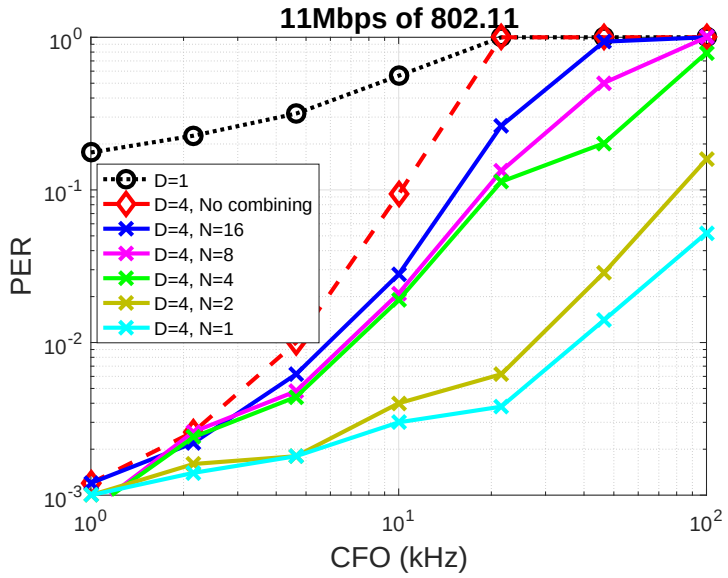

Fig. 4.14 Effects of combining period in 11 Mbps of IEEE 802.11.

period N to be 16, 8, 4, 2 and 1. The calculation of the CFO limit is shown in Table 4.2 and 4.3, and is confirmed by the simulation results.

4.4.3 RSSI Averaging Period

In this section, we evaluate the effect of RSSI averaging period M in IEEE 802.15.4 and IEEE 802.11 DSSS.

(a) IEEE 802.15.4

In order to see the effect of the negative-gain region, the CFO is linearly varied from 2 kHz to 20 kHz in this evaluation. The RSSI averaging period M is set to be 8, 4, 2, and

Table 4.4 Relationship between RSSI averaging periods and corresponding zero-gain frequencies in IEEE 802.15.4.

M	Zero-gain frequency
8	7.8 kHz
4	15.6 kHz
2	31.3 kHz
1	62.5 kHz

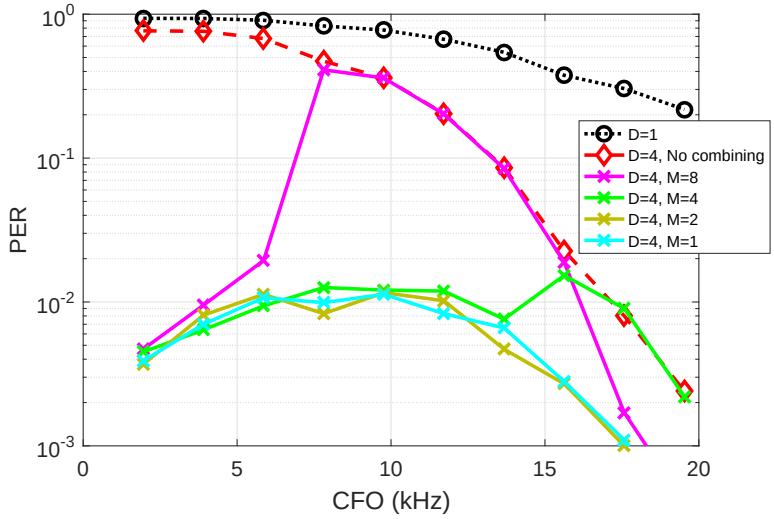

Fig. 4.15 Effects of RSSI averaging period in IEEE 802.15.4.

1. Table 4.4 shows the relationship between M and corresponding zero-gain frequencies. First, we study the effect of M in IEEE 802.15.4, and the number of diversity branches D is set to be 4. $\frac{E_B}{N_0}$ and M are set to be 20 dB and 1, respectively.

The results, as shown in Fig. 4.15, verify the effect of the negative-gain region, which starts when CFO is larger than a zero-gain frequency. In each case of M, when CFO falls in the corresponding negative-gain region, the improvement of PER disappears. In 802.15.4, the RSSI averaging period M is desired to be as low as possible.

(b) IEEE 802.11 DSSS

In this section, we test the RSSI averaging period M at M =32, 16, 8, 4 and 2 with varying CFO in IEEE 802.11 DSSS. The controlled parameters are set as follows: combining period $N = 1$, $\frac{E_B}{N_0} = 12$ dB, and $D = 4$. Table 4.5 and 4.6 shows the corresponding

Table 4.5 Relationship between RSSI averaging periods and corresponding zero-gain frequencies in 2 Mbps of IEEE 802.11.

M	Zero-gain frequency
32	31.25 kHz
16	62.5 kHz
8	125 kHz
4	250 kHz
2	500 kHz

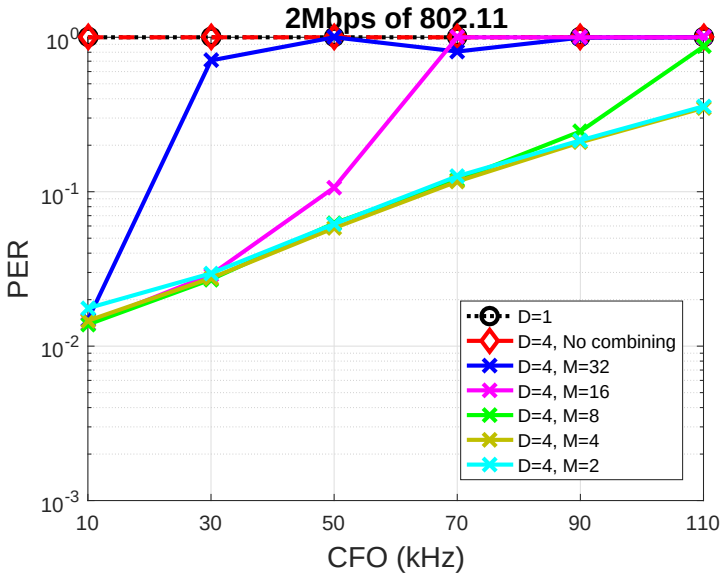

Fig. 4.16 Effects of RSSI averaging period in 2 Mpbs of IEEE 802.11.

zero-gain frequency of each RSSI averaging period M of 2 Mbps and 11 Mbps IEEE 802.11 standards, respectively.

Fig. 4.16 and 4.17 shows PER in each corresponding CFO of CT using 2 Mbps and 11 Mbps of IEEE 802.11, respectively. The simulation results verify that the RSSI-based PC cannot successfully combine packets when the CFO falls into the negative-gain frequency region. In addition, the RSSI averaging period M=4 is sufficient to provide good performance in the typical CFO region defined by IEEE 802.11 standards.

Table 4.6 Relationship between RSSI averaging periods and corresponding zero-gain frequencies in 11 Mbps of IEEE 802.11.

M	Zero-gain frequency
32	43 kHz
16	85.9 kHz
8	172 kHz
4	344 kHz
2	688 kHz

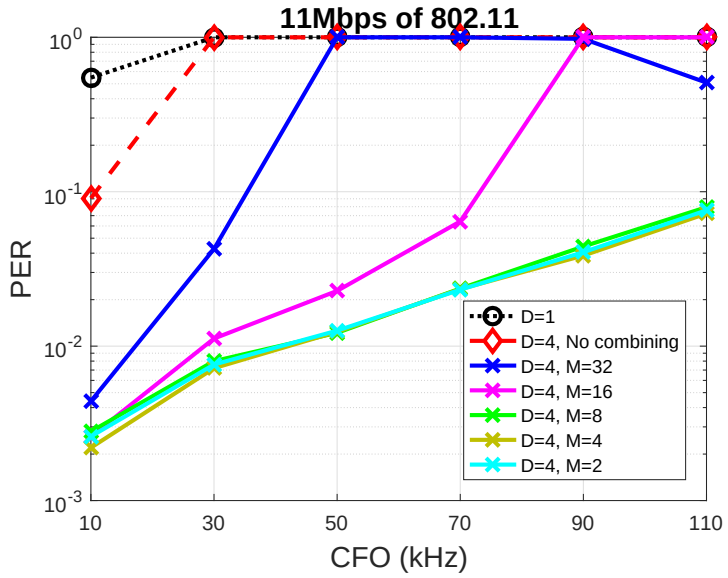

Fig. 4.17 Effects of RSSI averaging period in 11 Mpbs of IEEE 802.11.

4.4.4 Performance in IEEE 802.15.4

In this section, we evaluate the performance improvement provided by CT with RSSI-based PC in IEEE 802.15.4 physical-layer specifications. The evaluation is performed by using simulation and experiments based on the proof-of-concept implementation, as discussed in Section 4.3.4. The performance of CT itself in IEEE 802.15.4 has been proved to be good, and here we evaluate the further improvement given the RSSI-based PC.

(a) Simulation

In simulation, we study CT with a number of transmitters varying from 1 to 32 transmitters, where a channel from each transmitter to each branch of a receiver has random

gain A (depicted in Fig. 4.11) in Rayleigh distribution. The carrier frequency is assumed to be normal distribution with standard deviation of 19.2 kHz. This number is set according to the measurement from 80 TelosB nodes, and is equivalent to one-fifth of the maximum frequency deviation allowed by IEEE 802.15.4. Note that the IEEE 802.15.4 allows the maximum frequency deviation at ±40 ppm or approximately ±96 kHz for 2.4-GHz carrier frequency. N and M are set to be 1 in this simulation to investigate the upper-bound performance.

Fig. 4.18 (a) and (b) show the PER vs $\frac{E_b}{N_0}$ curve when $D = 2$ and $D = 4$, respectively. RSSI-based PC can provide 1-2 dB gain compared to a simple diversity scheme, which does not perform RSSI-based PC.

In addition, we investigate the search-based PC which performs exhaustive search to achieve an ideal combining. The ideal combining is assumed to achieve perfect error correction where a bit difference is detected. Fig. 4.19 shows the comparison between our proposed algorithm and the ideal algorithm when $D = 8$. The results show that our proposed method trades the reliability improvement for the practical complexity as discussed in Section 4.2. In the following section, we show the feasibility of our proposal in CT environments.

(b) Experiments

We perform an experiment to verify the simulation result and the feasibility of our proposal implemented on TelosB nodes. We create the CT environment with different f_B by using two TelosB nodes. Their carrier frequencies are confirmed before the experiments by using a spectrum analyzer. The transmission power is set to be -15 dBm. As shown in Fig. 4.20, receivers are put indoor at 24 locations with a distance from 8 meters from the transmitter pair. RSSI-based PC is performed with combining period $N = 4$ and RSSI averaging period $M = 8$. Therefore, the corresponding CFO limit is 7.8 kHz.

Fig. 4.21 show the experiment results in terms of average PER taken from all receivers. The lower plot depicts the PER improvement ratio, which is defined as the ratio between the PER when RSSI-based PC is not applied to the PER when RSSI-based PC is applied. The experiment results confirm the feasibility of RSSI-based PC in practice. Note that the PER between different CFO cases cannot be compared because signal power in each case is varied due to channel fluctuation and part-to-part differences among TelosB nodes.

Moreover, the use of RSSI makes the performance sensitive to co-channel interferences, which may falsify RSSI-based PC. The use of RSSI for detecting co-channel interference

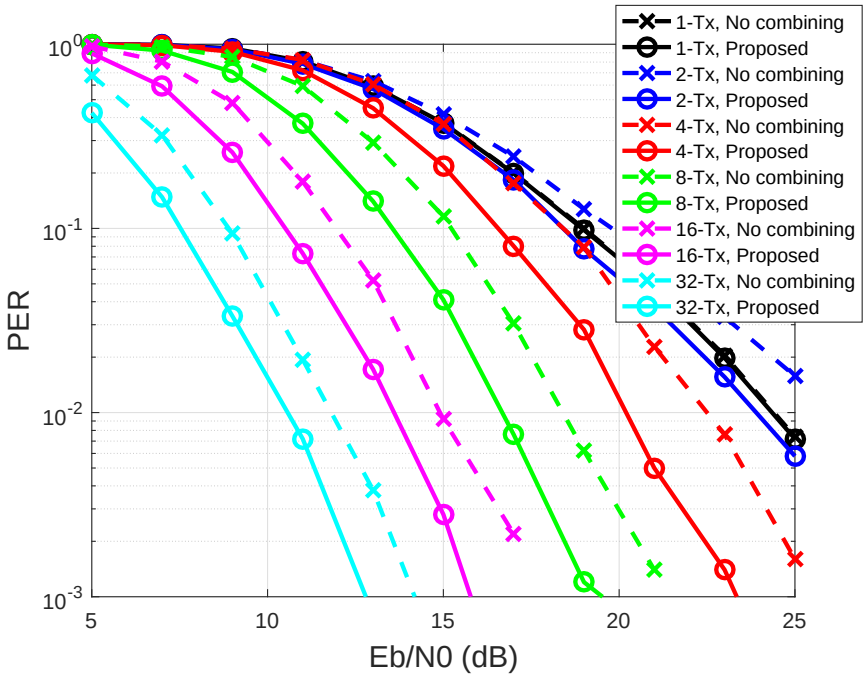

(a) $D = 2$.

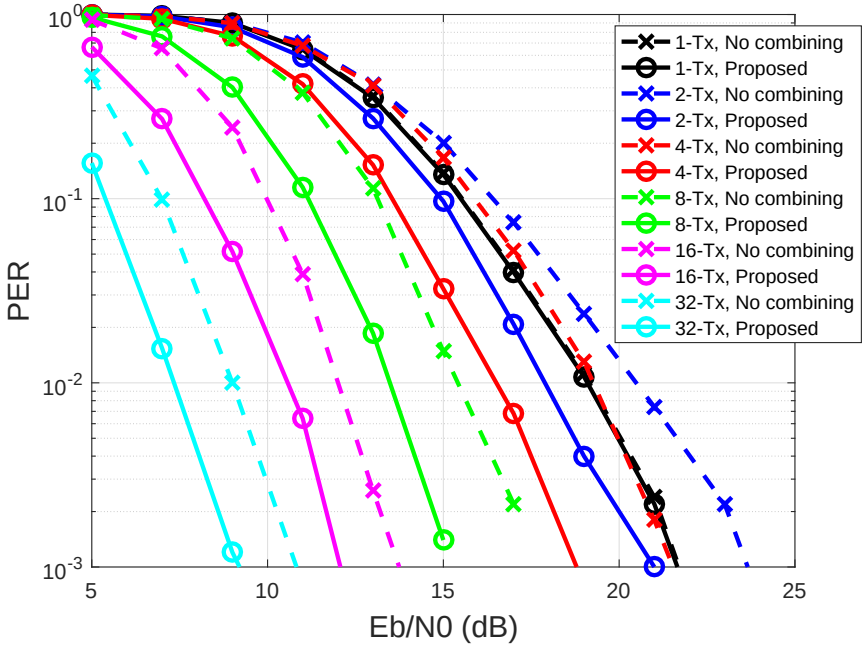

(b) $D = 4$.

Fig. 4.18 Performance of CT with RSSI-based PC in IEEE 802.15.4.

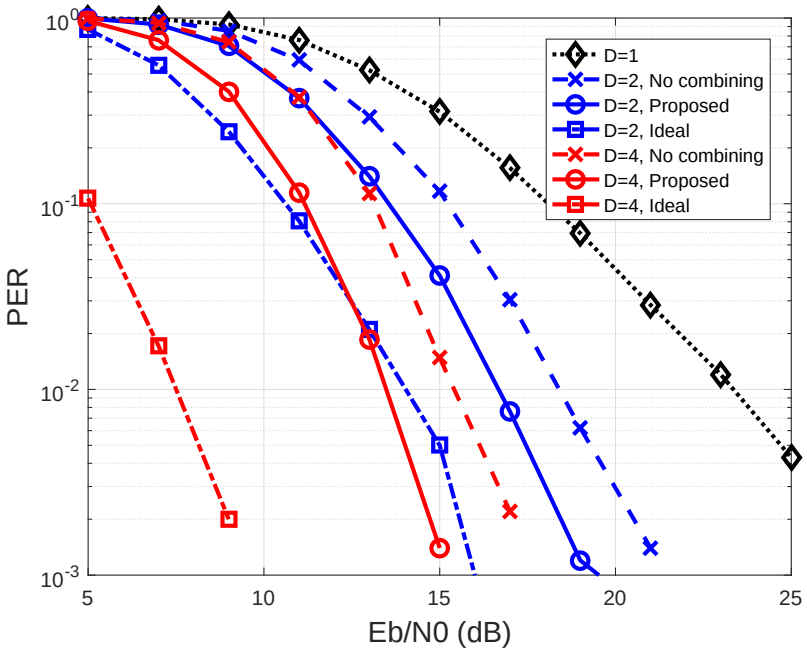

Fig. 4.19 Comparison with an ideal combining using exhaustive search.

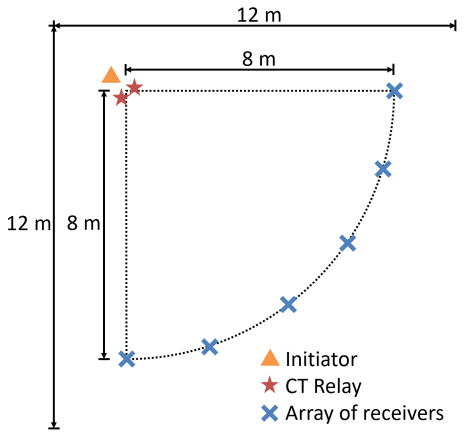

Fig. 4.20 Experiment setup.

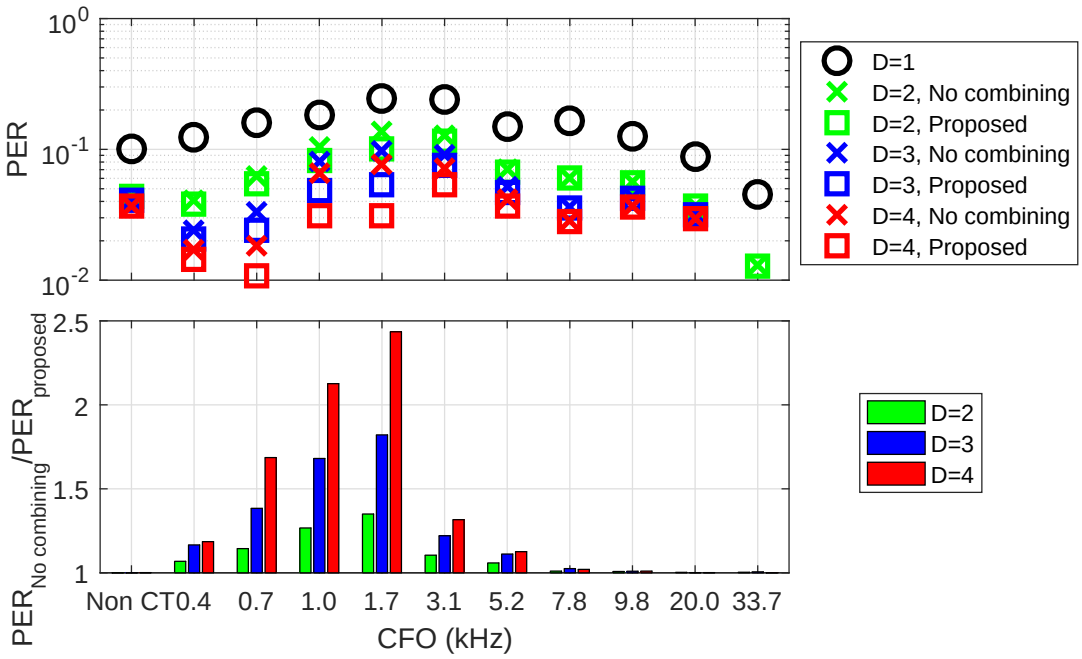

Fig. 4.21 Experimental results of RSSI-based PC.

and performing interference-aware PC could be a future work. Readers may refer to [80] regarding co-channel interference detection using RSSI.

4.4.5 Performance in IEEE 802.11 DSSS

This section evaluates the performance of CT with RSSI-based PC in IEEE 802.11 DSSS systems. Since the short symbol time of IEEE 802.11 is weak to the beat problem, CT

does not originally survive in IEEE 802.11 DSSS. We can expect RSSI-based PC to play an important role on enabling CT in this standard.

According to the understanding on the relationship of the beat frequency to the combining and RSSI averaging period from Section 4.4.2 and 4.4.3, we set N and M to be 1 and 4 symbols, respectively. IEEE 802.11 allows the maximum frequency deviation to ± 60 kHz. The carrier frequency is random by normal distribution with standard deviation of 12 kHz [*2].

In this evaluation, we first study the performance of CT with multiple transmitters (1, 2, 4, 8, and 16 transmitters) when RSSI-based PC is adopted. Fig. 4.22 and 4.23 show the PER results of systems with 2 Mbps and 11 Mbps transmission setting, respectively. In each of them, we separate the plots to (a) when RSSI-based PC is not applied and (b) when RSSI-based PC is applied. The results prove that RSSI-based PC is necessary to enable CT in IEEE 802.11 DSSS systems.

With 2-Mbps data rate, a 64-byte packet is usually longer than the beat period and this makes the received packet mostly fail to be decoded. Adding more transmitters results in shorter beat period and more frequent fading regions, thus further degrades the performance. Given the same packet length, 11-Mbps modulated packets takes significantly shorter time such that the packet length might be shorter than the beat period, which helps the demodulation of non-faded packets.

Next, we study the diversity gain by adding different numbers of diversity branches, i.e., $D = 1$, 2, and 4. We set the number of transmitters to be 8. Fig. 4.24 (a) and 4.24 (b) shows the PER of the 2 Mbps and 11 Mbps settings, respectively. The results show that more diversity branches can significantly reduce the error floor. In particular, the PER floor can drop lower than 10^{-3} when $D = 4$ is applied. This is because an extra diversity helps the receiver to receive different fading patterns of an identical signal and increase the change of successful combining.

4.5 Summary

In this chapter, we have proposed symbol-level PC using RSSI to alleviate a beat problem of CT. We have discussed not only the concept but also some important parameters

[*2] Based on the measurements of devices compliant with IEEE 802.15.4, the standard deviation is modelled to be one-fifth of the maximum frequency deviation.

which can affect the performance of RSSI-based PC. In addition, we show our implementation method and also verify it by porting it to off-the-shelf sensor nodes to show the feasibility in practice. The proposal is verified by computer simulations and hardware experiments. The results show that RSSI-based PC can significantly improve the reception reliability in both IEEE 802.15.4 and IEEE 802.11 DSSS specifications.

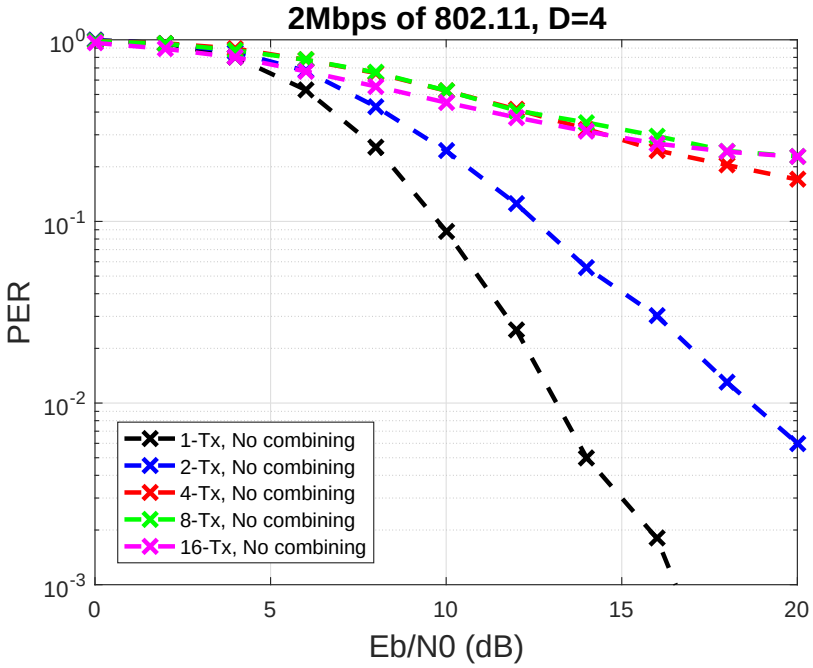

(a) No PC.

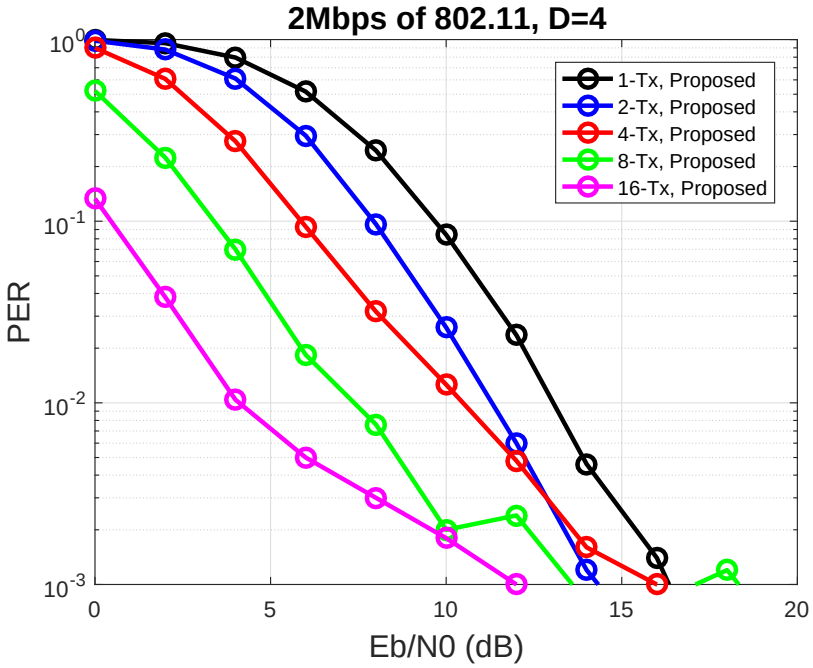

(b) RSSI-based PC.

Fig. 4.22 Performance of CT with RSSI-based PC in 2 Mbps of IEEE 802.11

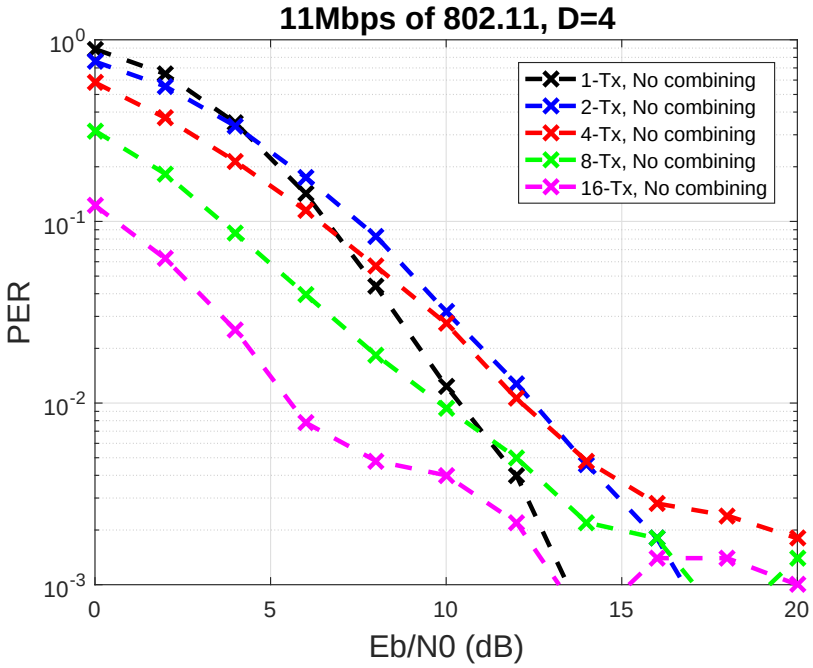

(a) No PC.

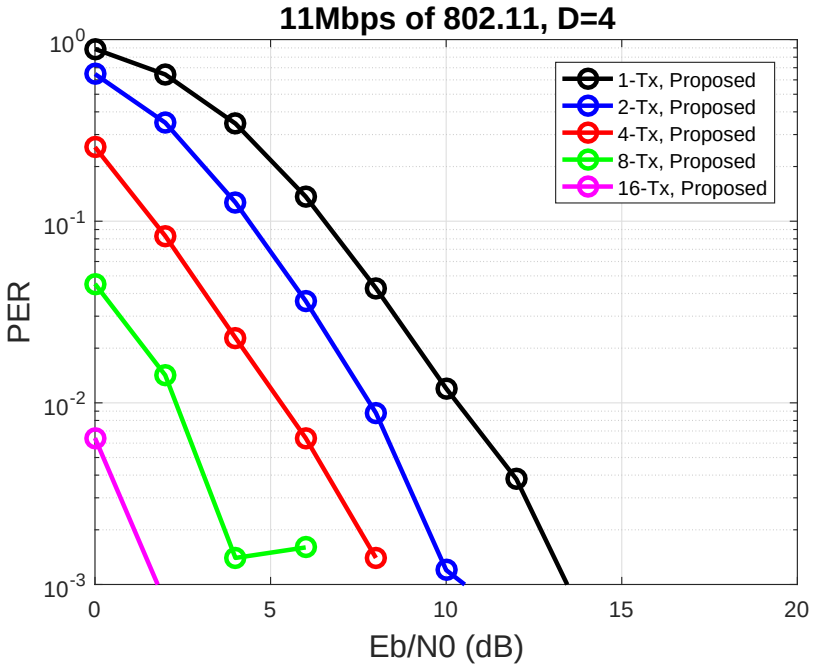

(b) RSSI-based PC.

Fig. 4.23 Performance of CT with RSSI-based PC in 11 Mbps of IEEE 802.11

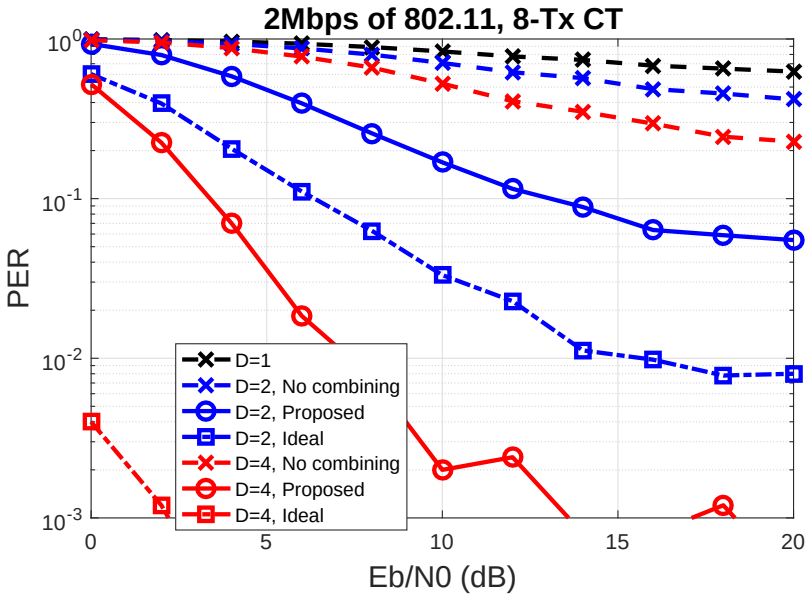

(a) 2 Mbps.

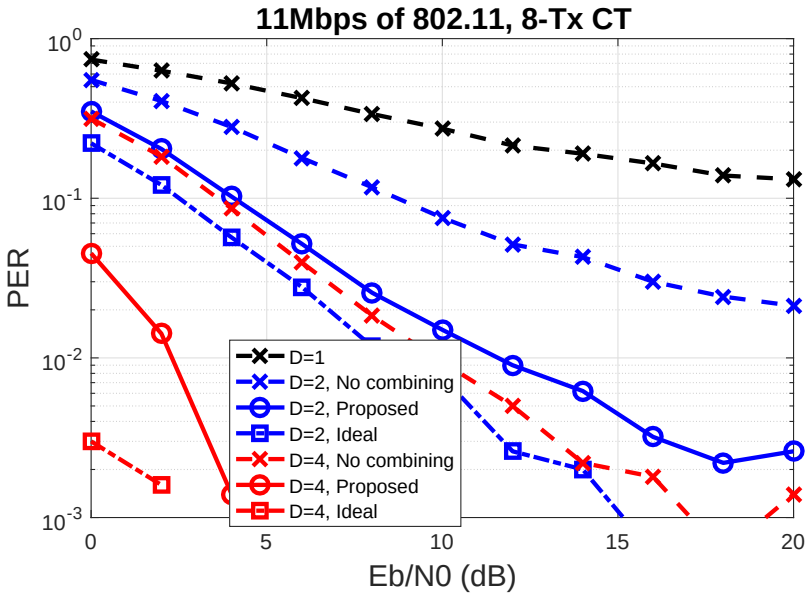

(b) 11 Mbps.

Fig. 4.24 PER improvement with different diversity branches in IEEE 802.11.

Chapter 5

Conclusions

5.1 Summary of This Thesis

In this thesis, we have addressed real-time and reliable industrial wireless communications via physical-layer approaches. To this end, we have clarified important mechanisms required in industrial wireless communications by means of investigation on related works. Previous studies are however limited to higher-layer design and still insufficient in terms of the real-time capability. This thesis has discussed the reduction of physical-layer transmission overheads including preamble transmission and transmit cooperation for improving the real-time capability, while maintaining good reliability. In particular, we have proposed

(1) **Subcarrier-selectable short preambles for real-time OFDM systems**

A subcarrier-selectable short preamble (SSSP) is proposed by introducing selectability to subcarrier sampling patterns, in such a way that it can provide full sampling coverage of all subcarriers. Compared to previous works which adopt either time-domain or frequency-domain channel correlation for channel estimation, the channel estimation by the SSSP is improved in fast fading channels and frequency-selective fading channels.

In addition to the preamble shortening method and preamble recovery method, we introduce adaptability to a channel estimation algorithm for the SSSP. Thus, the channel estimation of SSSP conforms to both fast and frequency-selective channels.

The proposed short preamble and the channel estimation algorithm are evaluated to validate the feasibility of the proposed method in terms of both reliability and real-time capability.

(2) **RSSI-based packet combining for reliable concurrent transmission**

RSSI-based packet combining is proposed to achieve not only real-time but also reliable concurrent transmission (CT). It adopts RSSI for post-decision symbol-level selection combining of multiple packets received by receive antenna diversity. By this way, not only the low-latency characteristic of CT can be preserved, but the extremely fast fading caused by the beat problem can also be solved.

Along with the proposal, we analyze the performance of the RSSI-based packet combining under CT environments. In particular, the effects of the combining cycle period and the RSSI averaging period on the error performance are studied. In addition, the lightweight on-the-fly combining process has been designed and implemented in off-the-shelf resource-constrained wireless nodes for proof of concept. This becomes possible because of the use of RSSI values, which allows us to promptly locate error-sensitive symbols.

The evaluation of the RSSI-based packet combining is conducted by computer simulation and real-world experiments. Essentially, CT with packet combining provides significant reliability improvement over a single-antenna system, while preserving real-time capability.

5.2 Future Works

This section suggests research items, which have not been addressed in this research and can be future extensions.

(1) **Experiments in factory environments**

Real-world testing is suggested to verify the simulation. In order to overcome channel model mismatch used in the simulation, experiments in factory environments can rather provide practical aspects in the performance evaluation.

(2) **Optimal SSSP patterns for timing and frequency synchronization**

A study of SSSP patterns is essential to achieve a robust synchronization performance. Although traditional algorithms for timing and frequency synchronization seems to be applicable to SSSP, the correlation-based algorithms need an optimal design of SSSP patterns to obtain a narrow plateau of correlation function for the accurate synchronizations.

(3) **Packet combining with tolerance to co-channel interference**

With the possibility of the coexistence in co-channel interference, RSSI values can be also used to detect and avoid the interference in symbol level. In addition to other interference mitigating mechanisms such as frequency hopping, a packet combining algorithm can adopt RSSI values to locate the interference and select less error-prone symbol to more likely receive a successful packet.

Acknowledgments

This research is properly achieved owing to good support from my supervisor. I would like to express my deepest gratitude to Professor Hiroyuki Morikawa for his guidance and persistent supports regarding researches and scholarships. I also appreciate invaluable advices and research guidance given by the former Research Associate of Morikawa Laboratory, Dr. Makoto Suzuki, and also the current Research Associate, Dr. Yoshiaki Narusue.

In addition, I would like to thank to all committee members who spend time checking and approving this dissertation as well as giving invaluable and constructive comments. Thank you to all of my friends in Morikawa Laboratory who have been assisting me. I appreciate not only their kind helps and friendly working atmosphere but also helpful life-related suggestions. Finally, I would like to gratefully thank you my family and friends, who always support and inspire me in every possible way.

Theerat Sakdejayont

June 2017

References

[1] C. Roser, "A critical look at industry 4.0," http://www.allaboutlean.com/industry-4-0/.

[2] "Framework and overall objectives of the future development of IMT for 2020 and beyond," *Draft New Recommendation ITU-R M, 22nd Meeting of Working Party 5D*, Jun. 2015.

[3] G. J. Pappas, "Wireless control networks: Modeling, synthesis, robustness, security," in *Proc. 14th International Conference on Hybrid Systems: Computation and Control (HSCC 2011)*, pp. 1–2, Apr. 2011.

[4] R. Zurawski, *Industrial communication technology handbook*. CRC Press, 2014.

[5] A. Buda, V. Schuermann, and J. F. Wollert, "Wireless technologies in factory automation," in *Factory Automation*. InTech, 2010.

[6] C. H. Liao, Y. Katsumata, M. Suzuki, and H. Morikawa, "Revisiting the so-called constructive interference in concurrent transmission," in *Proc. IEEE 41st Conference on Local Computer Networks (LCN 2016)*, pp. 280–288, Nov. 2016.

[7] P. Neumann, "Communication in industrial automation - what is going on?" *Control Engineering Practice*, vol. 15, no. 11, pp. 1332–1347, Nov. 2007.

[8] J. P. Thomesse, "Fieldbus technology in industrial automation," *Proceedings of the IEEE*, vol. 93, no. 6, pp. 1073–1101, Jun. 2005.

[9] B. Galloway and G. P. Hancke, "Introduction to industrial control networks." *IEEE Communications Surveys and Tutorials*, vol. 15, no. 2, pp. 860–880, 2013.

[10] P. A. Wiberg and U. Bilstrup, "Wireless technology in industry - applications and user scenarios," in *Proc. 8th IEEE International Conference on Emerging Technologies and Factory Automation (ETFA 2001)*, pp. 123–131, Oct. 2001.

[11] A. Frotzscher, U. Wetzker, M. Bauer, M. Rentschler, M. Beyer, S. Elspass, and H. Klessig, "Requirements and current solutions of wireless communication in industrial automation," in *Proc. IEEE International Conference on Communications Workshops (ICC 2014)*, pp. 67–72, Jun. 2014.

[12] A. Treytl, T. Sauter, and C. Schwaiger, "Security measures for industrial fieldbus systems – state of the art and solutions for ip-based approaches," in *Proc. IEEE International Workshop on Factory Communication Systems (WFCS 2004)*, pp. 201–209, Sep. 2004.

[13] D. Christin, P. S. Mogre, and M. Hollick, "Survey on wireless sensor network technologies for industrial automation: The security and quality of service perspectives," *Future Internet*, vol. 2, no. 2, pp. 96–125, Apr. 2010.

[14] I. F. Akyildiz, W. Su, Y. Sankarasubramaniam, and E. Cayirci, "A survey on sensor networks," *IEEE Communications magazine*, vol. 40, no. 8, pp. 102–114, Aug. 2002.

[15] G. Anastasi, M. Conti, M. Di Francesco, and A. Passarella, "Energy conservation in wireless sensor networks: A survey," *Ad hoc networks*, vol. 7, no. 3, pp. 537–568, May 2009.

[16] A. Willig, K. Matheus, and A. Wolisz, "Wireless technology in industrial networks," *Proceedings of the IEEE*, vol. 93, no. 6, pp. 1130–1151, Jun. 2005.

[17] P. Stenumgaard, J. Chilo, J. Ferrer-Coll, and P. Angskog, "Challenges and conditions for wireless machine-to-machine communications in industrial environments," *IEEE Communications Magazine*, vol. 51, no. 6, pp. 187–192, Jun. 2013.

[18] T. S. Rappaport, "Indoor radio communications for factories of the future," *IEEE Communications Magazine*, vol. 27, no. 5, pp. 15–24, May 1989.

[19] A. Willig, M. Kubisch, C. Hoene, and A. Wolisz, "Measurements of a wireless link in an industrial environment using an IEEE 802.11-compliant physical layer," *IEEE Transactions on Industrial Electronics*, vol. 49, no. 6, pp. 1265–1282, Dec. 2002.

[20] E. Tanghe, W. Joseph, L. Verloock, L. Martens, H. Capoen, K. Van Herwegen, and W. Vantomme, "The industrial indoor channel: large-scale and temporal fading at 900, 2400, and 5200 MHz," *IEEE Transactions on Wireless Communications*, vol. 7, no. 7, Jul. 2008.

[21] X. Li, D. Li, J. Wan, A. V. Vasilakos, C.-F. Lai, and S. Wang, "A review of industrial wireless networks in the context of industry 4.0," *Wireless networks*, vol. 23, no. 1, pp. 23–41, Jan. 2017.

[22] R. Steigmann and J. Endresen, "Introduction to WISA," white paper, ABB, 2006.

[23] Siemens AG, "Industrial wireless LAN," http://w3.siemens.com/mcms/industrial-communication/en/industrial-wireless-communication/iwlan-industrial-wireless-lan/pages/iwlan.aspx.

[24] "Wireless HART," http://en.hartcomm.org/.

[25] "ISA100.11," http://www.isa.org/isa100/.

[26] M. Nixon, "A comparison of WirelessHART and ISA100. 11a," *Whitepaper, Emerson Process Management*, pp. 1–36, Sep. 2012.

[27] Y.-H. Wei, Q. Leng, S. Han, A. K. Mok, W. Zhang, and M. Tomizuka, "RT-WiFi: Real-time high-speed communication protocol for wireless cyber-physical control applications," in *Proc. IEEE 34th Real-Time Systems Symposium (RTSS 2013)*, pp. 140–149, Dec. 2013.

[28] R. Viegas, L. A. Guedes, F. Vasques, P. Portugal, and R. Moraes, "A new MAC scheme specifically suited for real-time industrial communication based on IEEE 802.11e," *Computers & Electrical Engineering*, vol. 39, no. 6, pp. 1684–1704, Aug. 2013.

[29] M. Weiner, M. Jorgovanovic, A. Sahai, and B. Nikolie, "Design of a low-latency, high-reliability wireless communication system for control applications," in *Proc. IEEE International Conference on Communications (ICC 2014)*, pp. 3829–3835, Jun. 2014.

[30] D. K. Lam, Y. Shinozaki, K. Yamaguchi, S. Morita, Y. Nagao, M. Kurosaki, and H. Ochi, "A fast and safe industrial WLAN communication protocol for factory automation control systems," *Transactions of the Institute of Systems, Control and Information Engineers*, vol. 29, no. 1, pp. 29–39, Apr. 2016.

[31] N. A. Johansson, Y.-P. E. Wang, E. Eriksson, and M. Hessler, "Radio access for ultra-reliable and low-latency 5G communications," in *Proc. IEEE International Conference on Communication Workshop (ICCW 2015)*, pp. 1184–1189, Sep. 2015.

[32] C. Dombrowski and J. Gross, "EchoRing: a low-latency, reliable token-passing MAC protocol for wireless industrial networks," in *Proc. 21th European Wireless Conference*, pp. 1–8, May 2015.

[33] S. P. Karanam, H. Trsek, and J. Jasperneite, "Potential of the HCCA scheme defined in IEEE802.11e for QoS enabled industrial wireless networks," in *Proc. IEEE International Workshop on Factory Communication Systems (WFCS 2006)*, pp. 227–230, Jun. 2006.

[34] F. De Pellegrini, D. Miorandi, S. Vitturi, and A. Zanella, "On the use of wireless networks at low level of factory automation systems," *IEEE Transactions on Industrial Informatics*, vol. 2, no. 2, pp. 129–143, May 2006.

[35] G. Scheible, D. Dzung, J. Endresen, and J. E. Frey, "Unplugged but connected [design and implementation of a truly wireless real-time sensor/actuator interface]," *IEEE Industrial Electronics Magazine*, vol. 1, no. 2, pp. 25–34, Jul. 2007.

[36] X. Zhu, S. Han, P.-C. Huang, A. K. Mok, and D. Chen, "Mbstar: A real-time communication protocol for wireless body area networks," in *Proc. 23rd Euromicro Conference on Real-Time Systems (ECRTS 2011)*, pp. 57–66, Jul. 2011.

[37] W. Shen, T. Zhang, M. Gidlund, and F. Dobslaw, "SAS-TDMA: A source aware scheduling algorithm for real-time communication in industrial wireless sensor networks," *Wireless networks*, vol. 19, no. 6, pp. 1155–1170, Aug. 2013.

[38] D. Yang, Y. Xu, H. Wang, T. Zheng, H. Zhang, H. Zhang, and M. Gidlund, "Assignment of segmented slots enabling reliable real-time transmission in industrial wireless sensor networks," *IEEE Transactions on Industrial Electronics*, vol. 62, no. 6, pp. 3966–3977, Jun. 2015.

[39] W. Zhang, Y.-H. Wei, Q. Leng, and S. Han, "A high-speed, real-time mobile gait rehabilitation system," *The ACM Magazine for Students XRDS: Crossroads*, vol. 20, no. 3, pp. 46–51, Spring 2014.

[40] J. Zhang, J. Wu, Z. Han, L. Liu, K. Tian, and J. Dong, "Low power, accurate time synchronization MAC protocol for real-time wireless data acquisition," *IEEE Transactions on Nuclear Science*, vol. 60, no. 5, pp. 3683–3688, Oct. 2013.

[41] J. Silvo, L. M. Eriksson, M. Bjorkbom, and S. Nethi, "Ultra-reliable and real-time communication in local wireless applications," in *Proc. 39th Annual Conference of the IEEE Industrial Electronics Society (IECON 2013)*, pp. 5611–5616, Nov. 2013.

[42] E. Uhlemann and L. K. Rasmussen, "Incremental redundancy deadline dependent coding for efficient wireless real-time communications," in *Proc. 10th IEEE Conference on Emerging Technologies and Factory Automation (ETFA 2005)*, vol. 2, pp. 417–424, Sep. 2005.

[43] R. Blind and F. Allgöwer, "Is it worth to retransmit lost packets in networked control systems?" in *Proc. IEEE 51st Annual Conference on Decision and Control (CDC 2012)*, pp. 1368–1373, Dec. 2012.

[44] A. Willig, "How to exploit spatial diversity in wireless industrial networks," *Annual Reviews in Control*, vol. 32, no. 1, pp. 49–57, Apr. 2008.

[45] O. N. Yilmaz, Y.-P. E. Wang, N. A. Johansson, N. Brahmi, S. A. Ashraf, and J. Sachs, "Analysis of ultra-reliable and low-latency 5G communication for a factory automation use case," in *Proc. IEEE International Conference on Communication Workshop (ICCW 2015)*, pp. 1190–1195, Sep. 2015.

[46] A. Petropulu, R. Zhang, and R. Lin, "Blind OFDM channel estimation through simple linear precoding," *IEEE Transactions on Wireless Communications*, vol. 3, no. 2, pp. 647–655, Mar. 2004.

[47] M. C. Necker and G. L. Stuber, "Totally blind channel estimation for OFDM on fast varying mobile radio channels," *IEEE Transactions on Wireless Communications*, vol. 3, no. 5, pp. 1514–1525, Oct. 2004.

[48] F. Tufvesson and T. Maseng, "Pilot assisted channel estimation for OFDM in mobile cellular systems," in *Proc. IEEE 47th Vehicular Technology Conference (VTC 1997)*, vol. 3, pp. 1639–1643, May 1997.

[49] L. C. Godara, "Application of antenna arrays to mobile communications. II. Beamforming and direction-of-arrival considerations," *Proceedings of the IEEE*, vol. 85, no. 8, pp. 1195–1245, Aug. 1997.

[50] S. M. Alamouti, "A simple transmit diversity technique for wireless communications," *IEEE Journal on Selected Areas in Communications*, vol. 16, no. 8, pp. 1451–1458, Oct. 1998.

[51] W. Su, X.-G. Xia, and K. R. Liu, "A systematic design of high-rate complex orthogonal space-time block codes," *IEEE Communications Letters*, vol. 8, no. 6, pp. 380–382, Jun. 2004.

[52] K. Chutisemachai, T. Sakdejayont, C. H. Liao, M. Suzuki, and H. Morikawa, "Distributed antenna system using concurrent transmission for wireless automation system," in *Proc. IEEE 86th Vehicular Technology Conference (VTC 2017-Fall)*, Sep. 2017, (To appear).

[53] F. Ferrari, M. Zimmerling, L. Thiele, and O. Saukh, "Efficient network flooding and time synchronization with Glossy," in *Proc. ACM/IEEE 10th International Conference on Information Processing in Sensor Networks (IPSN 2011)*, pp. 73–84, Apr. 2011.

[54] M. Suzuki, Y. Yamashita, and H. Morikawa, "Low-power, end-to-end reliable collection using Glossy for wireless sensor networks," in *Proc. IEEE 77th Vehicular Technology Conference (VTC 2013-Spring)*, pp. 1–5, Jun. 2013.

[55] R. Petrovic and S. R. Filipovic, "Error floors of digital FM in simulcast and Rayleigh fading," *IEEE Transactions on Vehicular Technology*, vol. 47, no. 3, pp. 954–960, Aug. 1998.

[56] S. Souissi, S. Sek, and H. Xie, "The effect of frequency offsets on the performance of FLEX (R) simulcast systems," in *Proc. IEEE 49th Vehicular Technology Conference (VTC 1999)*, vol. 3, pp. 2348–2352, May 1999.

[57] "IEEE standard for information technology- telecommunications and information exchange between systems- local and metropolitan area networks- specific requirements part ii: Wireless lan medium access control (MAC) and physical layer (PHY) specifications," *IEEE Std 802.11g-2003*, pp. i–67, Jun. 2003.

[58] B. Ai, Z. X. Yang, C. Y. Pan, J. H. Ge, Y. Wang, and Z. Lu, "On the synchronization techniques for wireless OFDM systems," *IEEE Transactions on Broadcasting*, vol. 52, no. 2, pp. 236–244, Jun. 2006.

[59] A. V. Oppenheim, R. W. Schafer, and J. R. Buck, *Discrete-Time Signal Processing*, 3rd ed. Prentice Hall, 2010, ch. 8.

[60] H. Minn, V. K. Bhargava, and K. B. Letaief, "A combined timing and frequency synchronization and channel estimation for OFDM," *IEEE Transactions on Communications*, vol. 54, no. 3, pp. 416–422, Jun. 2006.

[61] T. J. Liang, W. Rave, and G. Fettweis, "On preamble length of OFDM-WLAN," in *Proc. 65th IEEE Vehicular Technology Conference (VTC 2007-Spring)*, pp. 2291–2295, Apr. 2007.

[62] J. J. van de Beek, M. Sandell, and P. O. Borjesson, "ML estimation of time and frequency offset in OFDM systems," *IEEE Transactions on Signal Processing*, vol. 45, no. 7, pp. 1800–1805, Jul. 1997.

[63] R. Mo, Y. H. Chew, T. T. Tjhung, and C. C. Ko, "A new blind joint timing and frequency offset estimator for OFDM systems over multipath fading channels," *IEEE Transactions on Vehicular Technology*, vol. 57, no. 5, pp. 2947–2957, Sep. 2008.

[64] Y. Wang, L. Yaroslavsky, and M. Vilermo, "On the relationship between MDCT, SDFT and DFT," in *Proc. 5th International Conference on Signal Processing (WCCC-ICSP)*, pp. 44–47, Aug. 2000.

[65] R. Van Nee and A. De Wild, "Reducing the peak-to-average power ratio of OFDM," in *Proc. 48th IEEE Vehicular Technology Conference (VTC 1998)*, pp. 2072–2076, May 1998.

[66] G. Liu, L. Zeng, H. Li, L. Xu, and Z. Wang, "Adaptive interpolation for pilot-aided channel estimator in OFDM system," *IEEE Transactions on Broadcasting*, vol. 60, no. 3, pp. 486–498, Sep. 2014.

[67] M. Henkel, C. Schilling, and W. Schroer, "Comparison of channel estimation methods for pilot aided OFDM systems," in *Proc. 65th IEEE Vehicular Technology Conference (VTC 2007-Spring)*, pp. 1435–1439, Apr. 2007.

[68] J. Cai, W. Song, and Z. Li, "Doppler spread estimation for mobile OFDM systems in Rayleigh fading channels," *IEEE Transactions on Consumer Electronics*, vol. 49, no. 4, pp. 973–977, Nov. 2003.

[69] J. Zheng and S. L. Miller, "Performance analysis of coded OFDM systems over frequency-selective fading channels," in *Proc. IEEE Global Telecommunications Conference (GLOBECOM 2003)*, pp. 1623–1627, Dec. 2003.

[70] "IEEE standard for local and metropolitan area networks–part 15.4: Low-rate wireless personal area networks (LR-WPANs)," *IEEE Std 802.15.4-2011*, pp. 1–314, Sep. 2011.

[71] "IEEE standard for information technology - telecommunications and information exchange between systems - local and metropolitan networks - specific requirements - part 11: Wireless lan medium access control (MAC) and physical layer (PHY) specifications: Higher speed physical layer (PHY) extension in the 2.4 GHz band," *IEEE Std 802.11b-1999*, pp. 1–96, Jan. 2000.

[72] H. Kubo and M. Miyake, "Beat interference suppression techniques by means of transmission time diversity and adaptive equalization," in *Proc. IEEE 51st Vehicular Technology Conference (VTC 2000-Spring)*, vol. 3, pp. 1874–1878, May 2000.

[73] T. Hattori and K. Hirade, "Multitransmitter digital signal transmission by using offset frequency strategy in a land-mobile telephone system," *IEEE Transactions on Vehicular Technology*, vol. 27, no. 4, pp. 231–238, Nov. 1978.

[74] Y. Fujino, S. Kuwano, S. Ohmori, T. Fujita, and S. Yoshino, "Cell range extension techniques for wide-area ubiquitous network," in *Proc. IEEE 10th International Symposium on Autonomous Decentralized Systems (ISADS 2011)*, pp. 35–40, Mar. 2011.

[75] E. Uhlemann and A. Willig, "Hard decision packet combining methods for industrial wireless relay networks," in *Proc. IEEE 2nd International Conference on Communications and Electronics (ICCE 2008)*, pp. 104–108, Jun. 2008.

[76] H. Dubois-Ferrière, D. Estrin, and M. Vetterli, "Packet combining in sensor networks," in *Proc. ACM 3rd International Conference on Embedded Networked Sensor Systems (SenSys 2005)*, pp. 102–115, Nov. 2005.

[77] Y. Liang and S. S. Chakraborty, "ARQ and packet combining with post-reception selection diversity," in *Proc. IEEE 60th Vehicular Technology Conference (VTC 2004-Fall)*, vol. 3, pp. 1853–1857, Sep. 2004.

[78] D. O'Rourke and C. Brennan, "Practical packet combining for use with cooperative and non-cooperative ARQ schemes in resource-constrained wireless sensor networks," *Ad Hoc Networks*, vol. 10, no. 3, pp. 339–355, May 2012.

[79] F. Adachi, "Postdetection selection diversity effects on digital FM land mobile radio," *IEEE Transactions on Vehicular Technology*, vol. 31, no. 4, pp. 166–172, Nov. 1982.

[80] X. Zheng, Z. Cao, J. Wang, Y. He, and Y. Liu, "ZiSense: Towards interference resilient duty cycling in wireless sensor networks," in *Proc. ACM 12th International Conference on Embedded Networked Sensor Systems (SenSys 2014)*, pp. 119–133, Nov. 2014.

Publications

Journal

[1] T. Sakdejayont, C. H. Liao, M. Suzuki, and H. Morikawa, "Subcarrier-selectable short preamble for OFDM channel estimation in real-time wireless control systems," IEICE Trans. Fundamentals, Special Section on Smart Multimedia and Communication Systems, Nov. 2017.

[2] T. Sakdejayont, M. Suzuki, and H. Morikawa, "Toward reliable concurrent transmission using RSSI-based packet combining," Wireless communications and mobile computing. (Under preparation)

International Conference

Oral Presentation

[3] T. Sakdejayont, C. H. Liao, M. Suzuki, and H. Morikawa, "Making preamble shorter in OFDM real-time wireless control systems," in Proc. APCC 2016, pp. 26-31, Yogyakarta, Indonesia, Aug. 2016.

[4] K. Chutisemachai, T. Sakdejayont, C. H. Liao, M. Suzuki, and H. Morikawa, "Distributed antenna system using concurrent transmission for wireless automation system," in Proc. VTC2017-Fall, Toronto, Canada, Sept. 2017.

[5] D. Lee, T. Sakdejayont, H. Sasaki, H. Fukumoto, and T. Nakagawa, "Performance evaluation of wireless communications using orbital angular momentum multiplexing," in Proc. ISAP 2016, Okinawa, Japan, Oct. 2016.

[6] T. Sakdejayont, D. Lee, Y. Peng, Y. Yamashita, and H. Morikawa, "Evaluation of memory-efficient 1-bit compressed sensing in wireless sensor networks," in Proc. R10-HTC 2013, pp.326–329, Sendai, Japan, Aug. 2013.

[7] T. Sakdejayont, N. Jindapornsopit, and S. Kittipiyakul, "Performance of gradient-based OFDMA subcarrier schedulers with TCP traffic," in Proc. ECTI-CON, Khon Kaen, Thailand, May 2011.

Poster Presentation

[8] T. Sakdejayont, C. H. Liao, M. Suzuki, and H. Morikawa, "Poster abstract: Beating the beat - RSSI-based packet combining in concurrent transmission sensor networks," in Proc. SenSys ' 16, Stanford, CA, Nov. 2016.

Technical Report

[9] T. Sakdejayont, C. H. Liao , M. Suzuki, and H. Morikawa, "Evaluation of packet combining using RSSI for reliable reception of concurrent transmission, " in IEICE Technical Report, RCS2016-223 (2016-12), Dec. 2016.

[10] T. Sakdejayont, C. H. Liao, H. Morikawa, "Evaluation of subcarrier-selected short preamble for OFDM wireless control systems, "in IEICE Technical Report, RCS2015-130 (2015-07), July 2015.

Domestic Conference

[11] T. Sakdejayont, M. Suzuki, and H. Morikawa, "Evaluation of RSSI-based packet combining on off-the-shelf wireless sensors in concurrent transmission environment," in IEICE Society Conference, B-5-98, Sept. 2016.

[12] T. Sakdejayont, C. H. Liao, M. Suzuki, and H. Morikawa, "Performance evaluation of real-time wireless control system using shortened preambles," in IEICE General Conference, B-5-151, March 2016.

[13] T. Sakdejayont, C. H. Liao, M. Suzuki, and H. Morikawa, "Adaptive channel estimation for OFDM wireless control systems using subcarrier-selected short preambles," in IEICE Society Conference, B-5-116, Sept. 2015.

[14] T. Sakdejayont, C. H. Liao, and H. Morikawa, "Short OFDM preamble for channel estimation in real-time wireless control systems," in IEICE General Conference, B-5-156, March 2015.

[15] K. Chutisemachai, T. Sakdejayont, C. H. Liao, M. Suzuki, and H. Morikawa, "Feasibility of distributed antenna system using concurrent transmission in real world," in IEICE General Conference, B-5-141, March 2017.

[16] K. Chutisemachai, T. Sakdejayont, C. H. Liao, M. Suzuki, and H. Morikawa, "Distributed antenna system using concurrent transmission with loose carrier frequency control in wireless factory," in IEICE Society Conference, B-5-99, Sept. 2016.

[17] R. Nakao, T. Sakdejayont, C. H. Liao, M. Suzuki, and H. Morikawa, "Packet combining using RSSI for beat interference rejection in concurrent transmission," in IEICE General Conference, B-5-155, March 2016. [in Japanese]

[18] D. Lee, T. Sakdejayont, H. Sasaki, H. Fukumoto, and T. Nakagawa, "A study on orbital angular momentum-based wireless communication," in IEICE General Conference, B-19-15, March 2016.

[19] T. Sakdejayont, D. Lee, and H. Morikawa, "Carrier frequency alignment in sub-Nyquist sampling receiver," in IEICE Society Conference, B-17-2, Sept. 2014.

[20] T. Sakdejayont, D. Lee, H. Morikawa, T. Yamada, H. Shiba, H. Sasaki, and T. Nakagawa, "Evaluation of sub-Nyquist sampling for BPSK/QPSK signals sparsely located in wideband spectrum," in IEICE General Conference, B-17-8, March 2014.

[21] H. Sasaki, T. Yamada, H. Shiba, T. Nakagawa, D. Lee, T. Sakdejayont, and H. Morikawa, "A study on sampling frequency of analog compressed sensing using overclocked devices," in IEICE General Conference, B-17-5, March 2014. [in Japanese]

[22] T. Sakdejayont, D. Lee, and H. Morikawa, "Analysis of overclocked PN sequences in sub-Nyquist sampling for wideband sparse signals," in IEICE Society Conference, B-17-11, Sept. 2013.

Patent

[23] 山田 貴之, 芝 宏礼, 笹木 裕文, 中川 匡夫, 李 斗煥, サクデーシャヨン　ティラット, 森川 博之, "信号処理システム及び信号処理方法, ", 特開 2015-162684, 出願　Feb. 2014.